THE UNVERSITY OF ALBERTA

RELEASE FORM

NAME OF AUTHOR ..... Richard B. Robertson .....

TITLE OF THESIS ..... Thermal Radiation as a Method of Deicing .....

DEGREE FOR WHICH THESIS WAS PRESENTED ..... Master of Science .....

YEAR THIS DEGREE GRANTED ..... 1976 .....

THE UNIVERSITY OF ALBERTA

THERMAL RADIATION AS A METHOD OF DEICING

by

© RICHARD B. ROBERTSON

A THESIS

SUBMITTED TO THE FACULTY OF GRADUATE STUDIES AND RESEARCH

IN PARTIAL FULFILMENT OF THE REQUIREMENTS FOR THE DEGREE

OF MASTER OF SCIENCE

DEPARTMENT OF MECHANICAL ENGINEERING

EDMONTON, ALBERTA

FALL, 1976

THE UNIVERSITY OF ALBERTA

FACULTY OF GRADUATE STUDIES AND RESEARCH

The undersigned certify that they have read, and recommend to the Faculty of Graduate Studies and Research, for acceptance, a thesis entitled THERMAL RADIATION AS A METHOD OF DEICING submitted by Richard B. Robertson in partial fulfilment of the requirements for the degree of Master of Science.

ABSTRACT

The icing of structures due to prevailing climatic conditions can present serious problems. Various methods to remove the ice build-up have been suggested. One of these is thermal radiation. However, before it can be used, the factors governing thermal radiation penetration in ice must be considered. A computer model was developed to simulate the transfer of collimated thermal radiation through an absorbing and scattering ice sheet. The model utilized a modified two flux representation of thermal radiation transfer first developed by Schuster (1905).

The validity of the model was checked by completing two sets of experiments. One set of experiments measured amounts of incident radiation absorbed and transmitted through various ice samples. In order to then compare these experimental results to the model, a second set of experiments were completed to measure the amount and distribution of scattered radiation produced in a thin ice sheet. Sufficient evidence was obtained by these experiments to verify the model.

The model was then used to calculate the amounts of incident energy that are absorbed, transmitted and reflected by an ice sheet for the various scattering characteristics of ice. This information provided an indication that thermal radiation might be useful as a deicing method.

ACKNOWLEDGEMENTS

The author wishes to express his appreciation to:

- Dr. R.R. Gilpin for his supervision and assistance during the completion of this thesis;

- Jim Kennedy for his help with the problems in computer programming;

- Dr. J.S. Kennedy for the work he did in obtaining the necessary financial support that was required.

TABLE OF CONTENTS

LIST OF TABLES

LIST OF FIGURES

LIST OF PLATES

LIST OF SYMBOLS

b	thickness of ice sheet
β	parametric constant
c_0	constant of integration for collimated radiation
c_1, c_2, c_3, c_4	constants of integration for diffuse radiation
c_I	cone angle constant
c_p	specific heat of ice at constant pressure
ε_i	total energy incident of the ice surface
ε_{ICE}	energy absorbed by ice sample
ε_L	energy transfer to ice mount
I_b	intensity of collimated radiation at x = b
I_0	intensity of collimated radiation at x = 0
I_s	intensity of radiation striking surface of ice sample during the experiments
I_x	intensity of collimated radiation at x
K	absorption coefficient of collimated radiation
K^1	absorption coefficient of diffuse radiation
κ	parametric constant
m_I	mass of ice sample

μ_1, μ_2	parametric constants
n	portion of scattering which is in the forward direction
π	parametric constant
R_1, R_2	parametric constants
r_b	reflection coefficient of collimated radiation at x = b
r_b^1	reflection coefficient of diffuse radiation at x = b
r_0	reflection coefficient of collimated radiation at x = 0
r_0^1	reflection coefficient of diffuse radiation at x = 0
r_s	scattering coefficient of collimated radiation
r_s^1	scattering coefficient of diffuse radiation
ζ	parametric constant
σ	extinction coefficient collimated radiation
σ^1	extinction coefficient diffuse radiation
ξ	parametric constant
t	time radiation source is applied to ice sample
τ	parametric constant
T_{rise}	temperature rise of ice sample
x	depth within an ice sheet from upper surface

Y	downward diffuse flux (positive x direction)
Y_0	downward diffuse flux at x = 0
Y_b	downward diffuse flux at x = b
Z	upward diffuse flux
Z_0	upward diffuse flux at x = 0
Z_b	upward diffuse flux at x = b

CHAPTER I

INTRODUCTION

The formation of ice on structures whether on the land, on the oceans, or in the air, can present very serious problems. When icing has occurred, if no viable method was available to prevent or failing that remove the ice build up, the result has been the collapse of power lines, the loss of ships and the downing of aircraft. Realizing the problem is only part of the answer. Next it will be necessary to propose and evaluate several methods which can be used to alleviate the icing problem.

Depending upon where the icing has occurred, various methods have been suggested and some have been tested under field conditions. On the land, the problem of icing has been solved by first evaluating conditions under which icing occurs. The structure is then designed to withstand the predicted ice load or is moved to a location where icing would not occur. On the oceans, the problem of ship icing has been tackled by again evaluating conditions under which icing occurs, however, the problem of preventing or removing the ice build up is more difficult to solve. Various researchers (1) have attempted to use foam mats and pneumatic tubes attached to ship surfaces to facilitate ice removal. In the air, the aircraft industry (3) has used

various methods including the use of engine exhaust, pneumatic tubes and specially treated surfaces to which ice has a low adhesion. The various methods of ice removal can be divided into two main categories - thermal and mechanical.

Under these two main categories are a variety of methods several of which have been illustrated in the preceeding paragraphs. The objective of this thesis will be to examine thermal radiation as a thermal method to aid in deicing surfaces. When using thermal radiation on an ice sheet, the objective is to allow penetration of the ice by the radiation resulting in its absorption at the ice-surface interface. By absorbing the heat energy at the bonding surface it is hoped that the bond could be broken allowing mechanical means of ice removal to be more effective. The model developed in this thesis, although it is intended primarily for study of ice removal techniques, could be used to predict such phenomena as transmission of solar radiation through lake ice.

For any problem involving thermal radiation penetration in an ice sheet, it is necessary to know the effects of the type of thermal radiation to be used and the various factors which govern its degree of penetration. Previously the approach to this problem has been to gather experimental data, on certain types of ice, in order to determine total extinction coefficients for a specific spectral distribution of thermal radiation. For example, Thomas (4) deter-

mined the effects of density and porosity on the extinction coefficients for snow and ice. The extinction coefficients were used in the Bouger-Lambert Law (i.e., $I = I_0 e^{-Kx}$) to evaluate light transmission. In these studies the roles of scattering and absorption were not considered separately merely their combined effect. A more generalized approach to thermal radiation penetration in ice is required if thermal radiation is to be evaluated as a deicing method.

The generalized approach used will consider the ice to behave like a diffusing material. That is, thermal radiation entering such a diffusing material is absorbed, transmitted and scattered within it. This approach was first developed by Schuster (5) to describe the absorption and scattering of radiation in what was termed a "foggy" atmosphere. The equations were further modified by Silberstein to take into account the passage of collimated thermal radiation through a diffuse material. S.Q. Duntley (7) discussed further some other alterations of the Schuster model to take into account such factors as dependency of scattering and absorption on wavelength, and the dependency of scattering and absorption on depth, and amounts of diffuse radiation.

It is now hoped that this model first developed by Schuster can now be applied with suitable modifications to solve thermal radiation penetration in an ice sheet. By comparing the theoretical results with those obtained from experimental tests, the model can be evaluated.

Information obtained from the model can then be used to indicate the possibility of using thermal radiation as a deicing method.

CHAPTER II

ANALYTICAL ANALYSIS OF THERMAL RADIATION TRANSMISSION IN A DIFFUSE MATERIAL

2.1 Introduction

For a collimated beam of thermal radiation of known energy striking the surface of an ice sheet, the problem is to determine how much of the incident energy is absorbed, transmitted and reflected by the ice sheet. To answer this a modified analysis of the equations presented by Dunkle and Bevens (8) will be applied. These differential equations along with the specific boundary conditions applicable to the problem will be used to obtain a set of expressions which give the magnitudes of upward and downward fluxes within the ice sheet as a function of depth.

2.2 Differential Equations

Consider an infinitesimal layer of ice located within an ice sheet subjected to a beam of collimated thermal radiation striking normal to the upper surface. For a given wavelength and a given interval of depth from $x - dx/2$ to $x + dx/2$ there exist three fluxes. These fluxes are a collimated flux and two diffuse fluxes - one in the upward and one in the downward direction caused by the scattering of the incident beam. To obtain the differential equations

some assumptions about the character of the absorbed and scattered radiation within a given layer must be made. First, the nature of the diffuse fluxes are such that upon leaving the infinitesimal layer they are isotropically distributed over a cone of given angle (9). Second, the proportion of the collimated beam scattered forward (n) is different from that scattered backward (1-n). And finally, the absorption and scattering coefficients for the collimated and diffuse fluxes are related by a constant determined by the cone angle of the diffuse radiation. That is, it is possible to relate the various absorption and scattering coefficients by

$$K^1 = K \times c_I$$

and

$$r_s^1 = (1-n)r_s \times c_I$$

where K and K^1 are the absorption coefficients for the collimated and diffuse fluxes respectively and similarly r_s and r_s^1 are the scattering coefficients. c_I is a parameter varying from 1.0 to 2.0 depending upon the cone angle. From the above assumptions three differential equations can be formulated (Figure 1)

$$dY = -K^1 Y dx - r_s^1 Y dx + r_s^1 Z dx + n r_s I_x dx \qquad (1)$$

$$dZ = K'Zdx + r_s'Zdx - r_s'Ydx - (1-n)r_sI_xdx \qquad (2)$$

$$dI_x = -r_sI_xdx - KI_xdx \qquad (3)$$

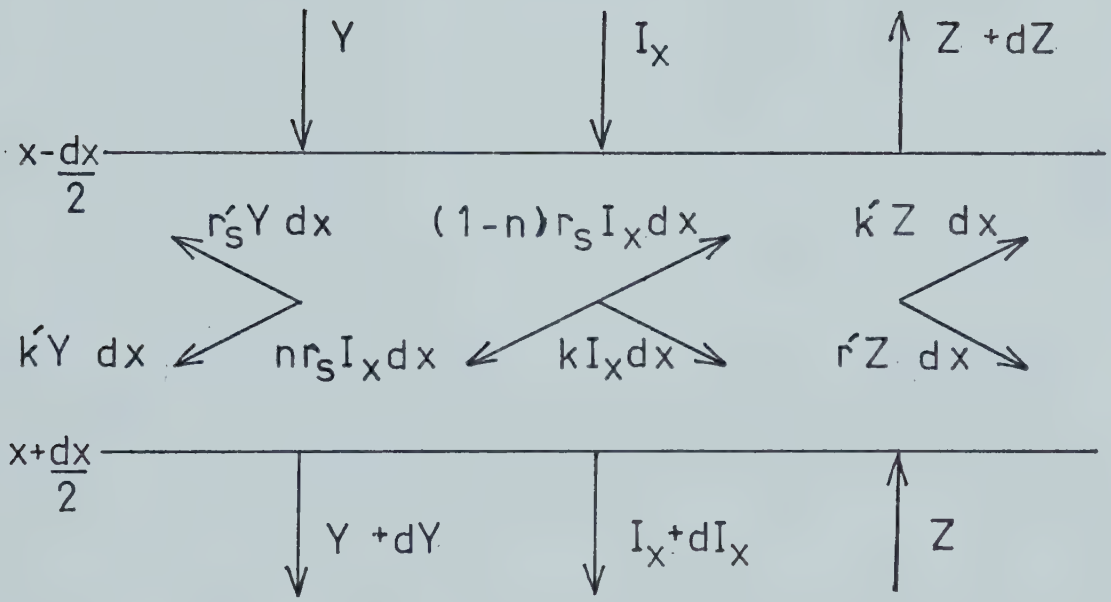

Figure 1. Radiation Fluxes Within an Ice Layer

2.3 Solution of the Differential Equations

The solution for the collimated radiation in equation (3) is an exponential function of the form $I_x = c_0e^{-\sigma x}$ where c_0 is a constant of integration and σ is

defined as $(r_s + K)$. Solving the remaining equations for the diffuse fluxes is accomplished by defining $u = Y + Z$ and $v = Y - Z$ and then adding and subtracting equations (1) and (2) to obtain

$$\frac{du}{dx} = -\sigma^1 v + (2n-1)r_s I_x \tag{4}$$

and

$$\frac{dv}{dx} = -K^1 u + r_s I_x \tag{5}$$

where σ^1 is defined as $\{2(r_s^1) + K^1\}$. Now by differentiating equation (1) by $\frac{d}{dx}$ plus substituting the equation for I_x the following equation is derived:

$$\frac{d^2u}{dx^2} = -\sigma^1 \frac{dv}{dx} - \sigma(2n-1)r_s c_0 e^{-\sigma x} \tag{6}$$

By utilizing equation (5) the differential equation becomes

$$\frac{d^2u}{dx^2} - \sigma^1 K^1 u = -\{\sigma(2n-1) + \sigma^1\} r_s c_0 e^{-\sigma x}$$

The solution of this equation is of the form

$$u = c_1 e^{\zeta x} + c_2 e^{-\zeta x} - \{\frac{\sigma(2n-1) + \sigma^1}{\sigma^2 - \zeta^2}\} r_s c_0 e^{-\sigma x} \qquad (7)$$

where ζ^2 is defined as $\sigma^1 K^1$ and c_1 plus c_2 are constants of integration determined by the boundary conditions. From the expression for u it is possible to obtain one for v by using equation (4) to get

$$v = -(\frac{\zeta}{\sigma^1}) c_1 e^{\zeta x} + (\frac{\zeta}{\sigma^1}) c_2 e^{-\zeta x}$$

$$- (\frac{\sigma}{\sigma^1}) \{\frac{\sigma(2n-1) + \sigma^1}{\sigma^2 - \zeta^2}\} r_s c_0 e^{-\sigma x}$$

$$+ \{\frac{(2n-1)}{\sigma^1}\} r_s c_0 e^{-\sigma x} \qquad (8)$$

By replacing some terms by simpler ones and then adding and subtracting equations (7) and (8), equations are obtained giving the upward and downward fluxes. These equations are

$$Y = c_3\{1 - \frac{\zeta}{\sigma^1}\} e^{\zeta x} + c_4\{1 + \frac{\zeta}{\sigma^1}\} e^{-\zeta x}$$

$$+ [\{1 + \frac{\sigma}{\sigma^1}\} \{\frac{\kappa}{\sigma^2 - \zeta^2} + \frac{\beta}{\sigma^1}] e^{-\sigma x}$$

and

$$Z = c_3\{1 + \frac{\zeta}{\sigma^1}\}e^{\zeta x} + c_4\{1 - \frac{\zeta}{\sigma^1}\}e^{-\zeta x}$$

$$+ [\{1 - \frac{\sigma}{\sigma^1}\}\{\frac{\kappa}{\sigma^2 - \zeta^2}\} - \frac{\beta}{\sigma^1}]e^{-\sigma x}$$

where $c_3 = \frac{c_1}{2}$; $c_4 = \frac{c_2}{2}$; $\kappa = -\{\sigma(2n-1) + \sigma^1\}(\frac{c_0}{2})r_s$;

$\beta = (2n-1)(\frac{c_0}{2})r_s$. A further consolidation of terms by letting

$\tau = \{1 - \frac{\zeta}{\sigma^1}\}$; $\xi = \{1 + \frac{\zeta}{\sigma^1}\}$; $\mu_1 = \{1 + \frac{\sigma}{\sigma^1}\}$; $\mu_2 = \{1 - \frac{\sigma}{\sigma^1}\}$;

$\pi = \{\frac{\kappa}{\sigma^2 - \zeta^2}\}$ leads to the equations in their final form.

$$Y = c_3\tau e^{\zeta x} + c_4\xi e^{-\zeta x} + \{\mu_1\pi + \frac{\beta}{\sigma^1}\}e^{-\sigma x} \qquad (9)$$

$$Z = c_3\xi e^{\zeta x} + c_4\tau e^{-\zeta x} + \{\mu_2\pi - \frac{\beta}{\sigma^1}\}e^{-\sigma x} \qquad (10)$$

and

$$I_x = c_0 e^{-\sigma x} \qquad (11)$$

2.4 Application of Boundary Conditions

In order to establish the values of the integration

constants in equations (9) through (11) the boundary conditions for the various wavelength intervals must be used. There exist three boundary conditions: one due to the reflection of the collimated radiation at the upper air-ice interface and two because of reflection of the upward and downward diffuse fluxes at the upper and lower air-ice surfaces respectively.

The boundary condition resulting from the passage of collimated radiation through the upper surface (Figure 2) implies that $c_0 = (1-r_0)I_0$ where r_0 is the coefficient of reflection for collimated radiation at the surface and I_0 is the intensity of incident energy on the ice sheet. Therefore equation (11) becomes $I_x = (1-r_0)I_0e^{-\sigma x}$.

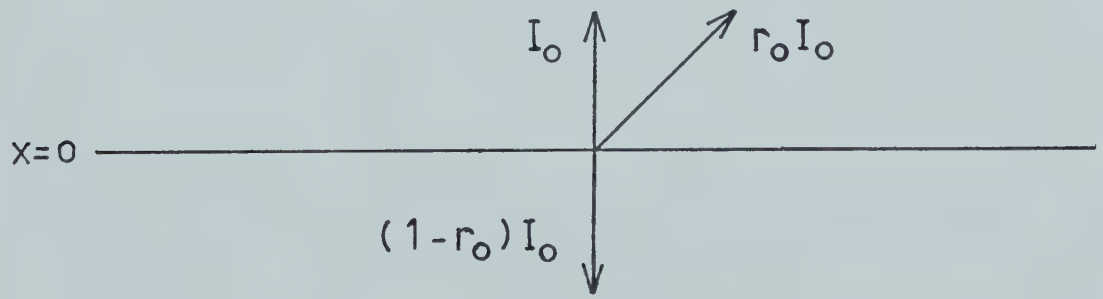

Figure 2. Collimated Boundary Condition

The other two boundary conditions are determined if as stated earlier the interaction of the diffuse fluxes with the upper and lower surfaces is considered. At the upper surface or air-ice interface the only portion of the downward flux existing is that due to the downward reflection of a portion of the upward flux such that $Y_0 = r_o^1 Z_0$ (Figure 3).

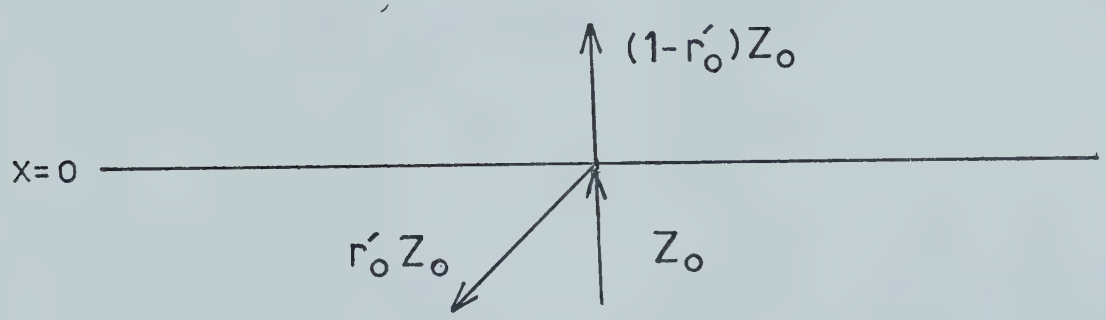

Figure 3. Diffuse Flux Boundary Condition

The reflection coefficient r_0^1 of the diffuse flux at $x = 0$ can be related to that of the collimated coefficient r_0 by the expression $r_0^1 = r_0 \times c_I$. To do this it must be

assumed that the reflection coefficient between the air-ice interface and the ice-air interface is approximately the same (10), which is true for angles of incidence less than 30 degrees, and that c_I can be used to relate the two coefficients. Similarly the reflection of the downward flux at the lower surface or ice-air interface plus the diffuse reflection of the collimated flux produces the final boundary condition (Figure 4).

$$Z_b = r_b^1 Y_b + r_b I_b$$

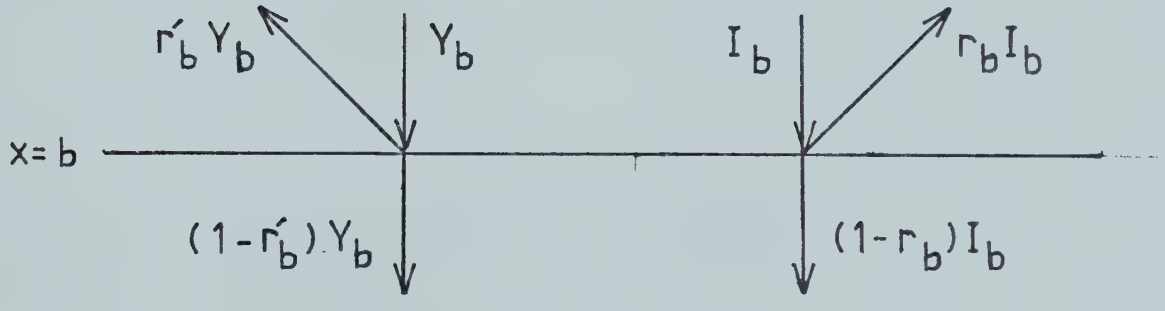

Figure 4. Diffuse Flux Boundary Condition

For the lower surface the relationship between r_b and r_b^1 is given by the expression $r_b^1 = r_b \times c_I$. Also it is assumed that the reflection of the collimated radiation is to be totally diffuse. From the above developed boundary conditions it is now possible to evaluate the integration constants for the diffuse fluxes.

If the equations derived earlier at a given wavelength are evaluated at x = 0 and x = b the diffuse flux equations become

$$Y_0 = c_3\tau + c_4\xi + \{\mu_1\pi + \frac{\beta}{\sigma^1}\}$$

$$Z_0 = c_3\xi + c_4\tau + \{\mu_2\pi - \frac{\beta}{\sigma^1}\}$$

$$Y_b = c_3\tau e^{\zeta b} + c_4\xi e^{-\zeta b} + \{\mu_1\pi + \frac{\beta}{\sigma^1}\}e^{-\sigma b}$$

and

$$Z_b = c_3\xi e^{\zeta b} + c_4\tau e^{-\zeta b} + \{\mu_2\pi - \frac{\beta}{\sigma^1}\}e^{-\sigma b}$$

Applying these flux equations to the boundary conditions two equations are obtained

$$c_3\{\tau - r_0^1\xi\} + c_4\{\xi - r_0^1\tau\} = R_1$$

where R_1 is $r_0^1\mu_2\pi - \mu_1\pi = \frac{\beta}{\sigma^1}\{1 + r_0^1\}$ and

$$c_3\{\xi - r_b^1\tau\}e^{\zeta b} + c_4\{\tau - r_b^1\xi\}e^{-\zeta b} = R_2e^{-\sigma b}$$

where R_2 is $r_b^1\mu_1\pi - \mu_2\pi + \frac{\beta}{\sigma^1}\{1 + r_b^1\} + r_b(1 - r_0)I_0$.

Solving the above equations expressions for the two constants are

$$c_3 = -\left\{\frac{R_1(\tau-r_b^1\xi)e^{-\zeta b} - R_2(\xi-r_0^1\tau)e^{-\sigma b}}{(\xi-r_0^1\tau)(\xi-r_b^1\tau)e^{\zeta b} - (\tau-r_0^1\xi)(\tau-r_b^1\xi)e^{-\zeta b}}\right\}$$

and

$$c_4 = \left\{\frac{R_1(\xi-r_b^1\tau)e^{\zeta b} - R_2(\tau-r_0^1\xi)e^{-\sigma b}}{(\xi-r_0^1\tau)(\xi-r_b^1\tau)e^{\zeta b} - (\tau- r_0^1\xi)(\tau-r_b^1\xi)e^{-\zeta b}}\right\}$$

CHAPTER III

COMPUTER SIMULATION

3.1 Computer Model

Using the equations developed in the preceding chapter, the radiation fluxes at a given wavelength and depth in an ice sheet can be found. These fluxes along with the absorption coefficients (Figure 5) - obtained from data presented by Goodrich (11) - are used to calculate the portion of incident energy that is absorbed by an ice sheet. The incident energy transmitted and reflected are evaluated using the radiation flux equations at the surfaces of an ice sheet.

To numerically evaluate the incident energy absorbed, the ice sheet is divided into a series of finite layers. The radiation fluxes existing in each layer are determined at the center of the layer and assumed constant over the remainder. Using the absorption coefficients, the energy absorbed within each ice layer is then found by multiplying the fluxes by these coefficients. Since this absorbed energy is evaluated at a given wavelength, the total radiation absorbed within each ice layer must be numerically integrated over the total spectrum. This is done by the trapezoidal rule. The total energy absorbed is then determined by adding the energy absorbed within each layer.

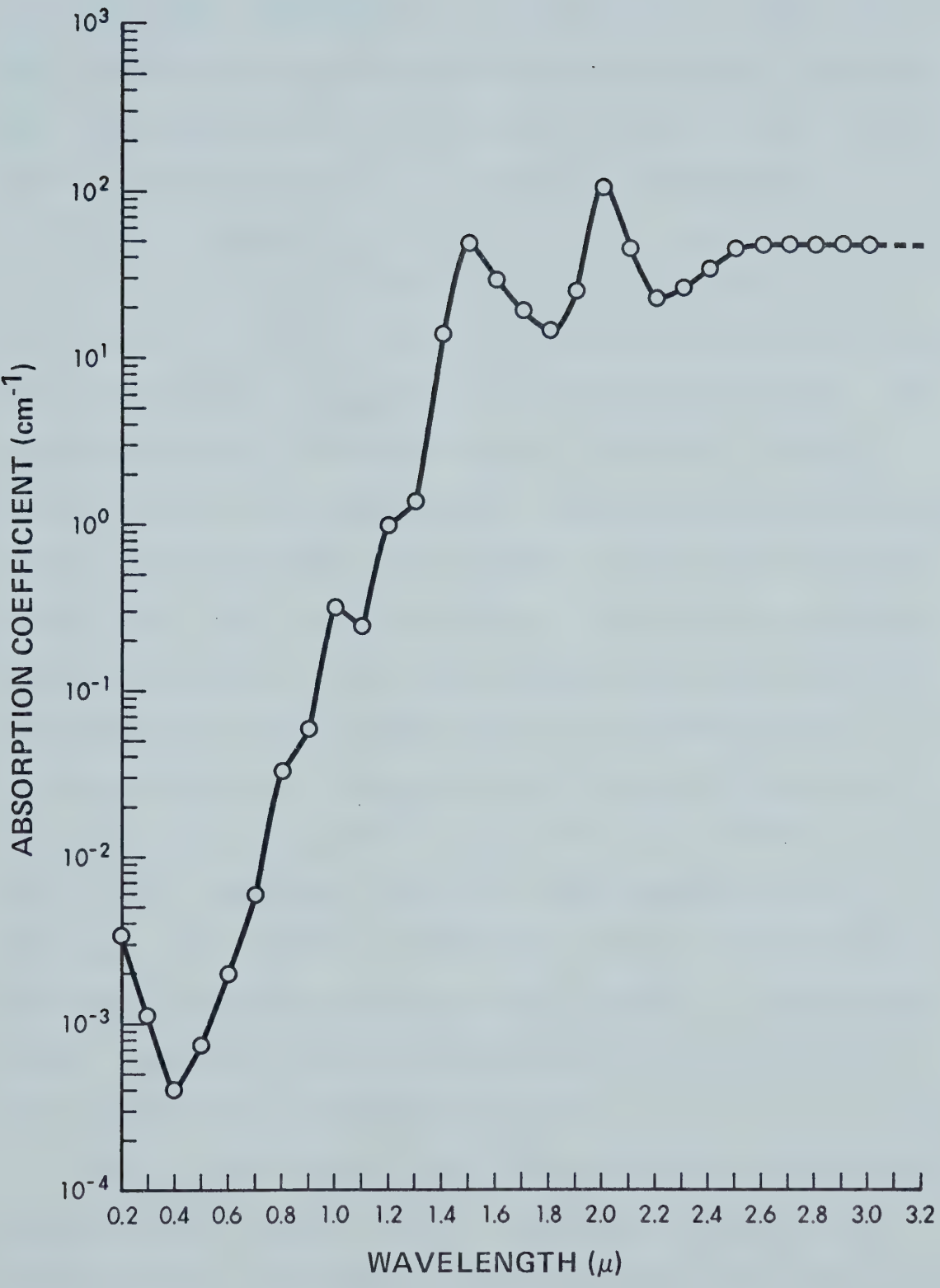

Figure 5. Clear Ice Absorption Coefficients

The same trapezoidal rule can be used to find the total incident energy transmitted and reflected. However, first the amounts of the transmitted and reflected radiation must be determined as a function of wavelength. To do this, the boundary conditions and the flux equations at the upper and lower surfaces must be used. The boundary condition are $(1-r_b^1)Y_b + (1-r_b)I_b$ for the transmitted radiation and $(1-r_0^1)Z_0 + r_0 I_0$ for the reflected radiation. To compare the effects produced by the different incident energy spectra used, the absorbed, transmitted and reflected energies are normalized with respect to the total incident energy. The total incident energy is obtained by numerically integrating over the total energy spectrum using the same method employed to determine the transmitted and reflected energies. By summing up the normalized values of the absorbed, transmitted and reflected energies, a check on the numerical accuracy of the computer model is obtained. The summation indicated that for a 20 cm thick ice sheet the maximum error was two percent. This particular ice sheet had been divided into 50 finite layers and had a scattering coefficient of 1.0/cm.

Due to the nature of the flux equations used, however, several special cases arise in computing the amounts of energy absorbed, transmitted and reflected. The first problem that occurs is when σ is equal to ζ and the term $\{\frac{K}{\sigma^2 - \zeta^2}\}$ appearing in the diffuse flux equations cannot be

evaluated. By setting $\sigma^2 = \zeta^2$ and then using the relationship between r_s and r_s^1 plus K and K^1, the critical condition is found to be

$$\{c_I^2 - 1\}^2K^2 + 2r_s\{(1-n)c_I^2 - 1\}K - r_s^2 = 0$$

Therefore, for a particular degree of scattering there exists a critical absorption coefficient for which the diffuse fluxes are impossible to evaluate. This numerical problem results from the form of the particular solution chosen to solve the diffuse flux equations. To overcome the problem the value of K is reset slightly when it falls on the critical value. Since this small change is insignificant considering the uncertainty in the absorption coefficients (11) no important error is produced. The next special case occurs when the absorption coefficients are 50 times greater than those for scattering at a given wavelength. When this situation occurs, it is assumed that the passage of the collimated radiation obeys the Bouger-Lambert law and that only absorption need be considered. The absorption is then determined by evaluating the difference between the collimated flux at each surface of the finite ice layers. Finally, numerical problems occur in the model when an ice sheet is optically very thick, that is, σ_b and ζ_b is very large. When this occurs the diffuse flux integration constants

$$c_3 = -\left\{\frac{R_1(\tau - r_b^1\xi)e^{-\zeta b} - R_2(\xi - r_0^1\tau)e^{-\sigma b}}{(\xi - r_0^1\tau)(\xi - r_b^1\tau)e^{\zeta b} - (\tau - r_0^1\xi)(\tau - r_b^1\xi)e^{-\sigma b}}\right\}$$

and

$$c_4 = \left\{\frac{R_1(\xi - r_b^1\tau)e^{\zeta b} - R_2(\tau - r_0^1\xi)e^{-\sigma b}}{(\xi - r_0^1\tau)(\xi - r_b^1\tau)e^{\zeta b} - (\tau - r_0^1\xi)(\tau - r_b^1\xi)e^{-\sigma b}}\right\}$$

can be approximated by

$$c_3 \simeq 0.0$$

and

$$c_4 \simeq \frac{R_1}{(\xi - r_0^1\tau)}$$

Utilizing the general case and the various special cases for radiation penetration in an ice sheet a series of computer outputs are obtained.

3.2 Results

The major parameters which affect the results are the temperature of the blackbody source, the degree of non-isotropic scattering (n), the scattering coefficients and

the diffuse cone angle constant (c_I). Two series of curves are generated. One series Appendix B gives the behavior of the absorbed, transmitted, and reflected energies for various combinations of the major parameters. The second series Appendix C gives similar sets of parametric curves for the rates of energy generation in the ice sheet due to absorption of the radiation fluxes. From these parametric curves the effect of varying the major parameters are evaluated.

A decrease in blackbody source temperature caused the radiant energy to shift to the longer wavelengths. Because of the higher absorption coefficients that exist at the longer wavelengths (Figure 5), this produces an increased absorption, decreased transmission and decreased reflection of the incident energy. As an example for a 12 centimeter thick ice sheet with no scattering, for a 3000°K source temperature 38 percent of the energy is transmitted while for the 5780°K source temperature 72 percent is transmitted.

The effect of scattering is quite important as far as the transmitted and reflected energies are concerned. In general, the effects of scattering on absorption are minimal. Increased scattering produces a decrease in transmission and an increase in reflection. This effect is particularly important for the high temperature source. Due to the higher absorption coefficients that exist at the wavelengths where the lower temperature source is the strongest, the effects of scattering on the transmitted and

reflected fluxes are less important. As would be expected these effects of scattering are not linear. That is, because of the exponentials in the flux equations, equal increments of scattering coefficients do not cause equal changes in the transmitted and reflected energies. The effect of scattering on absorption is minimal as stated earlier. However, changes in degree of forward scattering and scattering itself do produce some interesting phenomena. For example (5780°K and n = 0.90) an increase in scattering causes an increase in absorption for ice sheet thicknesses less than 12 centimeters. While for thicknesses greater than 12 centimeters, the absorption is decreased with increasing scattering. This behavior can be traced to two opposing effects caused by scattering. First, an increase in scattering produces a greater amount of diffuse radiation in the ice sheet. As a result of this, more incident energy is absorbed since diffuse radiation has effectively higher absorption coefficients compared to collimated radiation. Second, as more incident energy is scattered, a higher portion of energy is reflected out of the ice sheet. These two effects then counteract each other causing the observed behavior.

The degree of forward scatter as opposed to backward scatter also has an effect. Its most significant effect is that which it has on the incident energy absorbed. By increasing the degree of forward scatter (Appendix B, pages 93 to 98) the crossover of the absorption curves for the

various scattering coefficients is delayed. This delay is a result of less incident energy being reflected back out of the ice sheet. The other effects of increasing forward scatter are an increase in transmission.

To determine the effect of the diffuse cone angle constant (c_I) a comparison is made between the generation curves (Appendix C, pages 108 and 109). These are produced by varying the value of c_I from one to two at a given degree of scattering coefficients. This comparison indicates increasing c_I has a similar effect to a slight increase in scattering. Now, a further examination of thermal radiation penetration in an ice sheet will require input from experimental work. By completing these experiments representative values of the major parameters can be chosen.

CHAPTER IV

EXPERIMENTAL PROCEDURE AND RESULTS

4.1 Introduction

The two diffuse flux model with collimated flux superimposed will be tested for its validity by using two different types of experiments. The first type of experiment will establish the accuracy of the predictions for the amounts of incident radiation absorbed and transmitted; two different sources (Plate 1 and Plate 2) providing the necessary incident radiation. The second type of experiment will then be used to test assumptions about the character of the scattered radiation by determining what proportion is scattered forward and backward along with the scattered energy distributions. Finally, by comparing the information obtained from the experiments with that obtained from the computer model, some conclusions can be drawn about radiation transfer in ice.

4.2 Experimental Apparatus

4.2.1 Temperature Controlled Chamber and Ice Calorimeter

To determine the amounts of incident energy absorbed and transmitted, an ice sample is placed in a temperature controlled chamber (Figure 6 and Plate 2). This chamber is

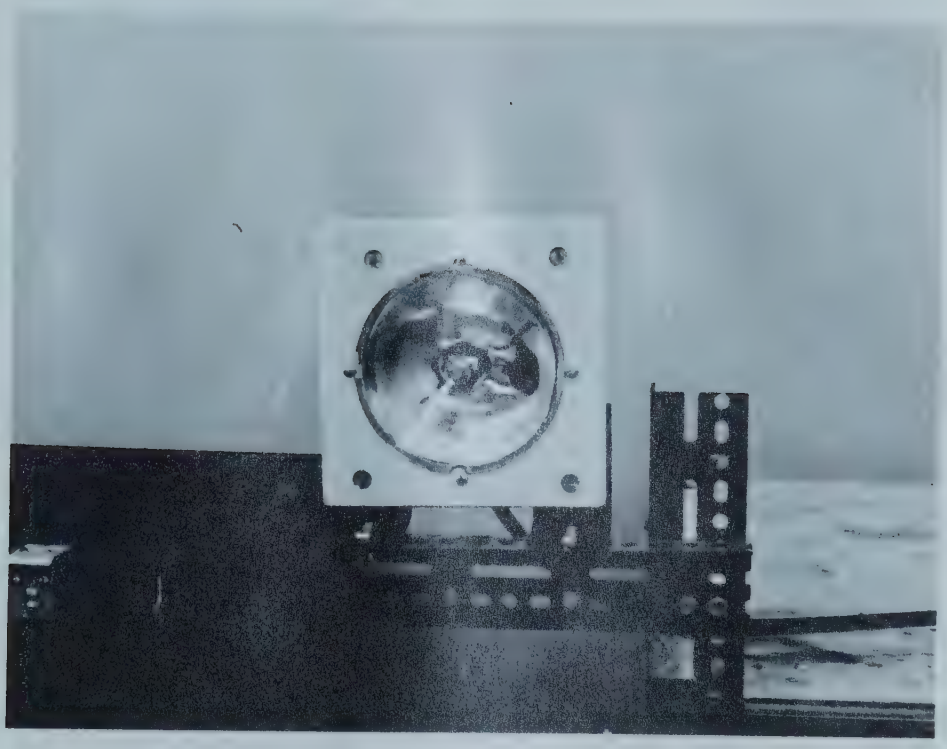

Plate 1 Tungsten Lamp

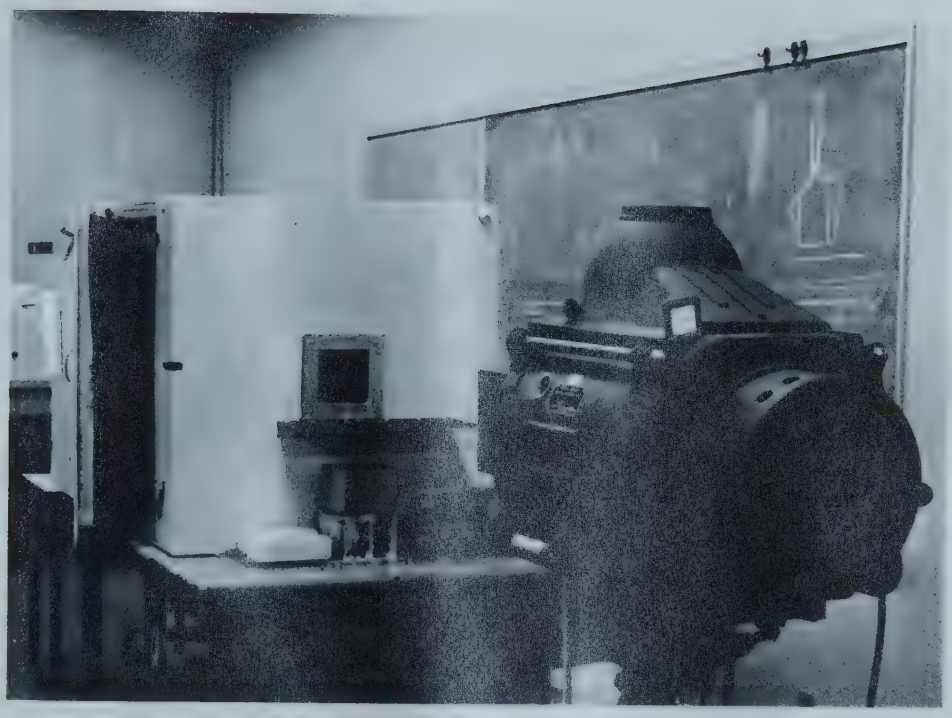

Plate 2 Solar Simulator and Temperature Controlled Chamber

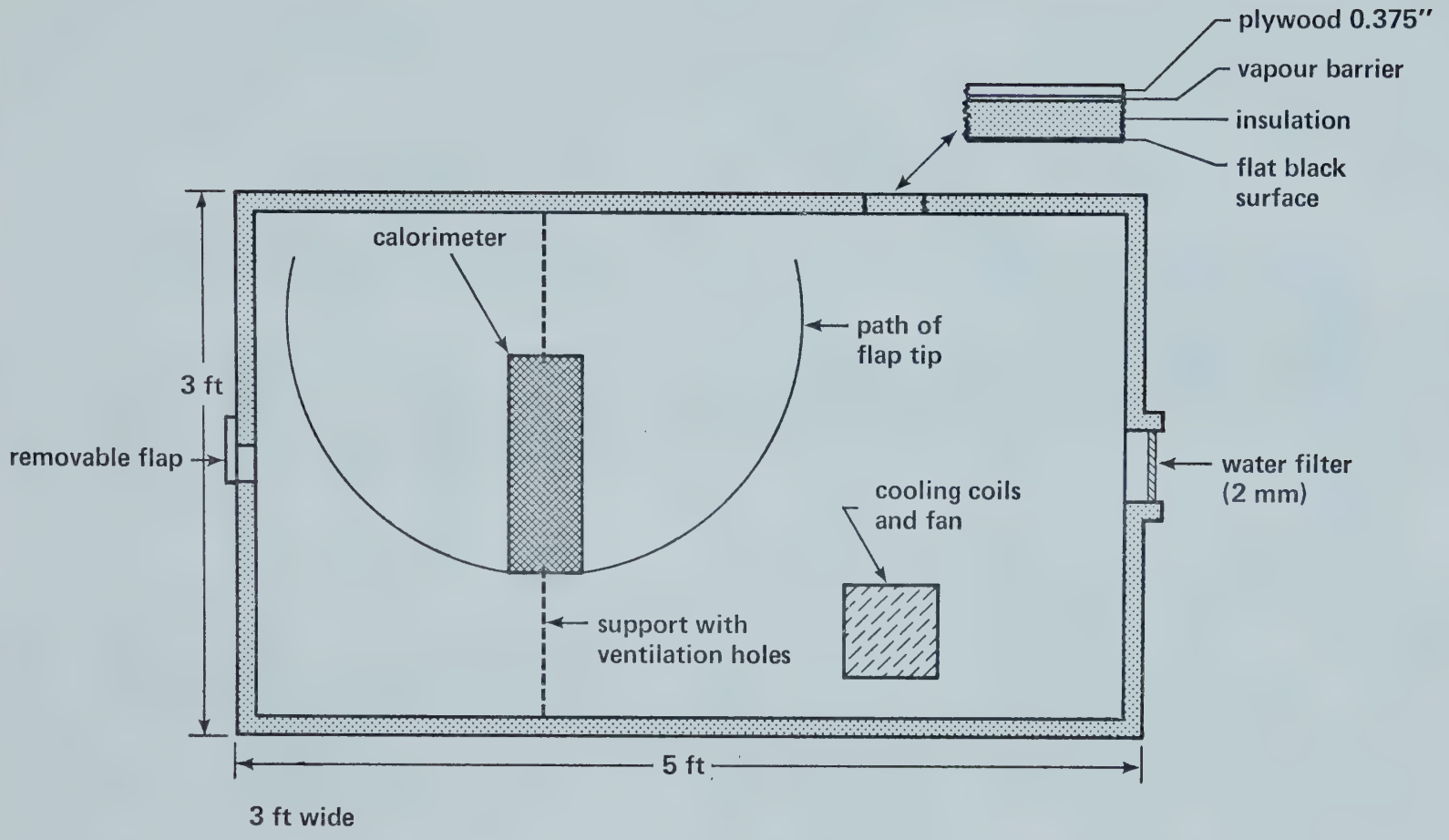

Figure 6. Temperature Controlled Chamber Schematic

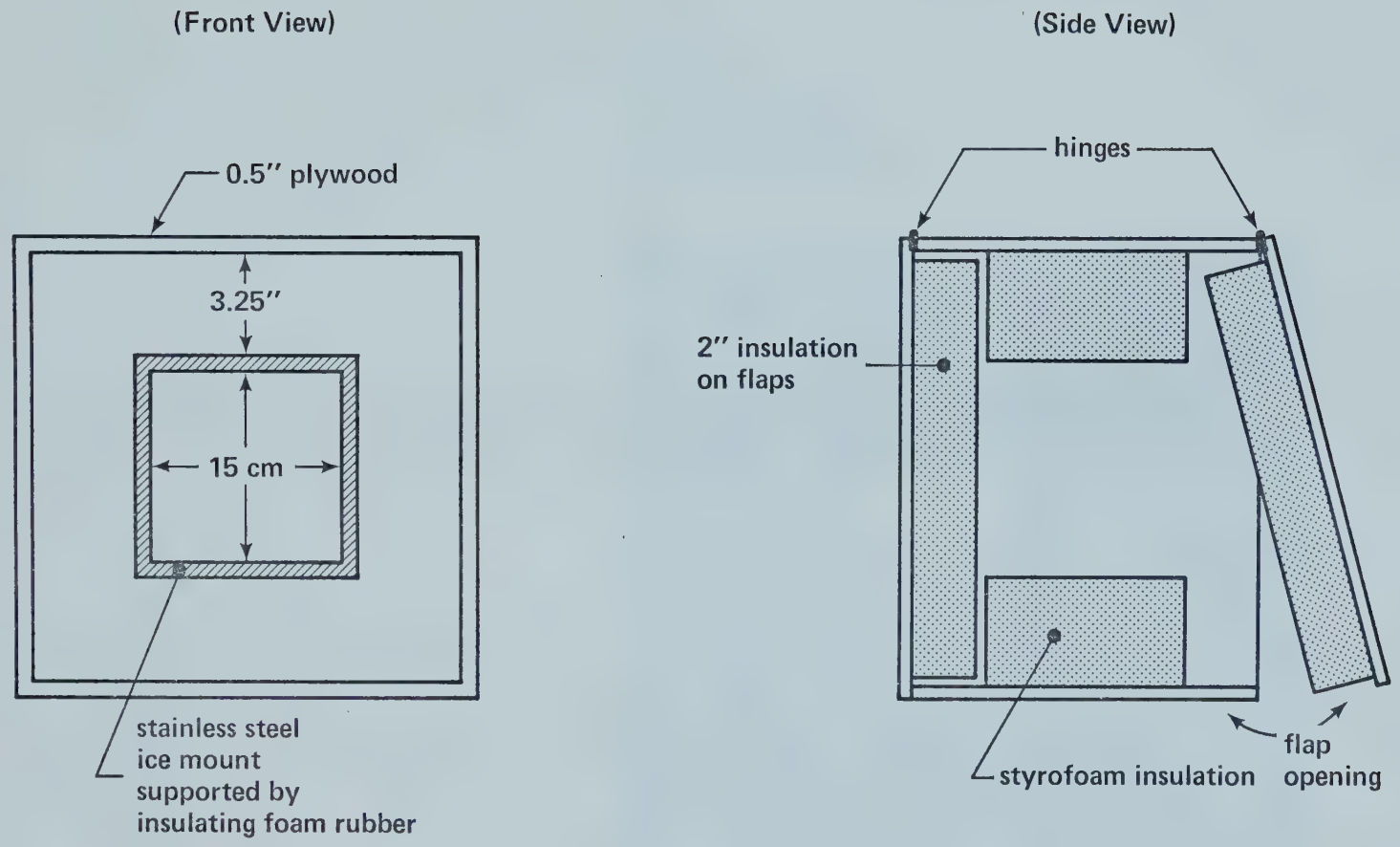

Figure 7. Ice Calorimeter

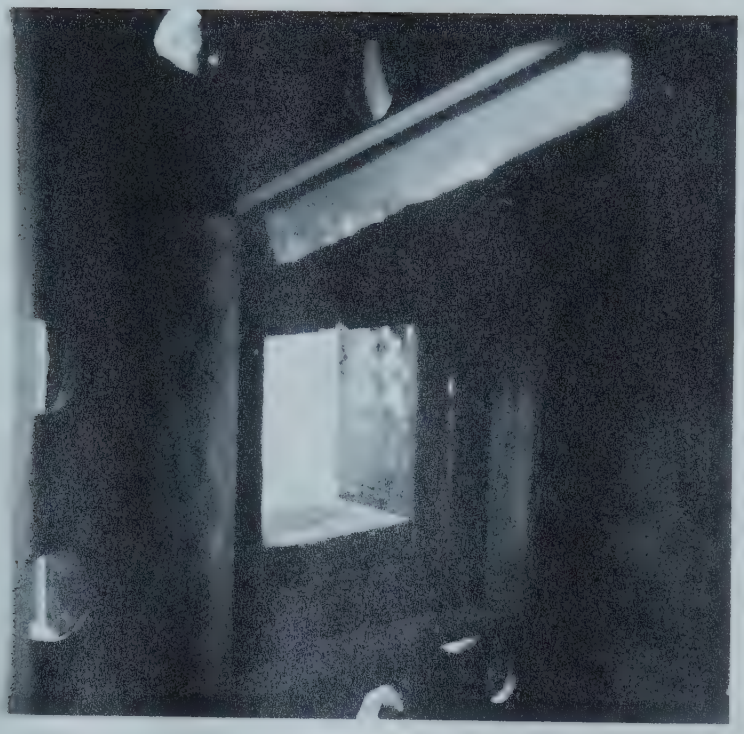

Plate 3 Calorimeter

maintained in the temperature range from -8°C to 0°C for the various absorption and transmission measurements. The ice sample has embedded in it three thermocouples which are frozen into the sample. Located within the chamber is an ice calorimeter (Figure 7 and Plate 3) into which the ice sample is placed. Surrounding the sides of the ice sample is a metal reflecting surface. Its purpose is to simulate, as far as the incident energy is concerned, a one-dimensional ice sheet. To allow the incident energy to strike the ice sample and then measure the portion of energy transmitted a flap is located on either end of the calorimeter. Two openings are also provided on either end of the temperature controlled chamber. Located on the front of the chamber is a two millimeter water filter (Figure 8). Its purpose is to eliminate the longer wavelengths contained within the incident energy spectra. The other end of the chamber is covered by a flap. By removing the flap, a thermal radiometer can be periodically exposed to the transmitted radiation.

4.2.2 Distribution of Scattered Radiation

The second experimental apparatus was employed to measure the distribution of scattered radiation from an ice sheet of approximately one centimeter in thickness. Basically it consists of a monocromatic beam of light (0.63 μ) produced with a laser and directed toward the ice sheet through a series of lenses. A more complete descrip-

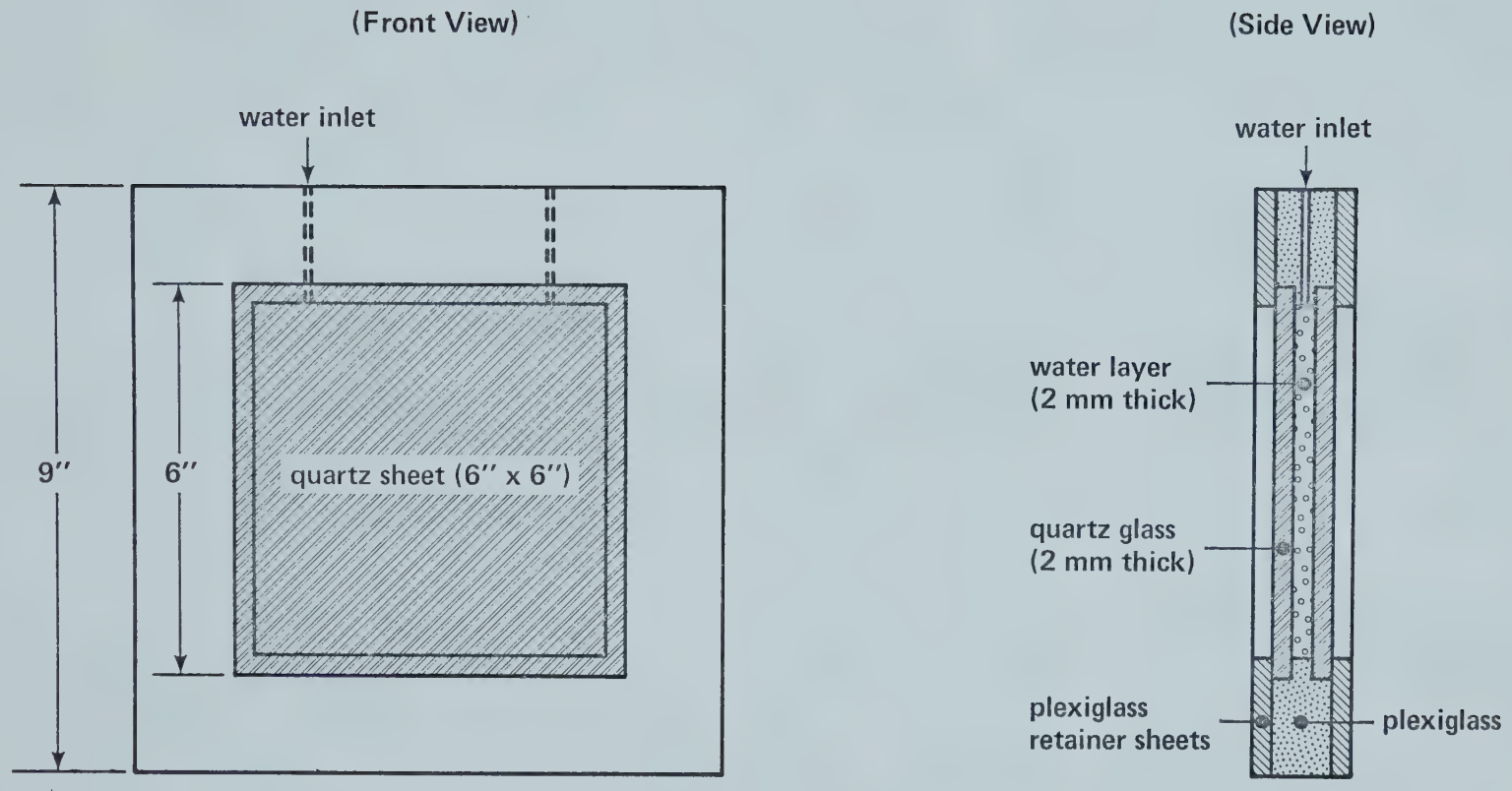

Figure 8. Water Filter

tion of the laser used as well as other instrumentation employed in the experiments is presented in Appendix D. Supporting the ice is a mount to which a quantum radiometer has been attached. The radiometer is attached in such a way that it is able to rotate through 60 degrees on either side of the laser beam (Plate 4). Using the apparatus, data was collected from which the angular distribution of scattered light was subsequently determined.

4.2.3 Instrumentation - Thermocouples and Radiometers

The copper constantan thermocouples placed in the ice sample are surrounded by a stainless steel shield (0.083 centimeters in outside diameter) and calibrated to within 0.05°C using a platinum resistance thermometer traceable to the National Bureau of Standards. These thermocouples are held in a plexiglass mount which is frozen into the chosen ice sample. This procedure allows the thermocouples to be embedded in the ice at 0.8 centimeter (thermocouple #1), 6.5 centimeters (#2) and 11.2 centimeters (#3) in relation to the upper surface. Figure 9 illustrates how the thermocouples are wired together to obtain the necessary temperature reading. These readings were recorded on a Hewlett Packard strip chart recorder.

As stated earlier two radiometers were employed to measure radiation intensities. To measure the intensity of the incident beam and the transmitted energy a Thermal Radiometer was used. This particular radiometer had a flat

Plate 4 Laser Scattering Apparatus

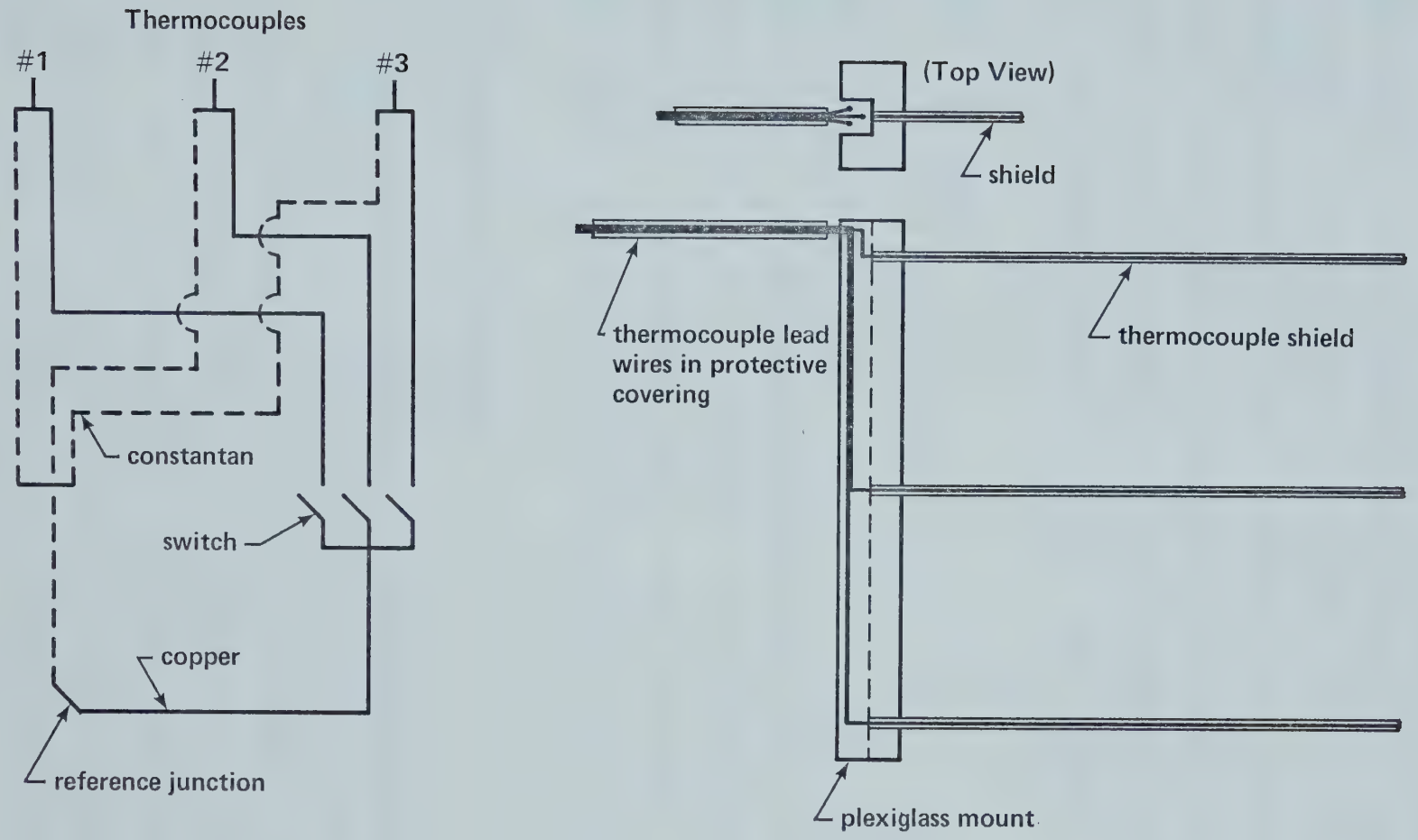

Figure 9. Thermocouple Wiring Diagram and Ice Mount

response for a range of wavelengths from 0.25 microns to 15.0 microns. To calibrate the radiometer a blackbody source was utilized (Figure 10 to Figure 11). For the measurement of the scattered radiation distributions a Quantum Radiometer was used. Although this radiometer does not have a flat response similar to the other probe, only one wavelength is involved in the measurements, therefore, no corrections are required to the probe's output.

4.2.4 Ice Mould

To produce uniformly sized ice samples, a plexiglass mould 15 centimeters square and 12 centimeters deep was constructed. On the bottom provision was made to attach a copper plate cooled by a chilled water-alcohol mixture (Figure 12). Depending on the desired ice sample, a plexiglass cover could also be attached on the top of the mould.

4.3 Experimental Procedure

4.3.1 Absorption, Transmission and Reflection Measurements

The experimental measurements of the absorbed, transmitted and reflected portions of the collimated incident energy were obtained for three ice samples and two radiation sources. The two sources used were a 650 watt tungsten-halogen projector lamp and a Metro-Lite solar simulator. Radiation intensities for the two sources with and without the water filter are compared to those of a blackbody

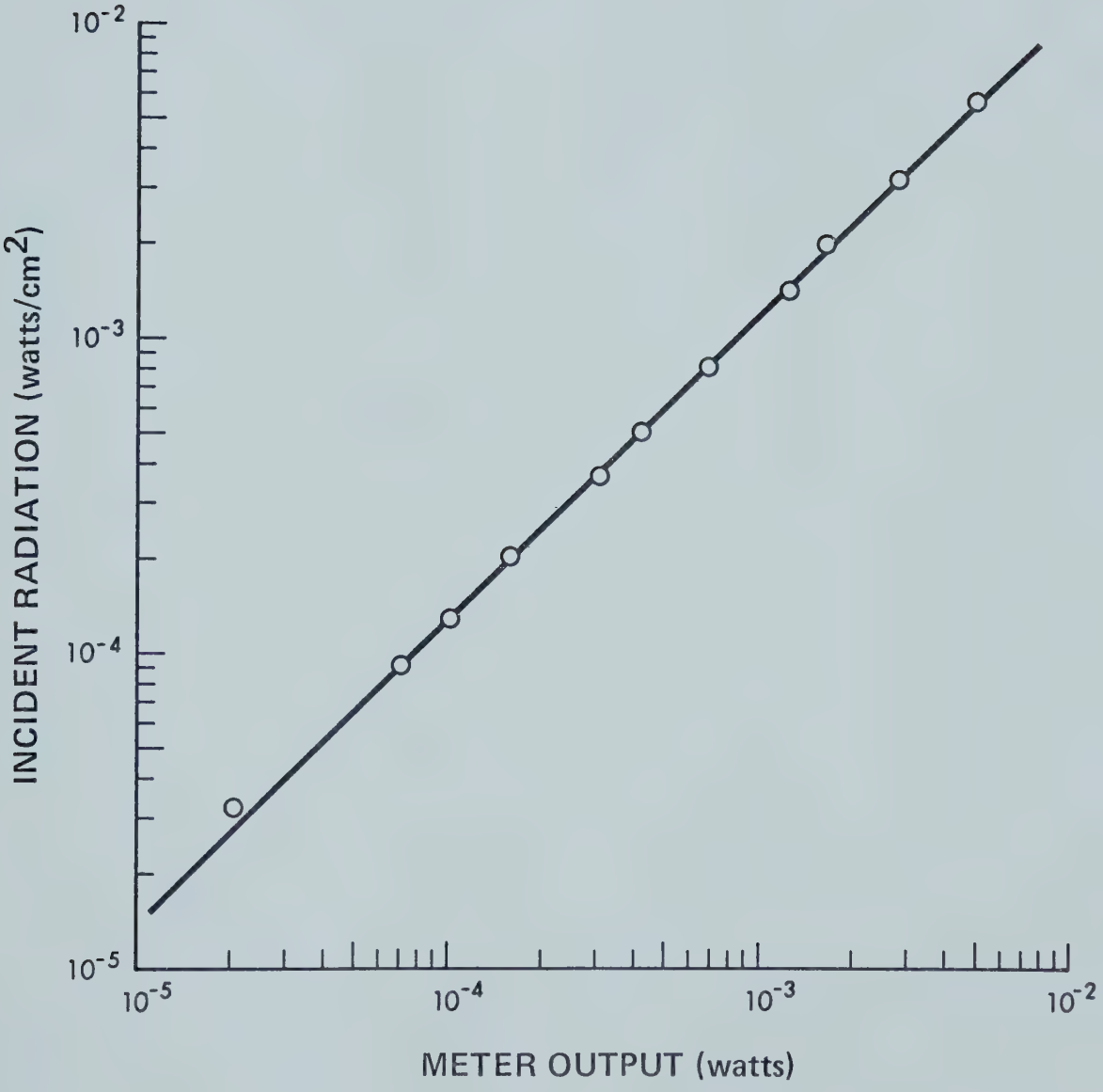

Figure 10. Calibration Curve Cintra Model 202

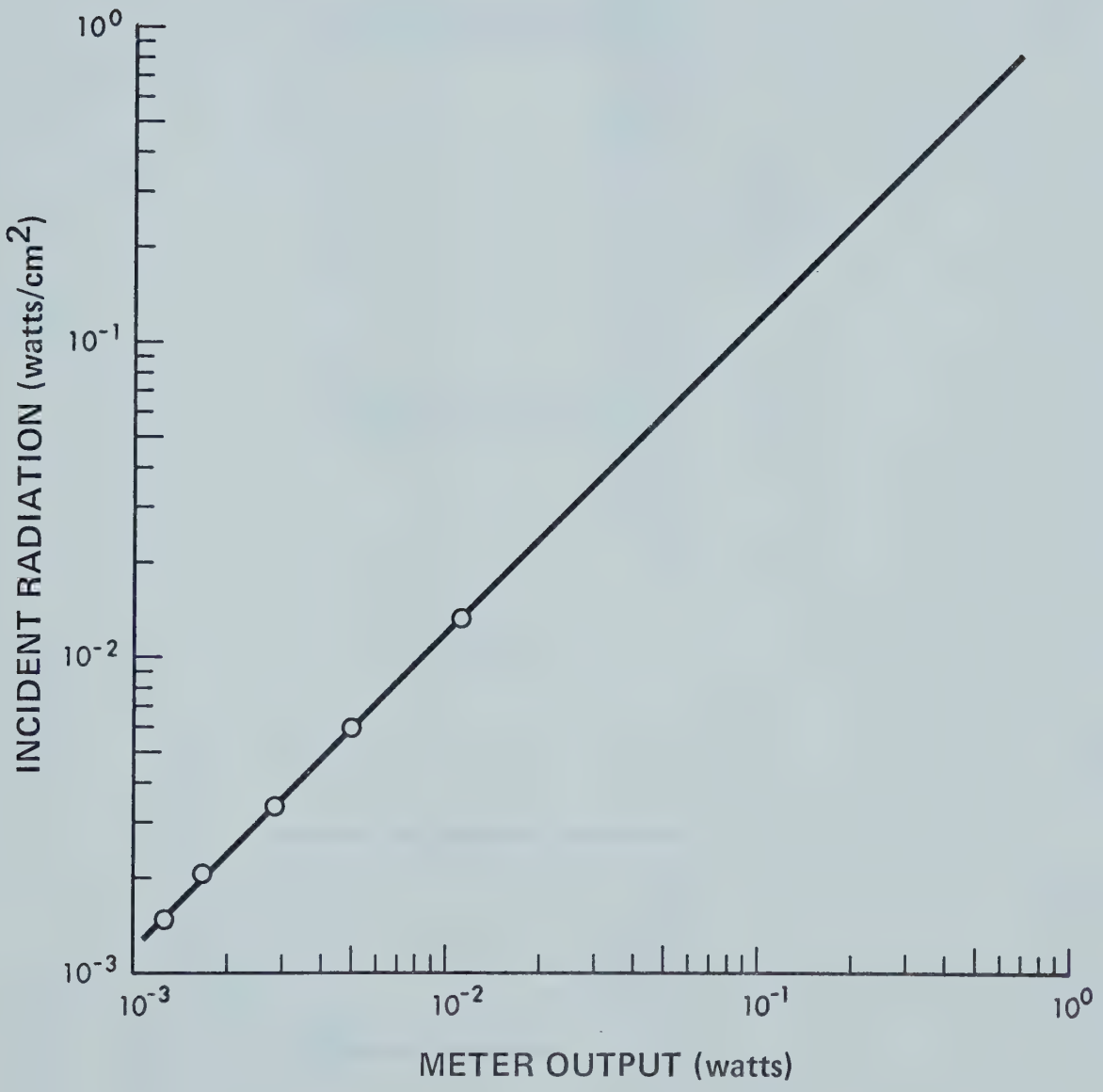

Figure 11. Extrapolated Calibration Curve

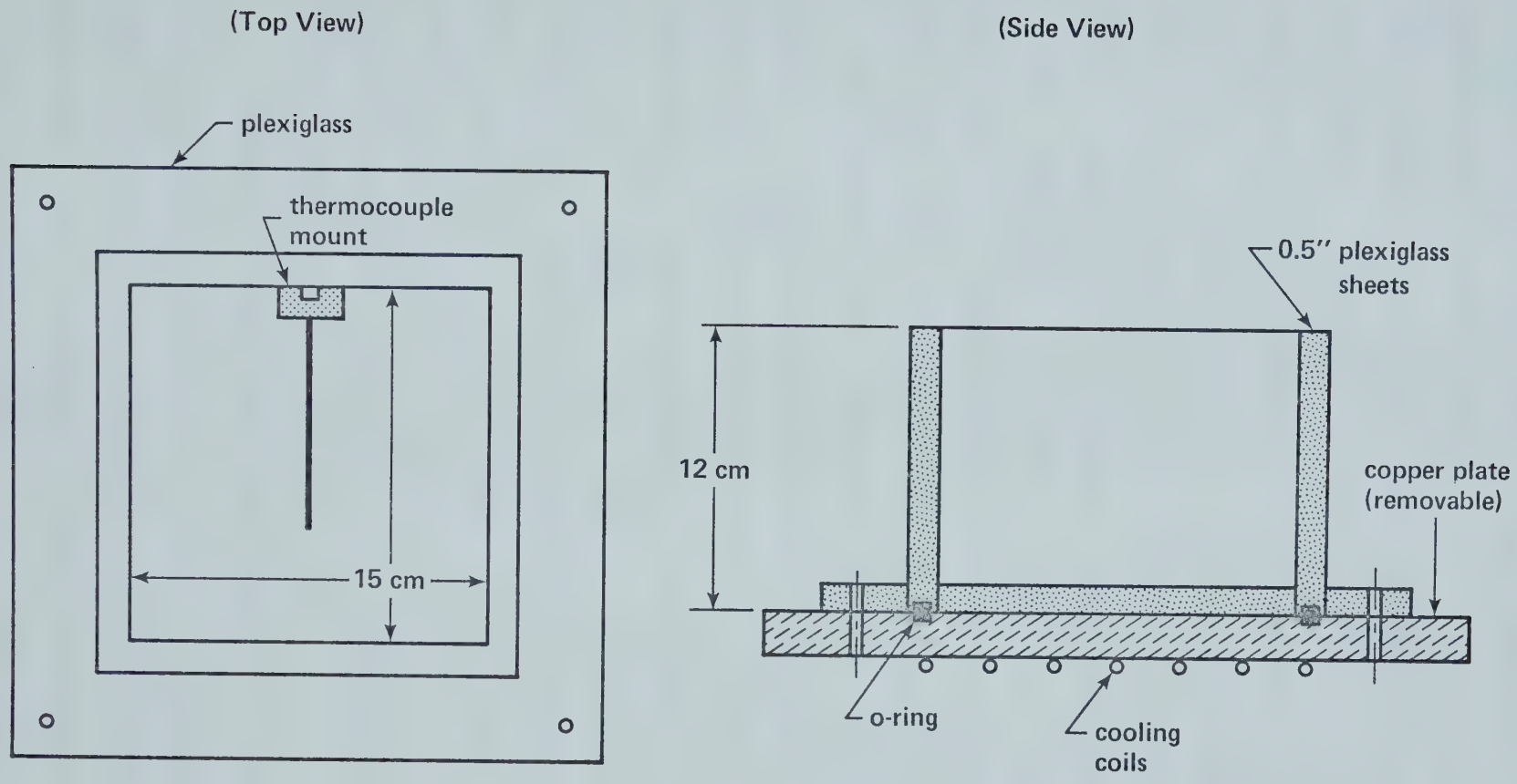

Figure 12. Ice Mould

(Figure 13 to Figure 16). These intensities and source temperatures having been obtained from Gilpin (16) are found to be comparable to those from an equivalent blackbody source. Before a given ice sample is exposed to the radiation, it is allowed to reach an equilibrium temperature with its surroundings. The sample is then exposed to the radiation source. If the tungsten lamp is used the time of exposure is 10 minutes and if the solar simulator is used then exposure is for 30 minutes. The flaps on the calorimeter are then lowered and the gradient of temperature within the ice is allowed to disappear. In the case of the tungsten lamp the time required is approximately 60 minutes. Similarly for the solar simulator the time required is approximately 40 minutes. One problem encountered in the experiments is that heat is transferred from the ice sample to the chamber during the experiments. To determine the amount of this heat transfer several tests were conducted in which temperature changes within the ice were measured as a function of time when no incident radiation was applied. The tests were conducted with the flaps open and also with the flaps closed.

Using the heat loss rates (Figure 17 and Figure 18) plus the thermocouple error (0.05°C), estimates of total error were made for the absorption measurement. The error produced by the thermocouples results in an uncertainty in the absorption measurements. However, that error produced by heat transfer between the ice sample and the chamber can

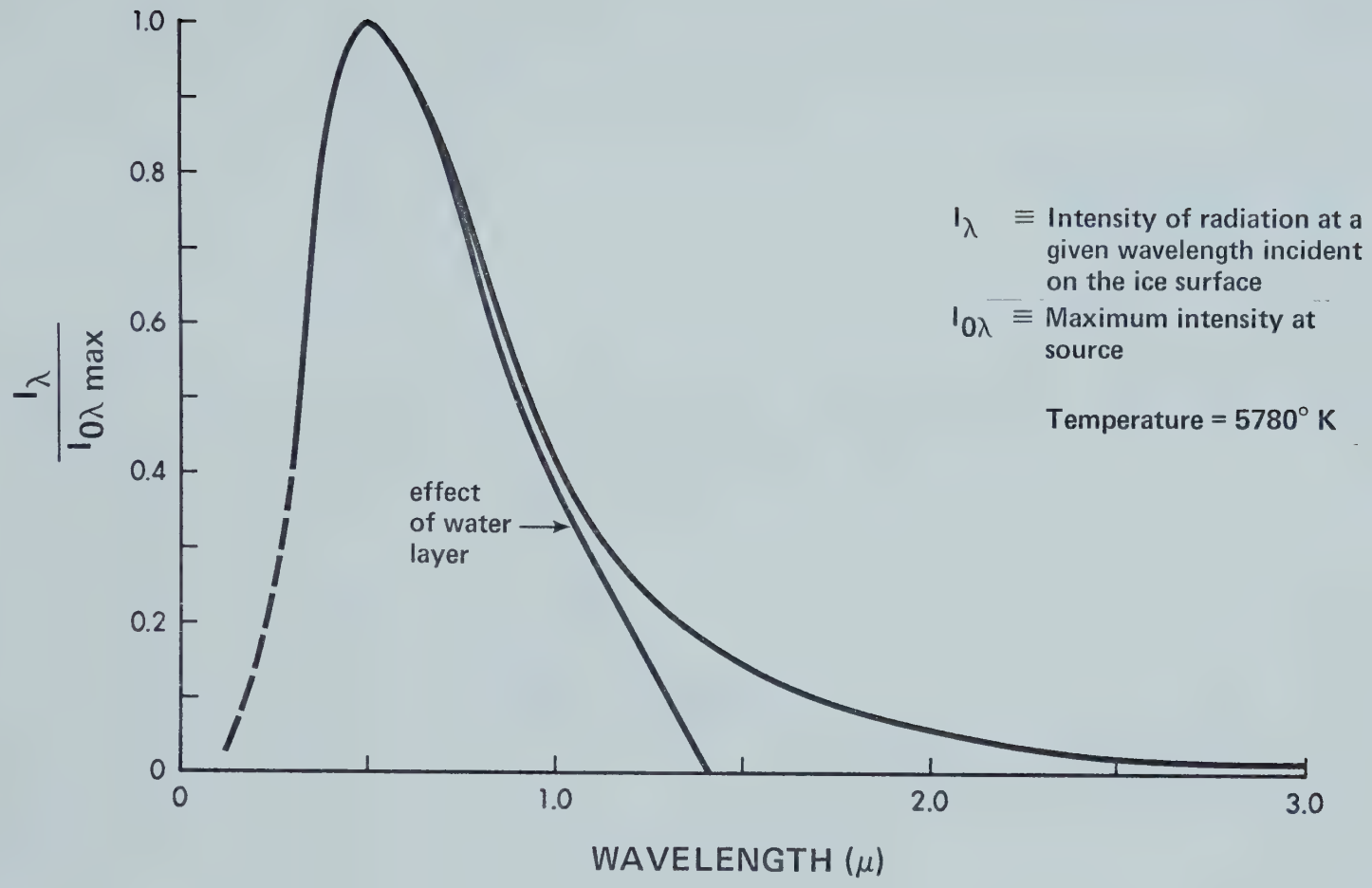

Figure 13. Blackbody Source with 2 mm Water Filter

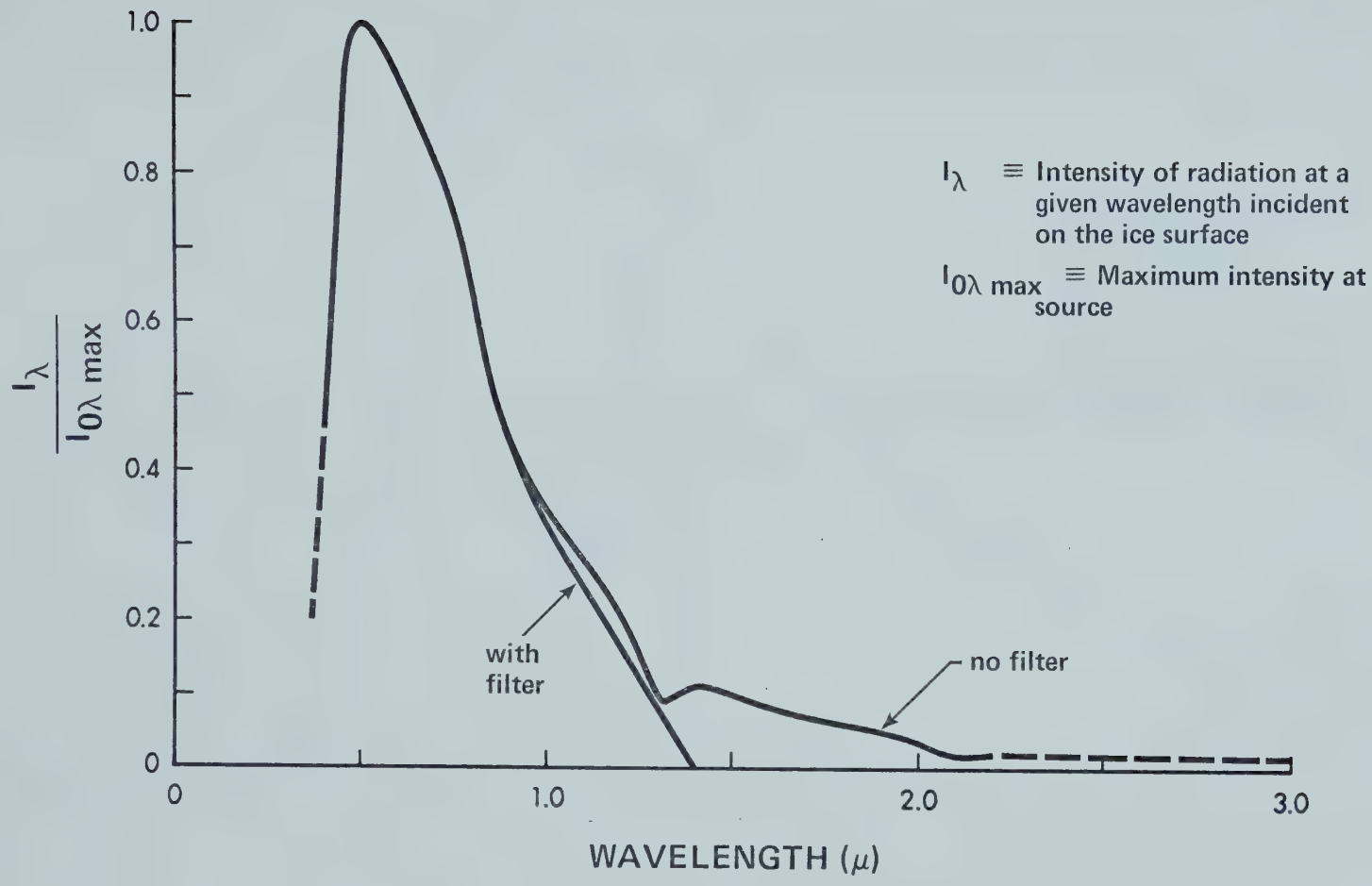

Figure 14. Metro-Lite Solar Simulator Output

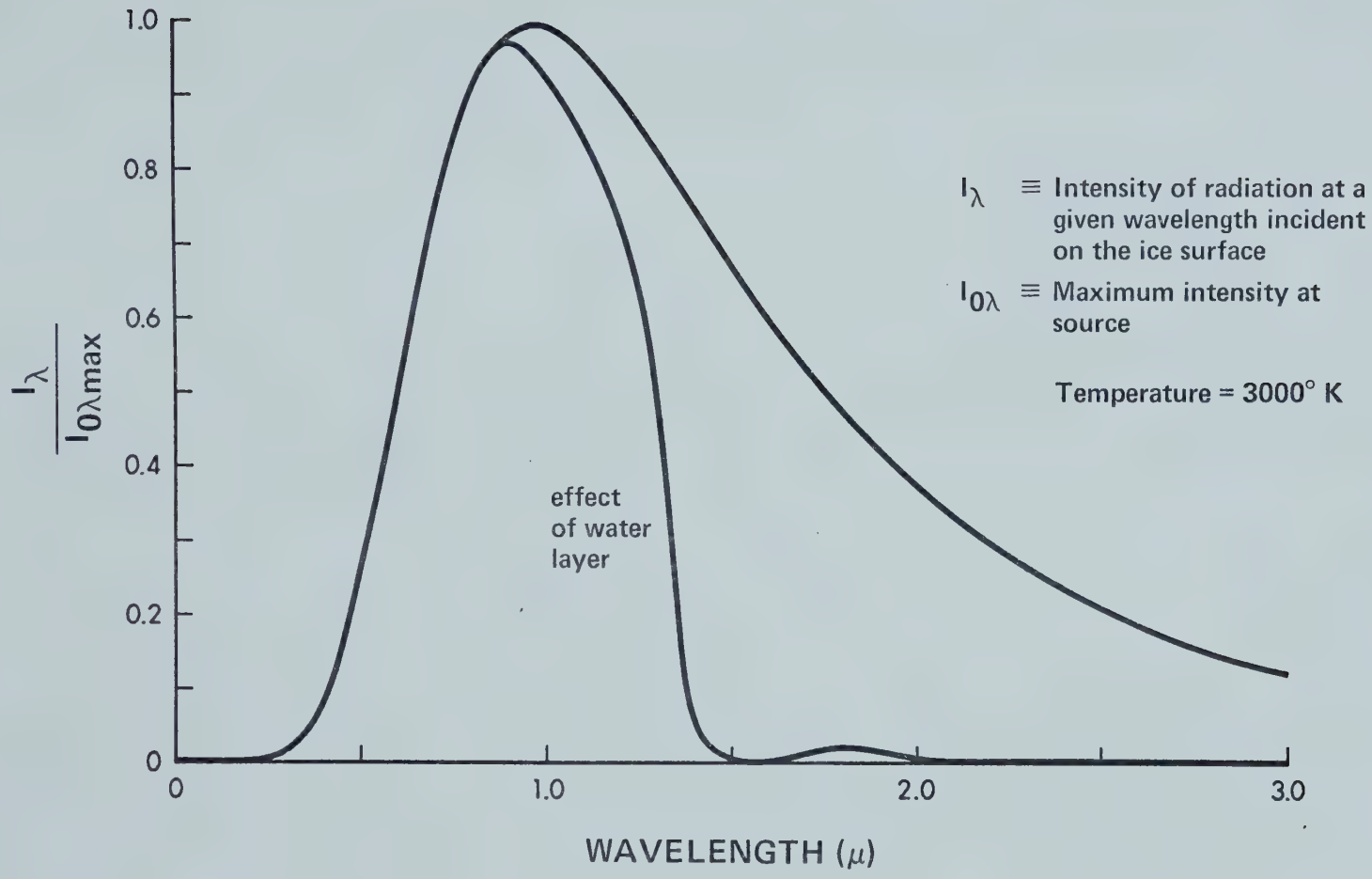

Figure 15. Blackbody Source with 2 mm Water Filter

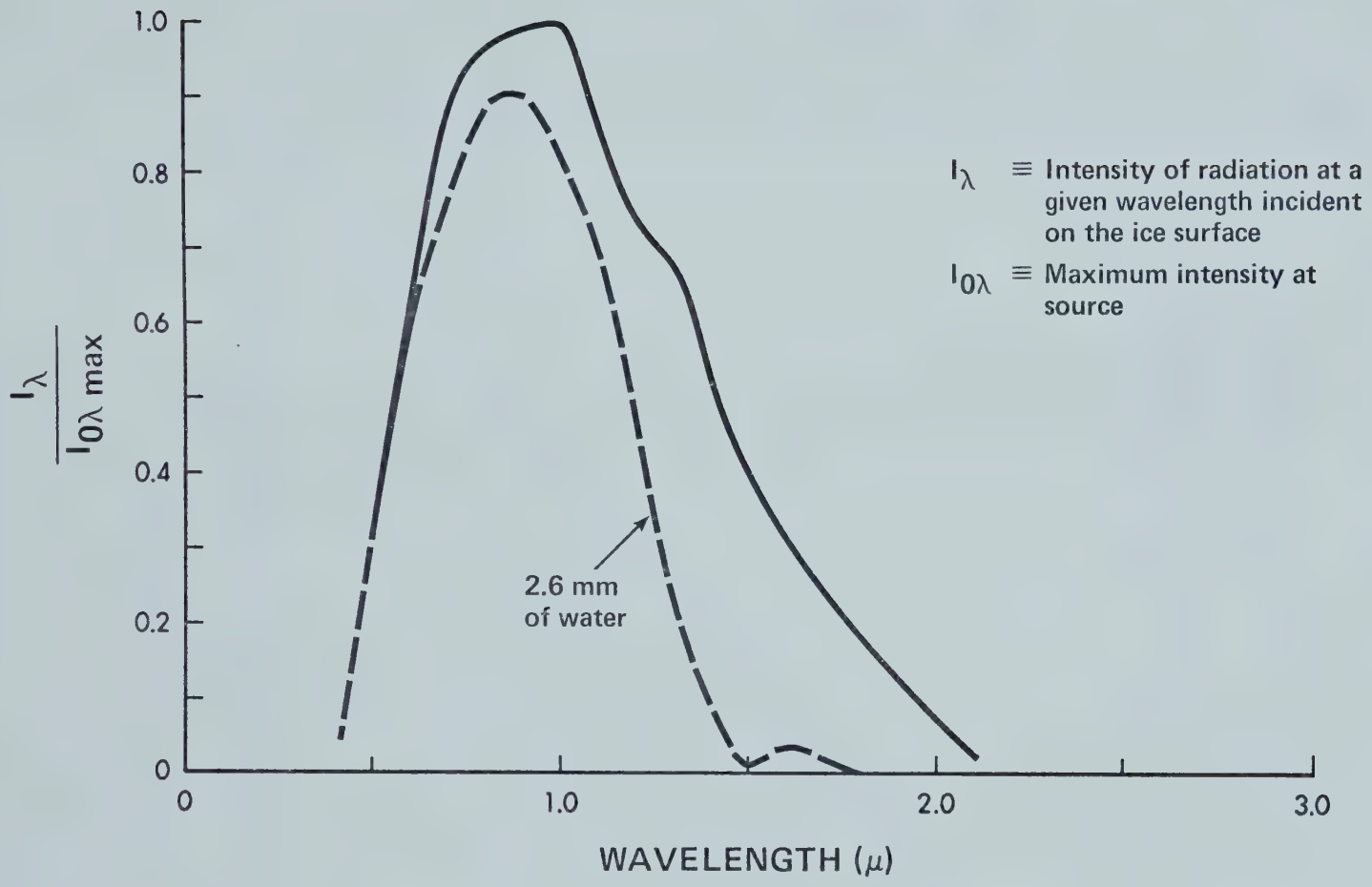

Figure 16. Tungsten Lamp Output

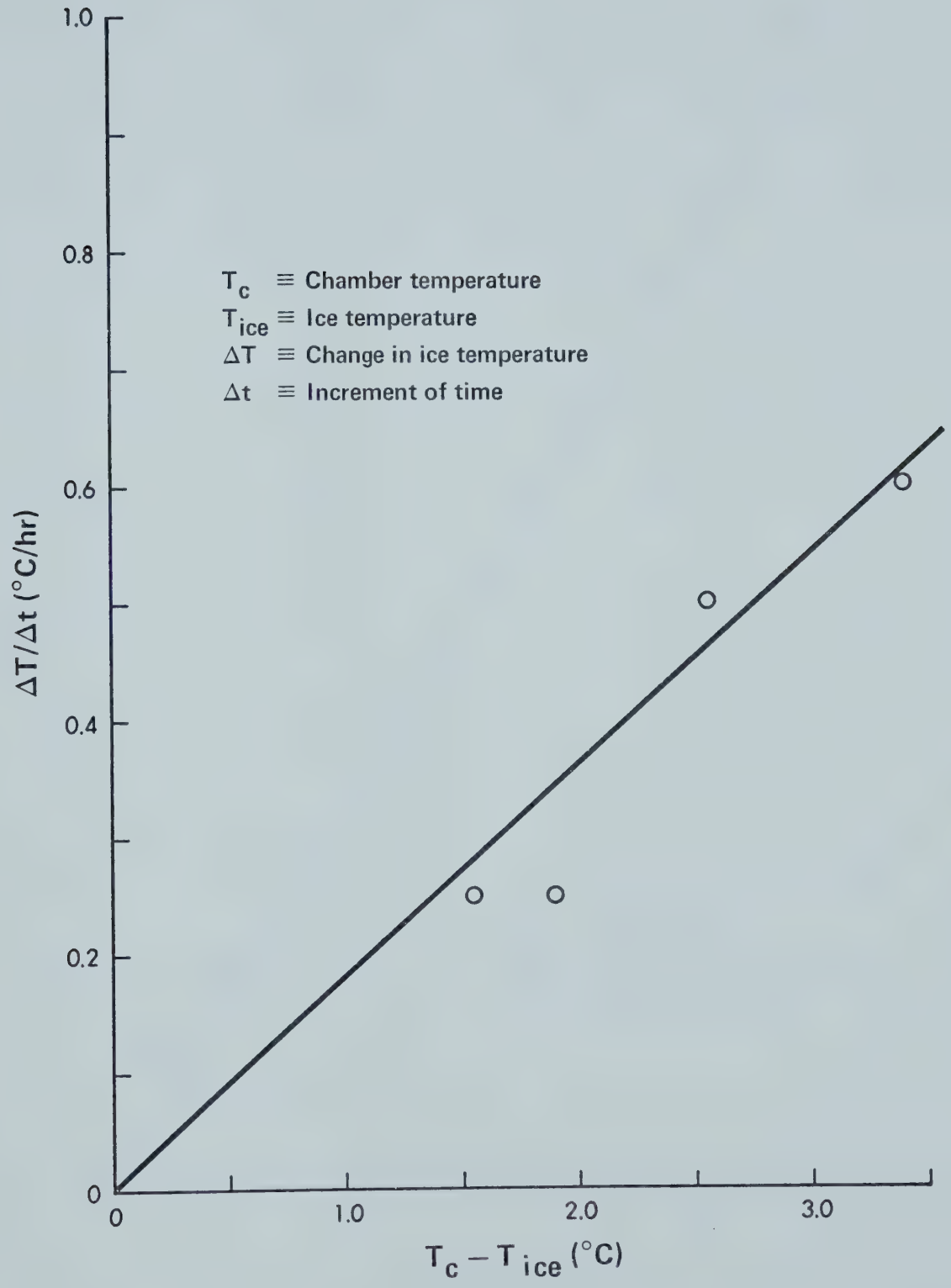

Figure 17. Heat Loss Flaps Closed

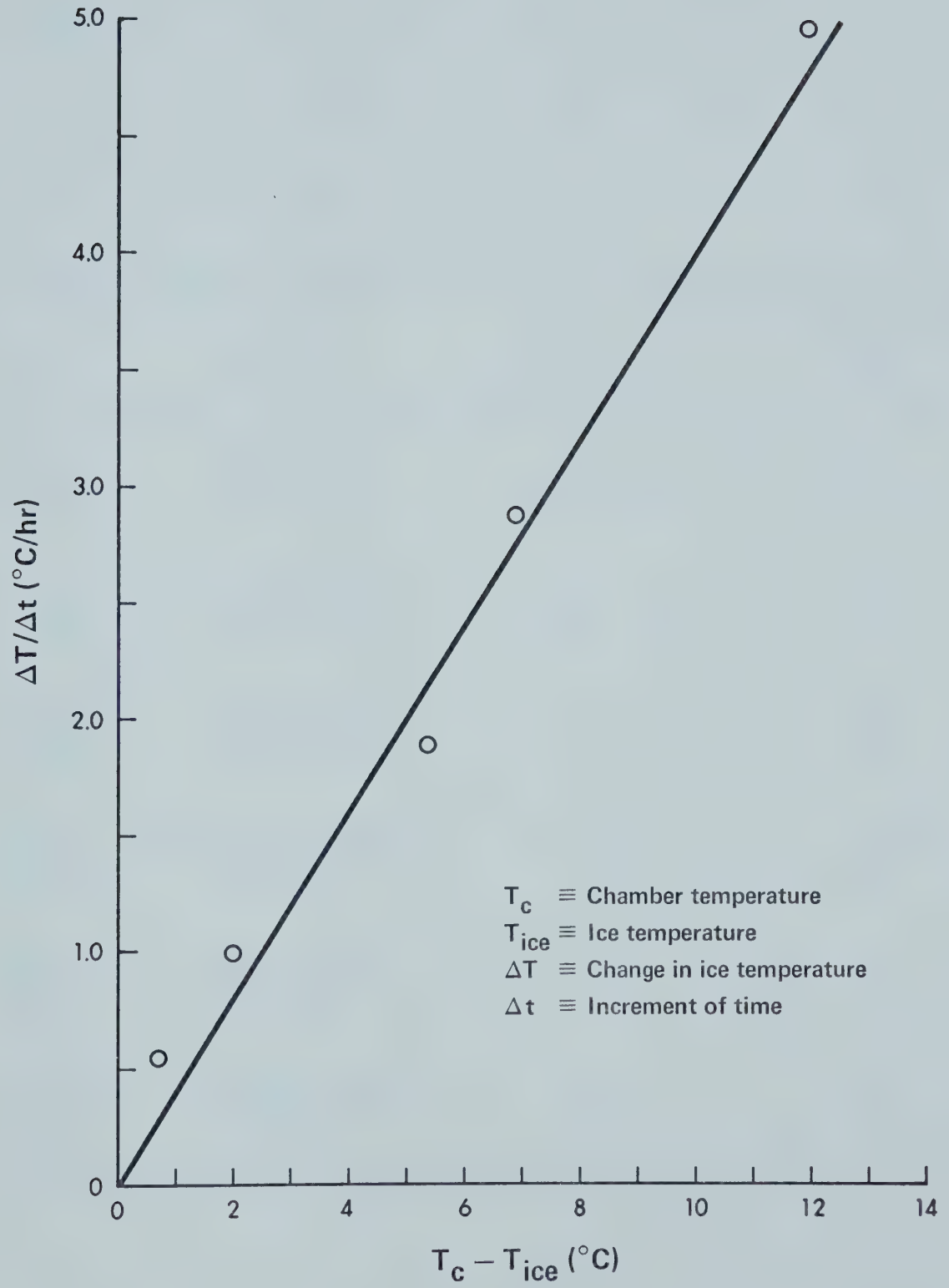

Figure 18. Heat Loss Flaps Open

TABLE I

LIST OF EXPERIMENTS

Test	Type of Source	Scattering (1/cm)	Application Time (min)
#1 through #3	Metro-Lite (5780°K)	0.0 (clear ice)	30.0
#4 through #6	Tungsten Lamp (3000°K)	0.0 (clear ice)	10.0
#7 through #9	Metro-Lite (5780°K)	2.15	30.0
#10 through #12	Tungsten Lamp (3000°K)	2.15	10.0
#13 through #15	Metro-Lite (5780°K)	1.90	30.0
#16 through #18	Tungsten Lamp (3000°K)	1.90	10.0

be approximately corrected for. Utilizing the average chamber and ice temperatures measured during each test, the heat transfer is estimated from Figures 17 and 18. These heat transfer rates are calculated separately for the flaps open and the flaps closed. The results are then used to estimate the apparent increase or decrease in the absorption measurements. The reliability of the absorption measurements was then ascertained by making three runs of any given ice sample and radiation source (Figure 19 and Figure 20). Each curve presented being the mean value of three individual runs.

During each run with the various ice samples, readings from each of the thermocouples are taken every 5 minutes when the flaps are open and every 10 minutes when the flaps are closed. The radiometer was used at the same time to measure the transmitted radiation. However, except for a clear ice sample (no scatter), this particular measurement was only taken after the final run of any given ice sample. This procedure was required since the thermal radiometer did not function when placed within the temperature controlled chamber if it was running. The reason for this change was that when the transmitted radiation was totally diffuse the measurements had to be taken as close to the ice sample as possible. Since the chamber was shut down for the transmission measurements, it was possible to take several measurements of the reflected energy before one of the ice samples deteriorated. By converting the

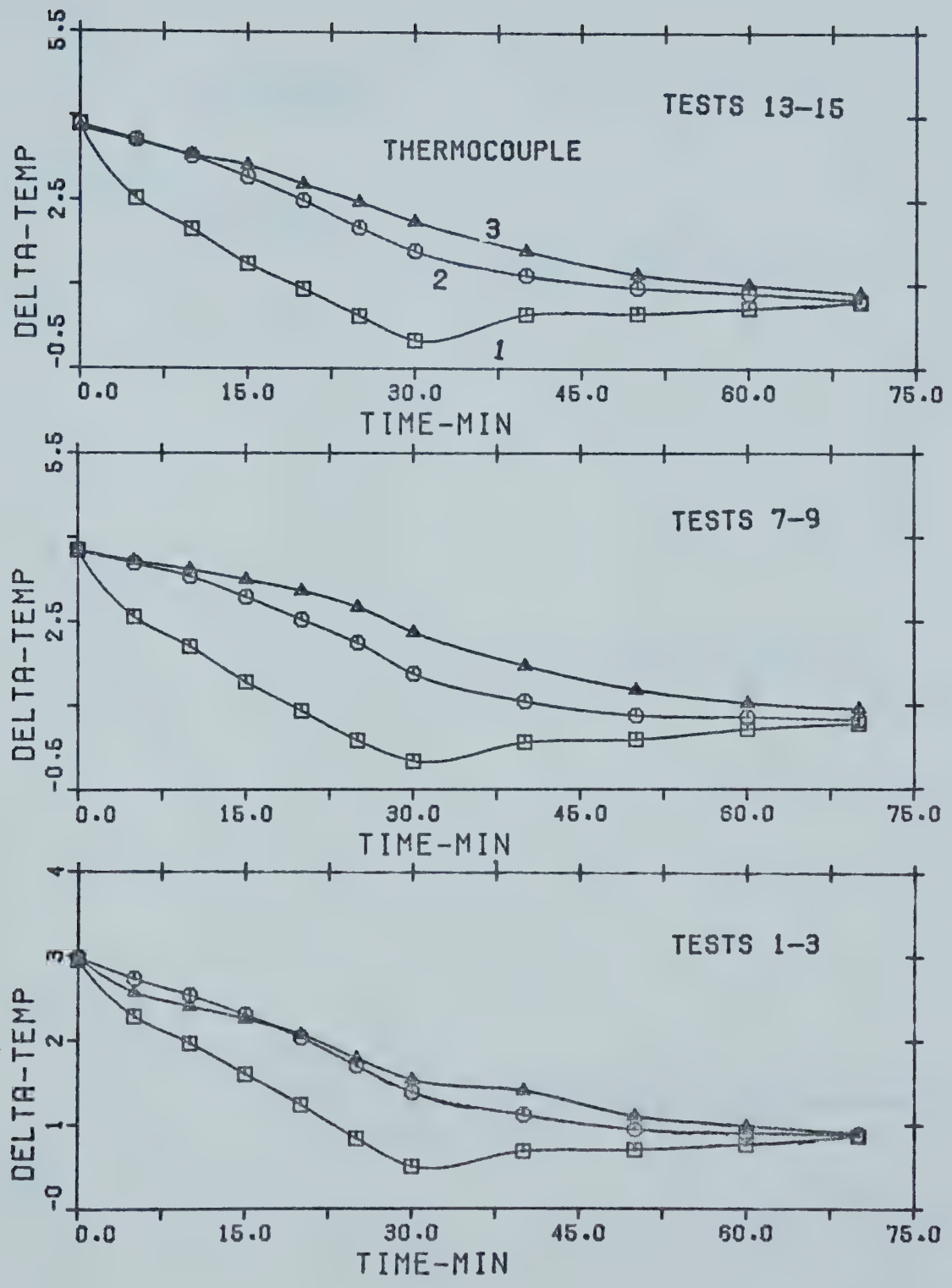
TESTS 13-15
THERMOCOUPLE
3
2
1
DELTA-TEMP
TIME-MIN
TESTS 7-9
DELTA-TEMP
TIME-MIN
TESTS 1-3
DELTA-TEMP
TIME-MIN
SUMMARY OF EXPERMENTAL RESULT

Figure 19.

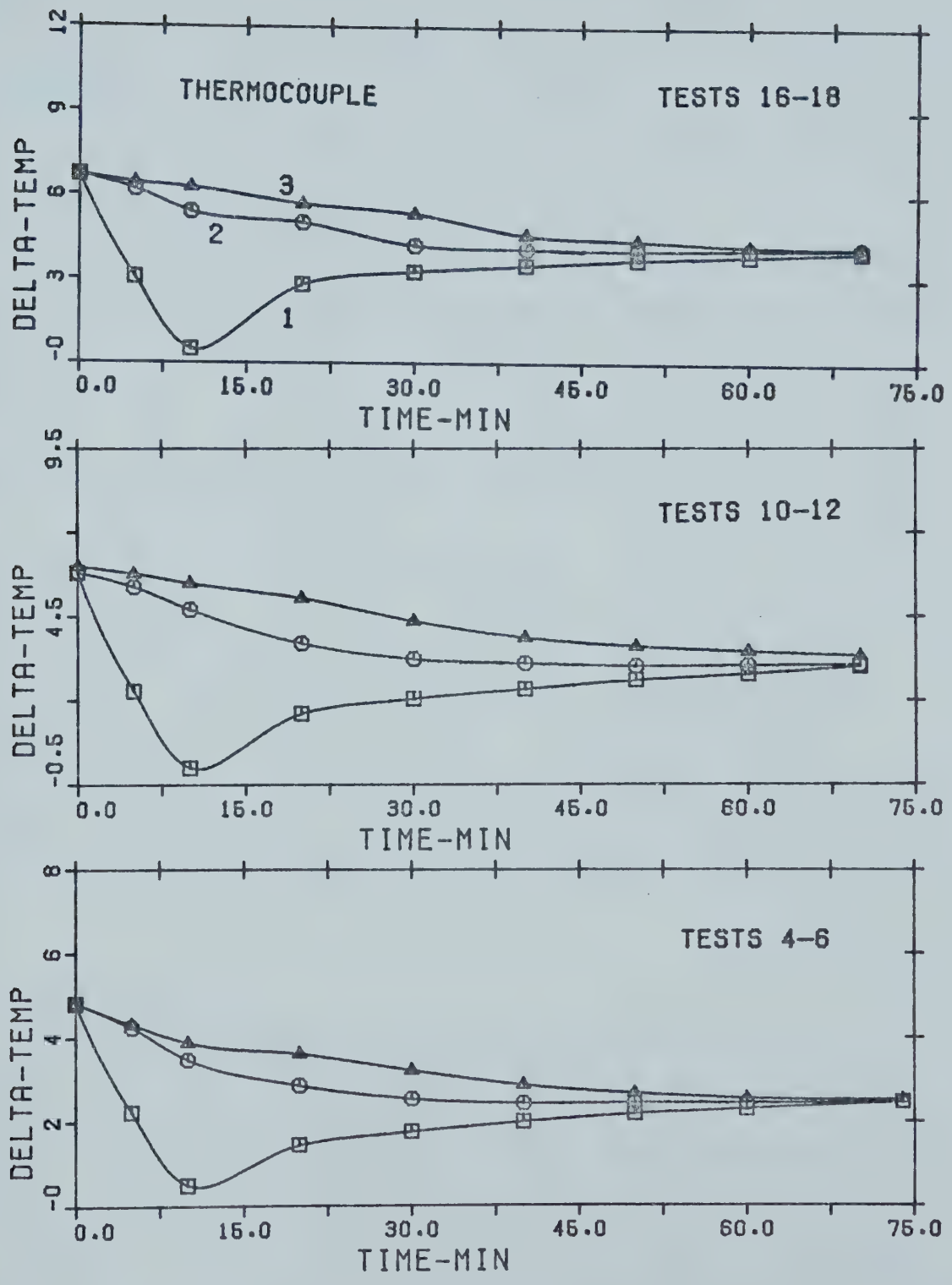

SUMMARY OF EXPERMENTAL RESULT

Figure 20.

raw data, the values of the absorbed, transmitted and reflected energies can be obtained in percent of the incident energy.

4.3.2 Scattering Distributions

By mounting a thin ice sheet in the laser apparatus, measurements of the energy distributions occurring due to scattering were taken with the quantum radiometer. The ice sheets were cut from the ice samples used in the first set of experiments. Each ice sheet had both its surfaces made parallel by placing the sheet on a heated copper plate. Total energies striking the radiometer's detector surface are recorded for angles measured from the direction of propagation. The angles are in 10 degree intervals from 60 degrees to 300 degrees and from 120 degrees to 240 degrees. Using the solid angle subtended by the detector, the intensities of scattered radiation can be calculated.

4.3.3 Ice Samples

In order to obtain the required ice samples with varying scattering characteristics, the dissolved gases present in water were entrapped during ice formation. By varying the rate of freezing or the initial gas content of the water, a desired ice sample is produced. The above method is used to produce three ice samples. Of the samples, one was clear and two contained gas pockets acting as scattering centers. In one scattering sample the gas cavi-

ties were a order of magnitude larger than the other. This particular sample was produced by rapid cooling of water containing dissolved carbon dioxide giving the ice sample a white appearance (Tests #7 to #12). As for the remaining scattering sample, it was produced by rapid freezing of heated tap water obtained from the City's water supply. This ice sample appeared to be gray in color similar to river ice (Tests #13 to #18).

4.4 Conversion of Raw Data

4.4.1 Calculation of Absorbed Energy

Let T_{rise} be the measured rise in ice temperature from the beginning to end of each run. Therefore, the energy absorbed by the ice is $\varepsilon_{ICE} = m_I c_p T_{rise}$ where m_I is equal to the mass of ice and c_p is the specific heat. Some of the collimated energy that is absorbed by the ice is conducted into a stainless steel support surrounding the ice sample. Assuming the support is at the same temperature as the ice, the energy lost to it is $\varepsilon_L = 0.0554\ T_{rise} \times 10^3$ cal where c_p of the stainless steel is 0.1 cal/gm°C and the mass of metal used is 554 grams. The percent of energy absorbed can now be determined if the total collimated energy striking the ice surface is found. To do this, the ice surface receiving the energy was assumed to be 225 square centimeters. Therefore, the energy incident on the ice sample is $\varepsilon_i = 3.23 \times 10^3\ I_s t$ calories where I_s is the

measured intensity of radiation at the ice surface obtained by using the thermal radiometer. The fraction of incident then absorbed is approximately $\{\frac{m_I c_p + (0.06)10^3 T_{rise}}{(3.23)10^3 I_s t}\}$.

4.4.2 Transmitted Energy

Two types of transmitted radiation are measured. The clear ice sample, since there was no scattering involved, produced a collimated beam while the two scattering samples produced a totally diffuse beam. When the radiation striking the thermal radiometer is diffuse, only a portion of the radiation is detected by the radiometer. This proportion is found by considering the internal geometry of the radiometer's detector. For this particular thermal radiometer employed, the portion of energy detected is 1.94×10^{-2}. The fraction of collimated energy transmitted is found by comparing the radiometer measurements, corrected if the radiation is diffuse, with those taken for the intensity of the unattenuated collimated beam.

4.4.3 Scattering Intensities

The quantum radiometer measurements of scattered radiation indicate the amounts of energy intercepted by the detector. To convert these measurements to radiation intensities, the solid angle subtended by the radiometer must be found. Using the detector area plus the distance between the centre of the thin ice sheet and the detector,

the solid angle was found to be 0.0676 steradians. The scattered radiation intensities are found by dividing the radiometer reading by the detector area and the solid angle. These radiation intensities are then normalized with respect to the incident energy striking the ice.

To determine the fraction of the collimated beam that is scattered, comparison between the energy incident on the detector when it was set at zero degrees with no ice sheet present and the output of the radiometer for the attenuated laser beam is made. The Bouger-Lambert law is then used to determine the scattering coefficient. By assuming absorption is small compared to scattering (true for 0.63 μ in ice), the law becomes $I = I_0 e^{-r_s x}$. Solving this equation gives the value of the scattering coefficient r_s.

4.5 Discussion of Results

The data obtained from the absorption and transmission experiments are presented in Tables I and II while those for the distribution of scattered radiation are presented in Figure 21 and Table III. From the experiments several observations can be drawn about radiation penetration in a 12 centimeter thick ice sample. The first of these involves the effects of scattering on absorption, transmission and reflection of the collimated incident radiation. Comparing the data obtained for clear ice to that for the remaining ice samples, shows an increase absorption, a decrease in transmission and for the limited data available an increase

TABLE II

EXPERIMENTAL RESULTS

Test	Absorption (α) %	Error (%) in Absorption (α) from Thermo-couple	Error (%) in Absorption (α) from Heat Transfer	Transmission (τ) %
#1	58.3	--	0.0	57.4
#2	44.3	--	4.66	53.2
#3	39.6	--	12.3	55.3
	$\bar{\alpha} \simeq 47.4$ $\sigma \simeq 9.7$	1.16	5.7	$\bar{\tau} \simeq 55.3$ $\sigma \simeq 2.1$
#4	69.3	--	7.88	39.2
#5	72.4	--	3.94	42.1
#6	78.7	--	2.90	47.7
	$\bar{\alpha} \simeq 71.7$ $\sigma \simeq 7.4$	1.58	4.9	$\bar{\tau} \simeq 42.3$ $\sigma \simeq 3.3$
#7	69.2	--	5.64	--
#8	64.9	--	5.86	--
#9	56.4	--	2.45	--
	$\bar{\alpha} \simeq 63.5$ $\sigma \simeq 6.5$	1.06	4.6	9.30
#10	72.8	--	4.48	--
#11	82.6	--	2.10	--
#12	75.6	--	3.5	--
	$\bar{\alpha} \simeq 77.0$ $\sigma \simeq 5.0$	1.40	3.4	5.75
#13	64.8	--	6.50	--
#14	61.8	--	7.10	--
#15	57.8	--	1.02	--
	$\bar{\alpha} \simeq 61.5$ $\sigma \simeq 3.5$	1.64	4.9	14.6
#16	90.5	--	8.22	--
#17	77.3	--	12.8	--
#18	90.5	--	6.91	--
	$\bar{\alpha} \simeq 86.1$ $\sigma \simeq 7.6$	1.02	9.3	8.29

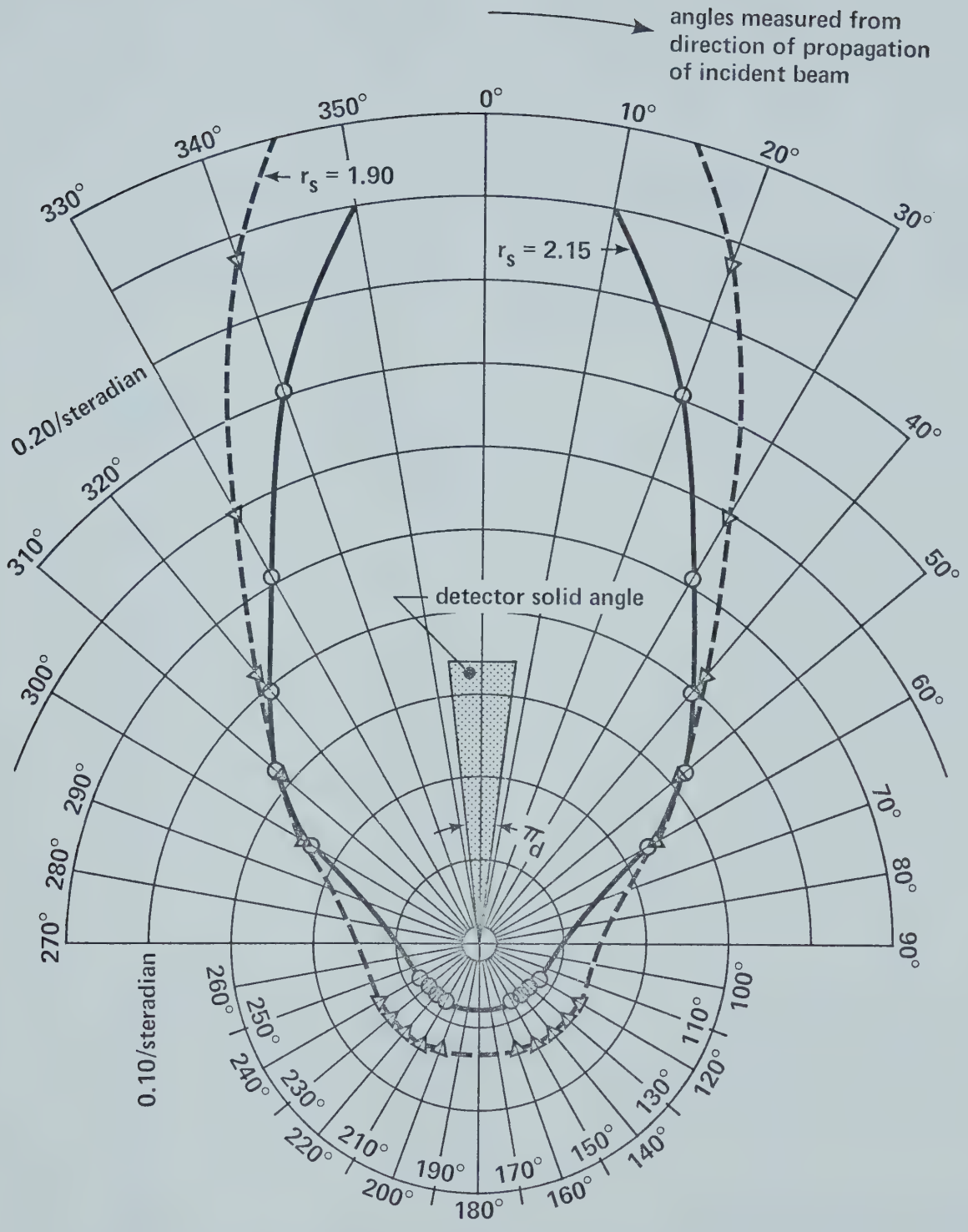

Normalized Scattering Distributions

Figure 21. Normalized Scattering Distributions

TABLE III

NORMALIZED SCATTERING DISTRIBUTIONS

Angle (Degrees)	Ice Sample r_s = 2.15/cm (1/Steredian)	Ice Sample r_s = 1.90/cm (1/Steredian)
0	1.750	2.170
10	0.475	0.629
20	0.178	0.219
30	0.131	0.149
40	0.100	0.106
50	0.082	0.079
60	0.060	0.061
.	.	.
.	.	.
.	.	.
120	0.019	0.033
130	0.020	0.036
140	0.020	0.036
150	0.020	0.036
160	--	0.036

in reflection. However, changes in absorption with increased scattering are less than those for the transmitted energy.

The estimates of experimental error for absorption measurements indicate that heat transfer from the chamber to the ice sample is significant. Since the average chamber temperatures were observed to be higher than the average ice temperatures, the heat transfer must cause an apparent increase in the absorption measurements. A more realistic value of the actual energy absorbed would, therefore, be obtained by subtracting the increase in absorption due to heat transfer from the absorption measurements based on the total temperature rise.

The final group of observations, about radiation penetrating in the ice sheet, are obtained from the scattering distributions. In general the radiation is scattered predominantly in the forward direction. When comparisons are then made between the forward and backward components of the scattered radiation, the scattered radiation distribution forward is dependent on the angle from the direction of propagation while the backward scattered radiation is isotropically distributed. The size of the scattering centers also has an effect on the scattering distributions with the smaller scattering centers producing a greater portion of backward scattered radiation. Since for the two scattering ice samples, the amount of radiation scattered from the collimated beam is the same, the reduction in size

of the scattering centers appears to reduce the fraction of energy scattered forward (i.e., n). Using the above observations comparisons can be made with those results generated by the computer model.

4.6 Experimental and Theoretical Results Comparison

The experimental data must now be compared with the theoretical computer model. Since the measurement of the angular distribution of scattered energy indicates a high forward scatter, the computer model with 90 percent forward scatter (n = 0.90) is used for these comparison purposes. In general, increased absorption is found with scattering (12 centimeter ice sheet) and transmission measurements are found to agree with the computer model (Figure 22 and Figure 23). Also the limited data available for the reflected radiation has good agreement with theory.

Any error that does exist can be traced to a variety of reasons. Some of these are related to the radiation sources used. Other sources of error are the possibility of non-uniform ice samples or the methods used to measure absorption and transmission. Comparisons of the radiation sources used for the experiments and the blackbody source with water filter are in close agreement (Figure 13 to Figure 16). From observations made during the experiments, the tungsten lamp is the steadier of the two sources used. Except for the clear ice sample, this did not seem to affect the transmission measurements which were all within 5 per-

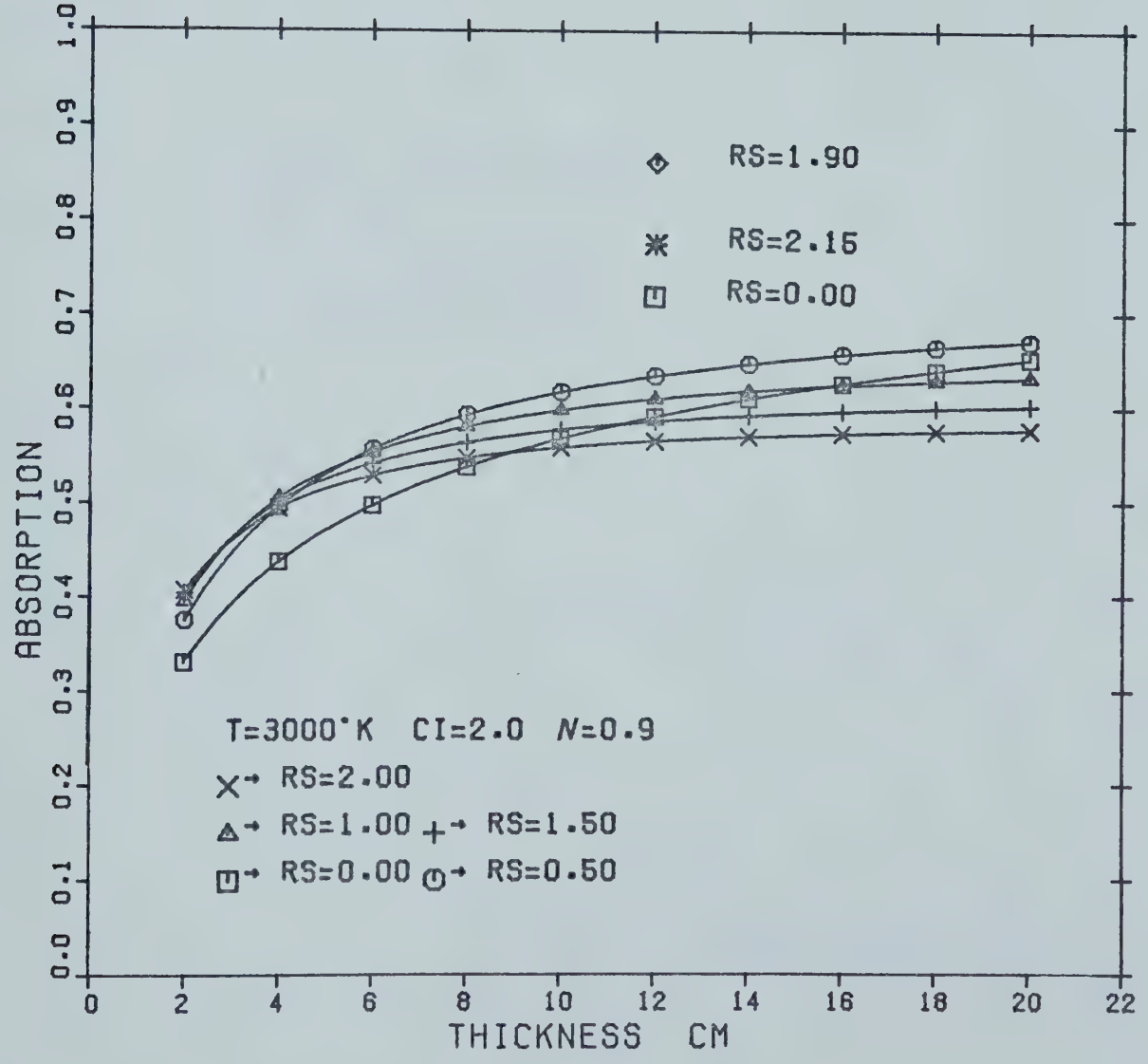

ICE SHEET EFFECTS ON THERMAL RADIATION

Figure 22a

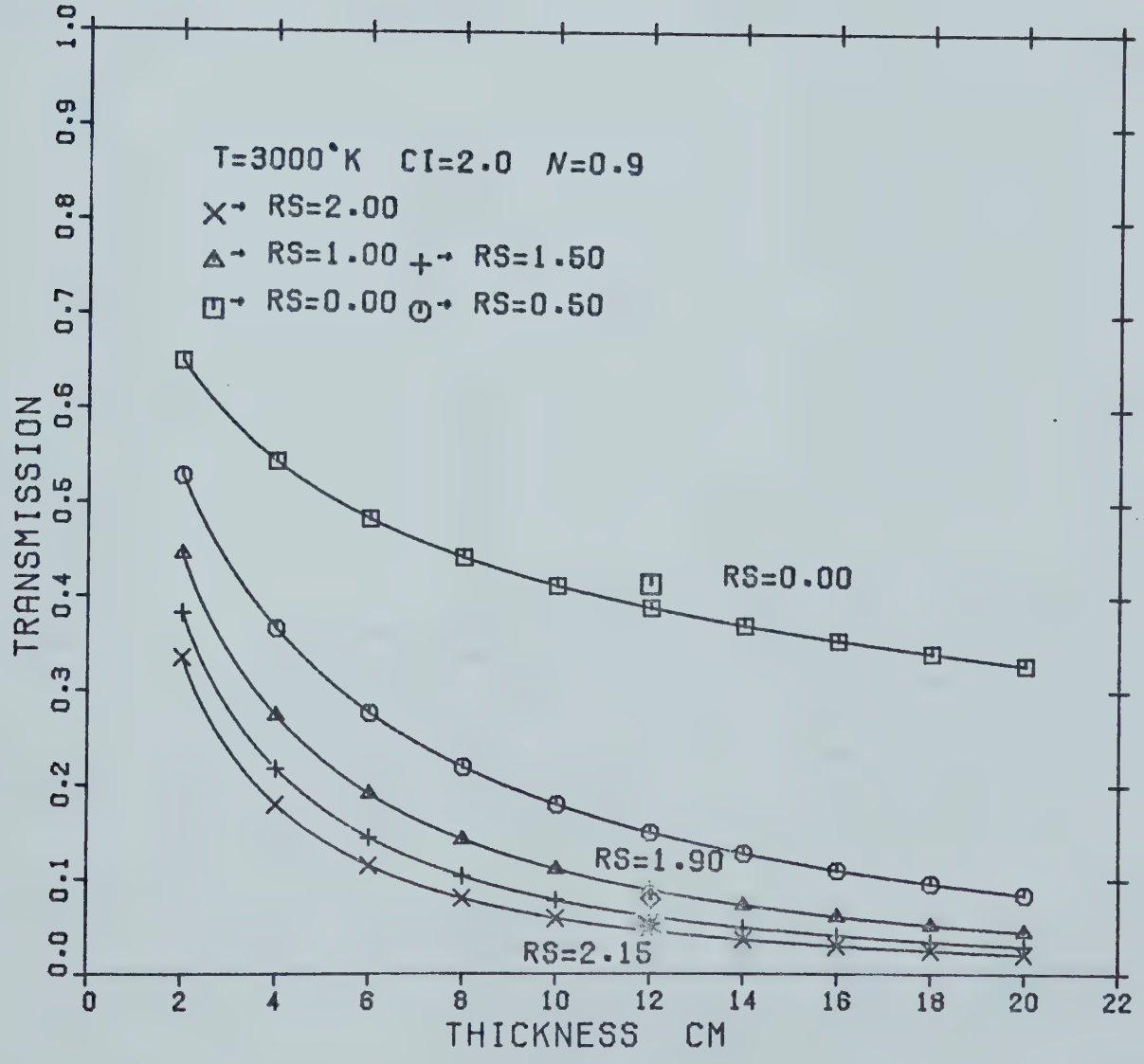

ICE SHEET EFFECTS ON THERMAL RADIATION

Figure 22b

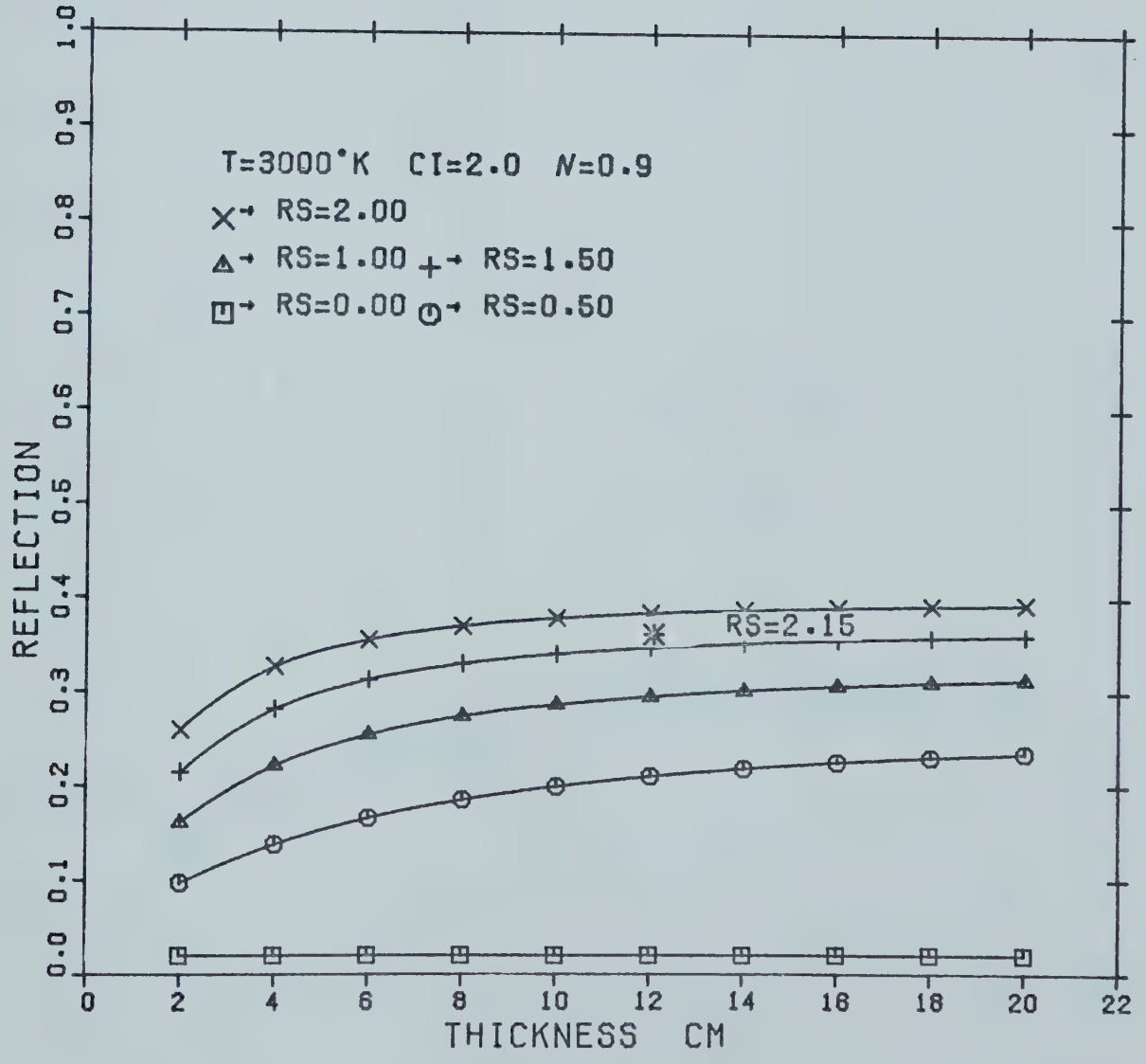

ICE SHEET EFFECTS ON THERMAL RADIATION

Figure 22c

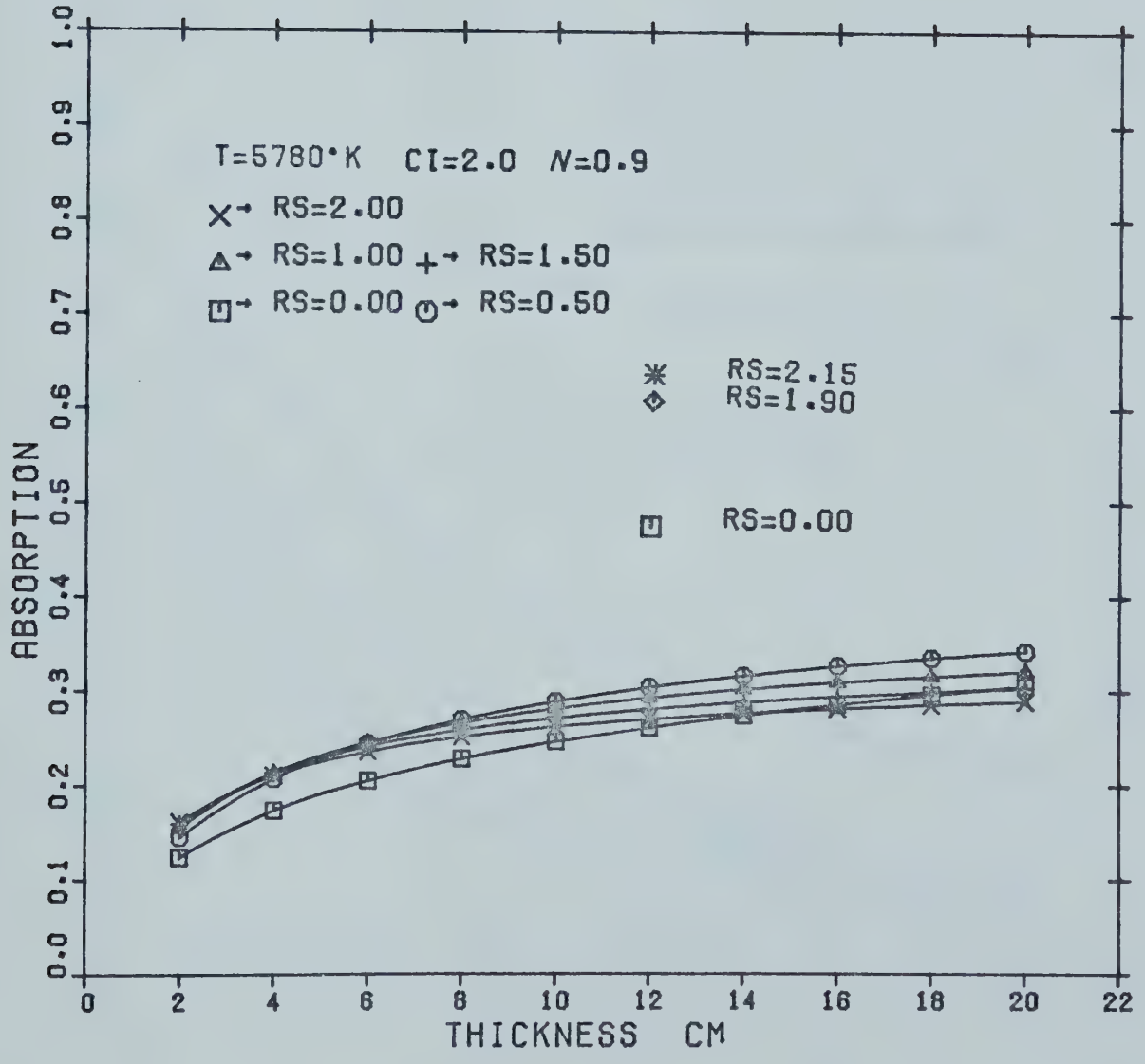

ICE SHEET EFFECTS ON THERMAL RADIATION

Figure 23a

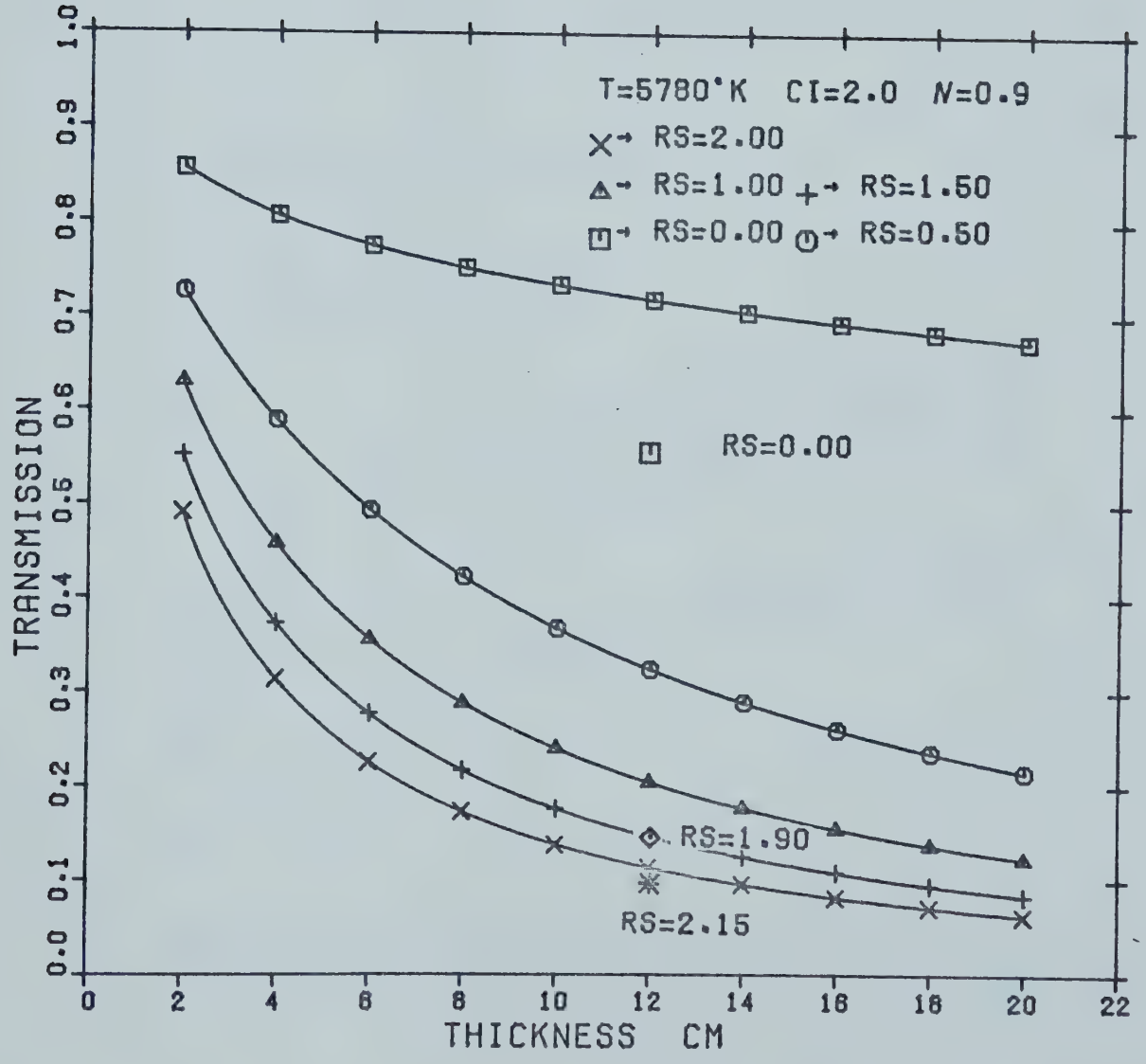

ICE SHEET EFFECTS ON THERMAL RADIATION

Figure 23b

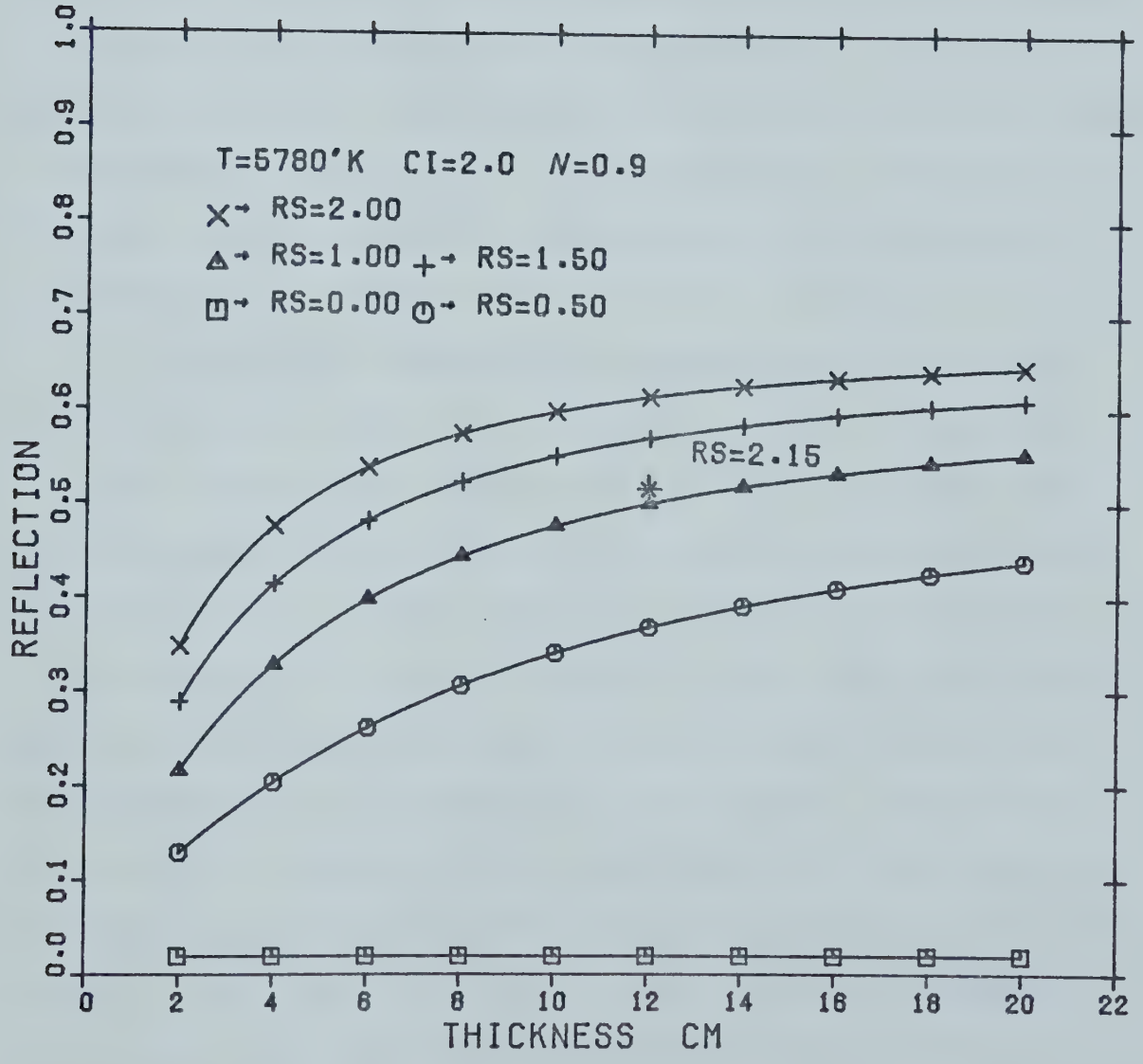

ICE SHEET EFFECTS ON THERMAL RADIATION

Figure 23c

cent of the theory. However, when the clear ice sample was exposed to the solar simulator, the measured transmission was 15 percent below that predicted by the computer model. This larger error is most likely due to the non-uniformities in the ice sample. Since these affect the higher temperature sources to a greater extent, the error is larger. These non-uniformities in the ice samples, however, do not affect the other transmission measurements. This is probably due to such a large degree of scattering that all radiation fluxes in the ice are totally diffuse. This point is born out by observing the transmitted radiation in the scattering ice samples which is totally diffuse.

Although the transmission measurements reasonably match the model, those for absorption do not. The error for the tungsten lamp source is 10 to 20 percent and that for the solar simulator is 20 to 30 percent based on total incident energy. Since the well accepted Bouger-Lambert law is used by the computer model for the clear ice cases, there must be some inherent error in the experiment itself. This error could be produced by two factors. One is the difficulty in simulating the one-dimensional ice sheet and the other is the heat transfer from the chamber to the ice sample. The lack of one-dimensional ice sheet affected absorption more than the transmission, since the transmission measurements are taken along the center line of the ice sample. Because of this, the radiation transmitted is not affected by the edge effects due to the presence of the

reflecting surface.

As described previously, the effect of heat transfer from the chamber to the ice sample was corrected for in the calculation of the energy absorbed by the ice. Having done this, the difference between the measured absorption and the absorption determined by the computer model was reduced. The resulting error for the tungsten source was reduced to 5 to 15 percent and that for the solar simulator to 15 to 25 percent. This difference between the experimental and theoretical absorption of ice, along with the large variance in the calculated absorption for the individual experimental runs, indicates that reliable measurement of absorption is extremely difficult. The problem being to expose an ice sample to thermal radiation and at the same time isolate the sample from its surroundings. However, significant agreement is available from the transmission and reflected energy measurements to verify the model chosen. Utilizing the information obtained from experiments and the computer model, the questions posed in the Introduction can be answered.

CHAPTER V

CONCLUSIONS

To determine the possibility of using thermal radiation as a deicing method, a knowledge of the behavior of thermal radiation in an ice sheet must first be obtained. To do this a model of radiative transfer in an ice sheet was first developed. The model assumed that ice behaved like a diffuse (turbid) material). Experiments were then carried out to evaluate validity of the model. From the data which was gathered, sufficient evidence was obtained to suggest that the model was reasonably accurate. Certainly within the accuracy necessary for practical purposes, this is true. That is, in field situations, the uncertainty about the scattering properties of ice would probably be greater than any error in the model itself.

The computer model is then used to provide the information required to evaluate thermal radiation as a deicing method. It generated for various combinations of radiation source temperatures and ice sheet scattering characteristics, the amounts of incident energy that were transmitted. In general, it was found that the higher source temperatures produced the larger amounts of transmitted energy. However, as source temperatures are increased, the effects of scattering became more pronounced.

To summarize the effect of scattering on transmission, consider the mean free path length of a photon before scattering of it occurs. The mean free path length is expressed as the reciprocal of the scattering coefficient (12). For example, if the scattering coefficient is 0.5/cm, the mean free path length of the photon is two centimeters. It would be expected that, the transmission of thermal radiation is not hindered greatly for ice sheet thicknesses less than one mean free path length. This is in fact born out by the computer model predictions for the 5780°K radiation source. The reduction in transmission (Appendix B, page 85) was approximately 15 percent lower than the clear ice transmission. A further examination of scattering and its effect on transmission can be obtained by considering for what ice sheet thicknesses scattering causes a 50 percent reduction in transmission. For the same 5780°K source temperature (Figure 23, page 63) the ice sheet must be about five mean free path lengths ($\frac{1}{r_s}$) thick. These conclusions can now be utilized in the consideration of thermal radiation as a deicing method.

In general, the computer results show that thermal radiation transmission through thin ice sheets (less than 2 cm) is significant regardless of scattering when a high temperature (5780°K) source is employed. This in turn indicates that thermal radiation would only prove valuable if the ice build-up was not excessive. Since certain objects such as antenna and guy wires cannot withstand a

large ice build-up, thermal radiation could be a viable method for deicing in those circumstances.

BIBLIOGRAPHY

1. Tadashi, Tabata, "Research on Prevention of Ship Icing", Defence Research Board Translation by E.R. Hope, July, 1968.

2. Tadashi, Tabata; Shuichi, Iwatu; Nobuo, Ono, "Studies of Ice Accumulation on Ships", Defence Research Board Translation, Vol. 1 and 2, November and December, 1967.

3. McConica III, T.H., "Bibliography of Ice and Frost Control", Arctic Research, Inc., WADC Tech. Report 56-338, January, 1968.

4. Thomas, C.W., "On the Transfer of Visible Radiation Through Sea Ice and Snow", Journal of Glaciology, Vol. 4, No. 34, 1963.

5. Schuster, A., "Astrophysics Journal", No. 21, pp. 1-22.

6. Silberstein, L., Phil. Mag., #4, 129 (1927).

7. Duntley, S.Q., "The Optical Properties of Diffusing Materials", J. Opt. Soc. Amer., Vol. 32, No. 2, February, 1942.

8. Dunkle, R.V., Bevens, J.T., "An Approximate Analysis of the Solar Reflectance and Transmittance of a Snow Cover", Journal of Meteorology, Vol. 13, April, 1956.

9. Hulbert, E.O., "Propogation of Radiation in a Scattering and Absorbing Medium", J.O.S.A., Vol. 33, January, 1943.

10. Viskanta, B.; Toor, J.S., "Radiant Energy Transfer in Waters", Water Resources Research, Vol. 8, No. 3, June, 1972.

11. Goodrich, L.E., "Review of Radiation Absorption Coefficients for Clear Ice in the Spectral Region 0.3 to 3 Microns", Technical Paper No. 331 of the Division of Building Research, NRCC 11761, December, 1970.

12. Sparrow, E.M.; Cess, R.D., "Radiation Heat Transfer", Brooks/Cole Publishing Company, Belmont, California, 1970.

13. Hottel, H.C.; Sarofim, A.F., "Radiative Transfer", McGraw-Hill, 1967.

14. Kottler, F., "Turbid Media with Plane-Parallel Surfaces", J. Opt. Soc. Amer., Vol. 50, No. 5, May, 1960.

15. Weeks, W.F.; Cox, G.F.N., "Laboratory Preparation of Artificial Sea and Salt Ice", Cold Regions Research and Engineering Laboratory, June, 1974.

16. Private Communication, Dr. R.R. Gilpin, Assistant Professor of Mechanical Engineering, University of Alberta.

APPENDIX A

COMPUTER PROGRAM

```
C  MAIN PROGRAM---USED TO PLOT DATA OBTAINED BY VARYING
C                 THE SCATTERING COEFFICIENT FOR THE
C                 DIFFERENT RANGES OF ICE THICKNESS'S.
C
      INTEGER TEMP
      DIMENSION ALFA(20),TRANS(10),REFLEC(10),ATTEN(10)
     Q  ,TH(10),XX(10),TSTORE(3,5,10)
101   FORMAT(F4.2,2X,I5,2X,I3,2X,F4.2)
201   FORMAT(20A4)
      READ(8,101) RS,TEMP,ITH,CI
      IOU=7
      DO 31 I=1,5
      RS1=RS*(I-1.0)
      CALL ICE(RS1,TEMP,ITH,CI,TRANS,REFLEC,ATTEN,TH)
      AS=ITH/5.0
      DO 32 J=1,10
      TSTORE(1,I,J)=TRANS(J)
      TSTORE(2,I,J)=REFLEC(J)
      TSTORE(3,I,J)=ATTEN(J)
32    CONTINUE
31    CONTINUE
C
C       PLOTTING OF DATA
      DO 33 K=1,3
      READ(8,201) (ALFA(II),II=1,20)
      DO 34 L=1,5
      NF=L
      IF(L.EQ.5.AND.K.EQ.3) NF=-5
      DO 35 M=1,10
      XX(M)=TSTORE(K,L,M)
35    CONTINUE
      CALL CGPL(TH,XX,TH,10,NF,1,1,3,1,0.0
     Q  ,AS,5.5,0.0,0.2,5.0,ALFA,IOU)
34    CONTINUE
33    CONTINUE
      STOP
      END
C
C  SUBROUTINE ICE---CALLED BY MAIN PROGRAM TO EVALUATE
C                   THE TRANSMITTANCE,REFLECTANCE,AND
C                   ABSORBTANCE FOR TEN DIFFERENT ICE
C                   SHEET THICKNESS'S. THIS SUBROUTINE
C                   CONTAINS WITHIN IT FOUR OTHER
C                   SUBROUTINES USED TO CALCULATE INCIDENT
C                   RADIATION,ESTIMATE PROGRAM ACCURACY,
C                   AND HANDLE SPECIAL CASES OCCURING IN
C                   ICE.
C
```

```
      SUBROUTINE ICE(PVR,TEMP,ITH,CI,TRANS
     Q ,REFLEC,ATTEN,TH)
      INTEGER Z,TEMP
      REAL KAPPA,MEW,MMEW,IN,N
        COMMON WL,IN,T,X(50),CABS(50)
      DIMENSION  ABS(50,28),TABS(50),EXC(50),TOT(28)
     Q ,TRANS(10),REFLEC(10),ATTEN(10),TH(10)
C       ICE THICKNESS AND SOURCE TEMP
C
        T=TEMP
        N=0.90
        RC=0.02
        RC1=RC
        DELWL=0.1*1.0E-04
        DO 01  LL=1,10
        TH(LL)=(ITH*LL)/10.0
        DELX=TH(LL)/50
        X(1)=TH(LL)/100
        DO 02 L=2,50
        X(L)=X(L-1)+DELX
02      CONTINUE
        TOTIN=0.0
        ATTEN(LL)=0.0
C
C
100      FORMAT(F4.2,4X,E7.1)
200    FORMAT('1',15X,'RADIATION ATTENUATION IN AN ICE
     Q LAYER')
300     FORMAT(' ',10X,'ATTENUATION',2X,F6.3)
310     FORMAT(' ',10X,'RADIATION SUMATION',2X,F6.3)
400    FORMAT('0',7X,F7.3,17X,F7.5,10X,F8.5)
500     FORMAT(' ',5X,'DEPTH',15X,'ABSORTION'
     Q,10X,'EXTINCTION COEFFCIENT')
700     FORMAT('0',25X,I2)
800     FORMAT(' ',2X,5(E15.7,2X))
900     FORMAT('0',20X,E15.7)
920     FORMAT('0',2X,4(E15.7,3X))
1000    FORMAT('0',10X,'REFLECTED RADIATION TOP
     Q  SURFACE',2X,F6.3,10X,'TRANSMITTED RADIATION',2X
     Q ,F6.3)
1100    FORMAT('0',10X,'TEMPERATURE=',F8.2,10X,'THICKNESS
     Q =',F6.2)
C      ATTENUATION EVALUATION
1200    FORMAT('0',15X,'RS=',F5.3)
C
       DO 03 Z=1,28
       READ(5,100) WL,PVK
        WL=WL*1.0E-04
```

```
      CALL ENERGY
       GO TO 28
29     PVK=0.95*PVK
28     PVK1=PVK*CI
       PVR1=(1.0-N)*PVR*CI
       IN=IN*EXP(-PVK*0.20)
      SIGMA=PVR+PVK
       TOT(Z)=IN*DELWL
       IF(PVR.EQ.0.0.OR.PVK.GT.(PVR*50)) GO TO 04
       SIGMA1=(2*PVR1)+PVK1
       KAPPA=-(SIGMA1+SIGMA*(2.0*N-1.0))*(1-RC)*IN*(PVR/2.0)
       ROW=(SIGMA1*PVK1)**0.5
       IF((ROW/SIGMA).GT.0.995.AND.(ROW/SIGMA).LT.1.005)
     Q  GO TO 29
      PI=KAPPA/((SIGMA**2)-(ROW**2))
       BETA=((2.0*N-1.0)*(PVR/2.0)*(1-RC)*IN)
       IF((ROW*TH(LL)).GT.50.OR.(SIGMA*TH(LL))
     Q .GT.50) GO TO 05
       TAW=1-(ROW/SIGMA1)
       SI=1+(ROW/SIGMA1)
       MEW=1+(SIGMA/SIGMA1)
       MMEW=1-(SIGMA/SIGMA1)
C         CONSTANT EVALUATION
      R=((RC*CI)*PI*MMEW)-(BETA/SIGMA1)*(1.0+(RC*CI))
     Q -(PI*MEW)
       RR=RC1*(1-RC)*IN+RC1*CI*MEW*PI-MMEW*PI
     Q +(BETA/SIGMA1)*(1.0+(RC1*CI))
       A=(SI-(RC1*CI)*TAW)
       AA=(TAW-(RC1*CI)*SI)
      B=(SI-(RC*CI)*TAW)
        BB=(TAW-(RC*CI)*SI)
       DIV=((A*B*EXP(ROW*TH(LL)))-(AA*BB/EXP(ROW*TH(LL))))
      CON=-((R*AA/EXP(+ROW*TH(LL)))-(RR*B/EXP(+SIGMA*TH(LL)
     Q )))/DIV
      CCON=((R*A*EXP(ROW*TH(LL)))-(RR*BB/EXP(+SIGMA*TH(LL)
     Q )))/DIV
C     DETERMINE ATTENUATION
C
        DO 07 L=1,50
       DOWN=(CON*TAW*EXP(ROW*X(L)))+(CCON*SI/EXP(+ROW*X(L)))
     Q  +((PI*MEW+(BETA/SIGMA1))/EXP(+SIGMA*X(L)))
      UP=(CON*SI*EXP(ROW*X(L)))+(CCON*TAW/EXP(+ROW*X(L)))
     Q   +((PI*MMEW-(BETA/SIGMA1))/EXP(+SIGMA*X(L)))
       ABS(L,Z)=((PVK1*(DOWN+UP))+((IN*(1-RC))/EXP
     Q (SIGMA*X(L)))
     Q  *PVK)*DELX
       IF(L.EQ.1)  BCT=(RC*IN)+(1-(RC*CI))*((CCON*TAW)
     Q  +(CON*SI)+((PI*MMEW-(BETA/SIGMA1))))
```

```
      IF(L.EQ.50)  BCB=(1-(RC1*CI))*((CON*TAW*EXP(ROW
     Q  *TH(LL)))+(CCON*SI/EXP(ROW*TH(LL)))+
     Q ((PI*MEW+(BETA/SIGMA1))/EXP(
     Q  SIGMA*TH(LL))))+((IN*(1-RC))/EXP(SIGMA*TH(LL)))
     Q *(1-RC1)
07    CONTINUE
      GO TO 08
05    CALL ISHEET(ROW,SIGMA,PI,CI,DELX,PVR,PVK
     Q ,RC,SIGMA1,BETA,BCT)
      BCB=0.0
      DO 09 J=1,50
      ABS(J,Z)=CABS(J)
09    CONTINUE
      GO TO 08
04    TH1=TH(LL)
       CALL ABSORB(DELX,PVK,RC,SIGMA,TH1,BCT,BCB)
      DO 14 JJ=1,50
      ABS(JJ,Z)=CABS(JJ)
14    CONTINUE
08    CALL RAD BAL (BCT,BCB,Z,DELWL)
03    CONTINUE
C
      DO 10 KK=1,27
      TOTIN=0.5*(TOT(KK)+TOT(KK+1))+TOTIN
10    CONTINUE
C
C     TOTAL ATTENUATION
      DO 11 L=1,50
      DO 12 Z=1,27
      BABS=(DELWL*0.5)*(ABS(L,Z)+ABS(L,Z+1))
       IF(Z.EQ.1)  TABS(L)=0.0
       TABS(L)=BABS+TABS(L)
12    CONTINUE
      TABS(L)=TABS(L)/TOTIN
      ATTEN(LL)=TABS(L)+ATTEN(LL)
11    CONTINUE
       BCT=BCT/TOTIN
       BCB=BCB/TOTIN
       TRANS(LL)=BCB
       REFLEC(LL)=BCT
C
       DO 13 II=1,50
       EXC(II)=TABS(II)/(TH(LL)/50)
13     CONTINUE
       TEXC=ATTEN(LL)/(TH(LL))
       SUM=ATTEN(LL)+BCB+BCT
C
C
```

```
      WRITE(6,200)
      WRITE(6,1100) T,TH(LL)
      WRITE(6,1200) PVR
      WRITE(6,500)
     WRITE(6,400)  (X(L),TABS(L),EXC(L),L=1,50)
      WRITE(6,300) ATTEN(LL)
      WRITE(6,300) TEXC
      WRITE(6,310) SUM
      WRITE(6,1000) BCT,BCB
01    CONTINUE
      RETURN
      END
C
C  ENERGY---CALCULATES INCIDENT RADIATION ASSUMING BLACK
C           BODY DISTRIBUTION.
C
     SUBROUTINE  ENERGY
       REAL IN
       COMMON WL,IN,T,X(50),CABS(50)
     ET=((1.4387)/(WL*T))
     VET=(EXP(ET)-1.0)
     IN=((3.740E-05)/((WL**5)*VET))/3.14159
     RETURN
     END
C
C  ABSORB---DETERMINE ABSORBED,REFLECTED,AND TRANSMITTED
C           RADIATION OCCURING WHEN SCATTERING COEFFICIENT
C           IS ZERO OR INSIGNIFICANT COMPARED TO THE
C           ABSORBTION COEFFICIENT.
C
      SUBROUTINE ABSORB(DELX,PVK,RC,SIGMA,TH1,BCT,BCB)
      REAL IN
       COMMON WL,IN,T,X(50),CABS(50)
      DO 01 J=1,50
      IF((X(J)*PVK).GT.50) GO TO 03
      ABS1=((1-RC)*IN)*EXP(-PVK*(X(J)-(DELX/2)))
      ABS2=((1-RC)*IN)*EXP(-PVK*(X(J)+(DELX/2)))
      CABS(J)=ABS1-ABS2
      IF(J.EQ.1)  BCT=RC*IN
      IF(J.EQ.50)  BCB=(IN*(1-RC))/EXP(SIGMA*TH1)
      GO TO 01
03    CABS(J)=0.0
      IF(J.EQ.1)  CABS(1)=(1-RC)*IN
      IF(J.EQ.1)  BCT=RC*IN
      IF(J.EQ.50)  BCB=0.0
01    CONTINUE
      RETURN
      END
```

```
C
C  RAD BAL---SUMMATION OF ALL RADIATION ABSORBED,REFLECTED
C            ,AND TRANSMITTED.
C
      SUBROUTINE RAD BAL (BCT,BCB,Z,DELWL)
      INTEGER Z
      DIMENSION  T(28),B(28)
      T(Z)=BCT
      B(Z)=BCB
      IF(Z.LT.28) GO TO 01
      CB=0.0
      CT=0.0
      DO 02 J=1,27
      TT=(DELWL*0.5)*(T(J)+T(J+1))
      BB=(DELWL*0.5)*(B(J)+B(J+1))
      CT=TT+CT
      CB=BB+CB
02    CONTINUE
      BCB=CB
      BCT=CT
01    RETURN
      END
C
C   ISHEET---USED TO DETERMINE AMOUNTS OF ABSORBED AND
C            REFLECTED RADIATION WHEN NO RADIATION IS
C            TRANSMITTED TO THE LOWER SURFACE.
C
C
      SUBROUTINE ISHEET(ROW,SIGMA,PI,CI,DELX,PVR,PVK
     Q ,RC,SIGMA1,BETA,BCT)
      REAL MEW,MMEW,IN
      COMMON WL,IN,T,X(50),CABS(50)
      PVK1=PVK*CI
      TAW=1-(ROW/SIGMA1)
      SI=1+(ROW/SIGMA1)
      MEW=1+(SIGMA/SIGMA1)
      MMEW=1-(SIGMA/SIGMA1)
      R=((RC*CI)*PI*MMEW)-(BETA/SIGMA1)*(1+(RC*CI))
     Q -(PI*MEW)
      B=(SI-(RC*CI)*TAW)
      DO 01 J=1,50
      IF((ROW*X(J)).GT.70) GO TO 02
      IF((SIGMA*X(J)).GT.70) GO TO 03
      DOWN=(R/B)*SI/EXP(ROW*X(J))+
     Q (PI*MEW+(BETA/SIGMA1))/
     Q EXP(SIGMA*X(J))
      UP=(R/B)*TAW/EXP(ROW*X(J))+
     Q (PI*MMEW-(BETA/SIGMA1))/
```

```
     Q EXP(SIGMA*X(J))
       CABS(J)=((PVK1*(DOWN+UP))+((IN*(1-RC))/EXP
     Q (SIGMA*X(J)))
     Q  *PVK)*DELX
       IF(J.EQ.1)  BCT=(RC*IN)+(1-(RC*CI))*(((R/B)
     Q *TAW)+((PI*MMEW-(BETA/SIGMA1))))
       GO TO 01
02     IF((SIGMA*X(J)).GT.70)  GO TO 03
       CABS(J)=(((IN*(1-RC))/EXP(SIGMA*X(J)))
     Q  *PVK)*DELX
       IF(J.EQ.1)  BCT=(RC*IN)
       GO TO 01
03     CABS(J)=0.0
       IF(J.EQ.1)  BCT=(RC*IN)
01     CONTINUE
       RETURN
       END
```

APPENDIX B

ICE SHEET EFFECTS ON THERMAL RADIATION

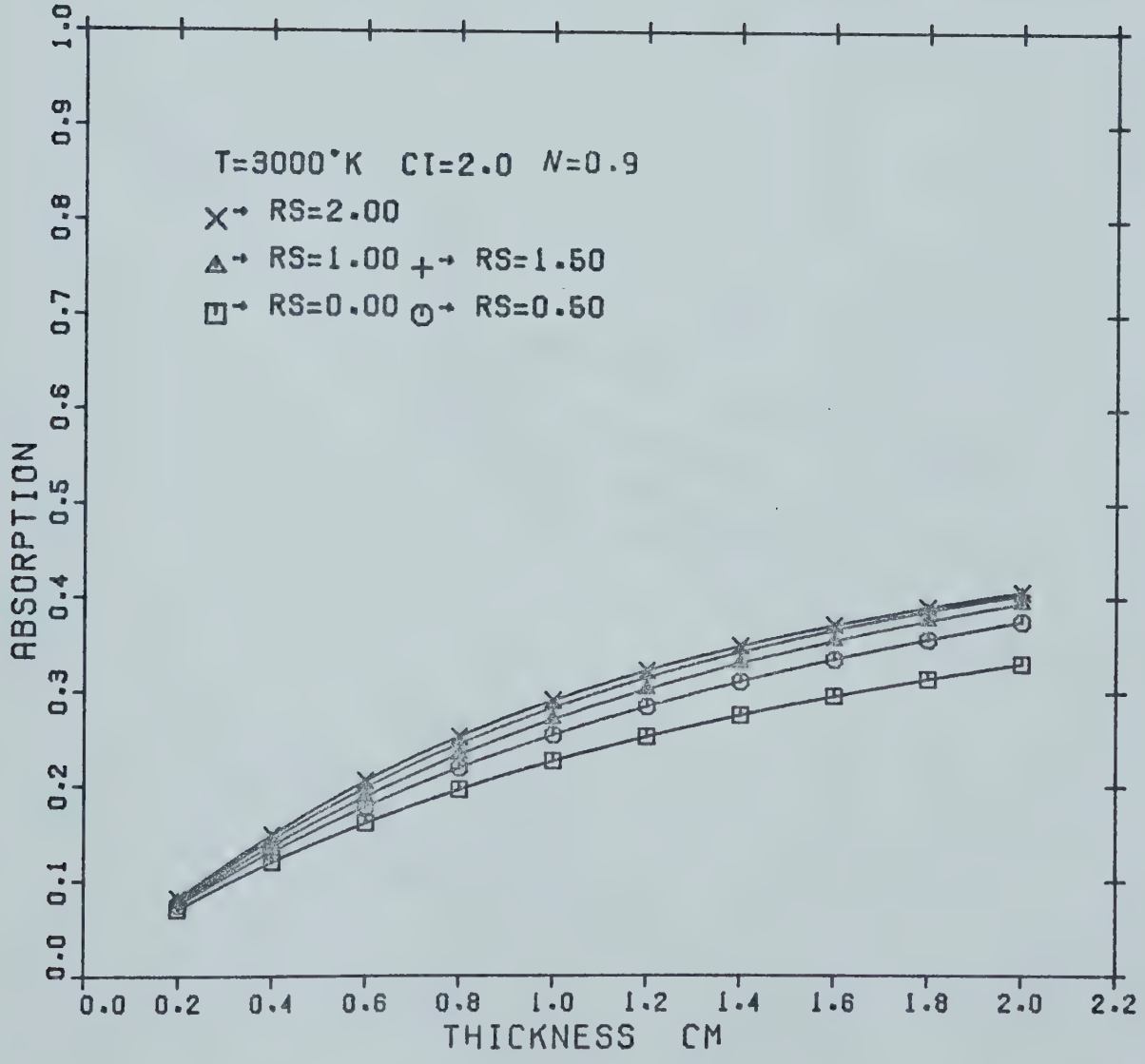

ICE SHEET EFFECTS ON THERMAL RADIATION

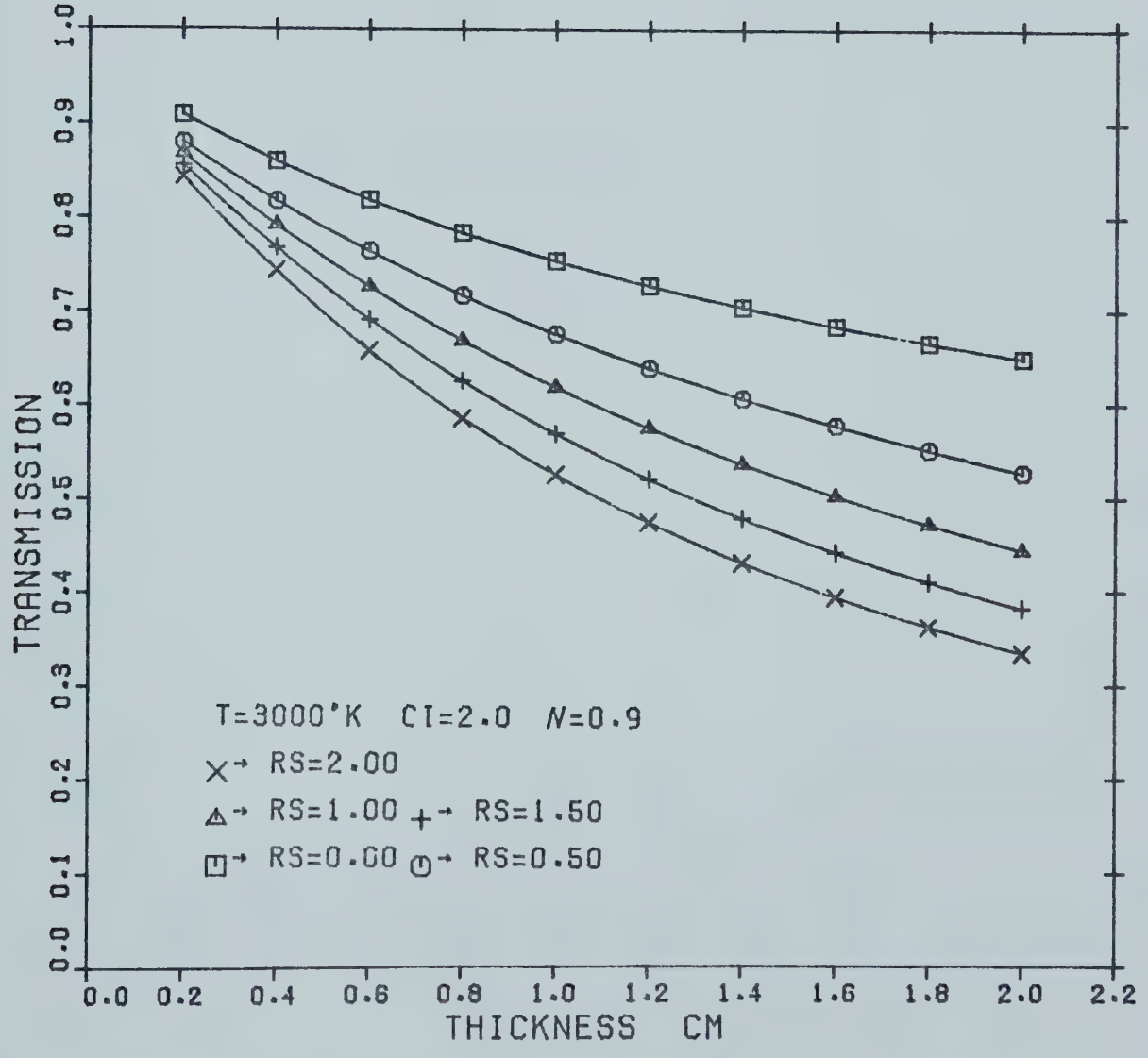

ICE SHEET EFFECTS ON THERMAL RADIATION

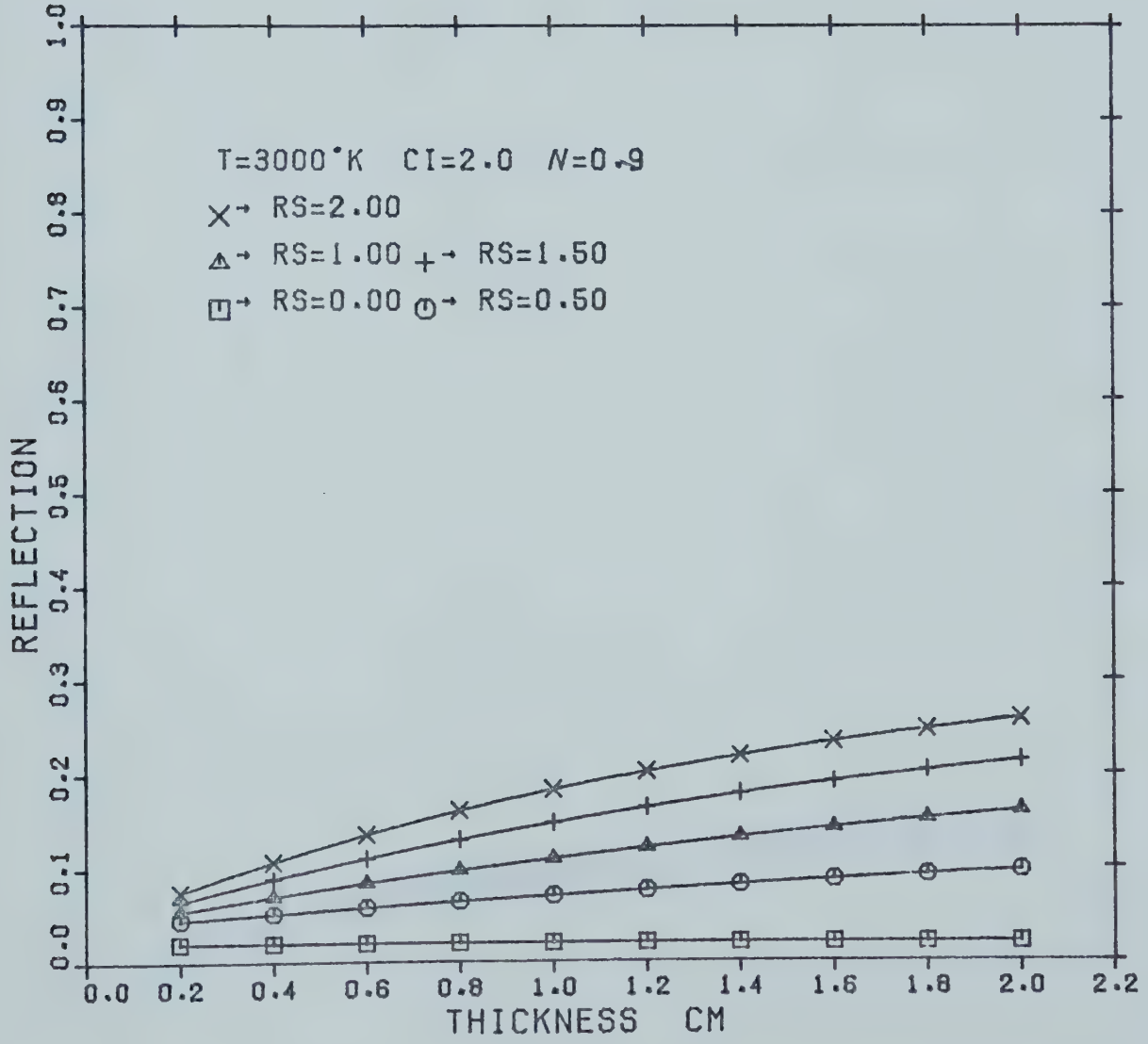

ICE SHEET EFFECTS ON THERMAL RADIATION

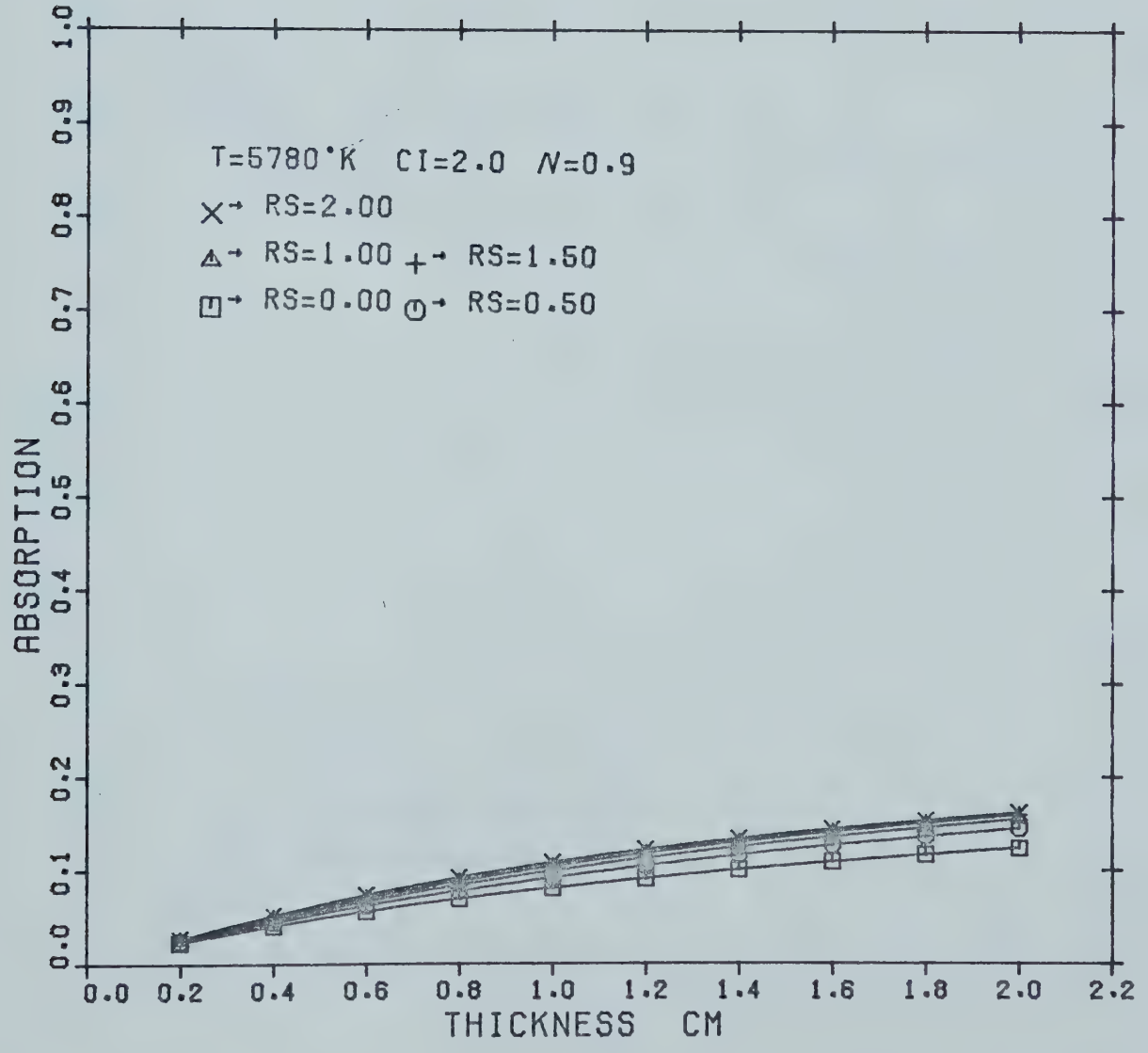

ICE SHEET EFFECTS ON THERMAL RADIATION

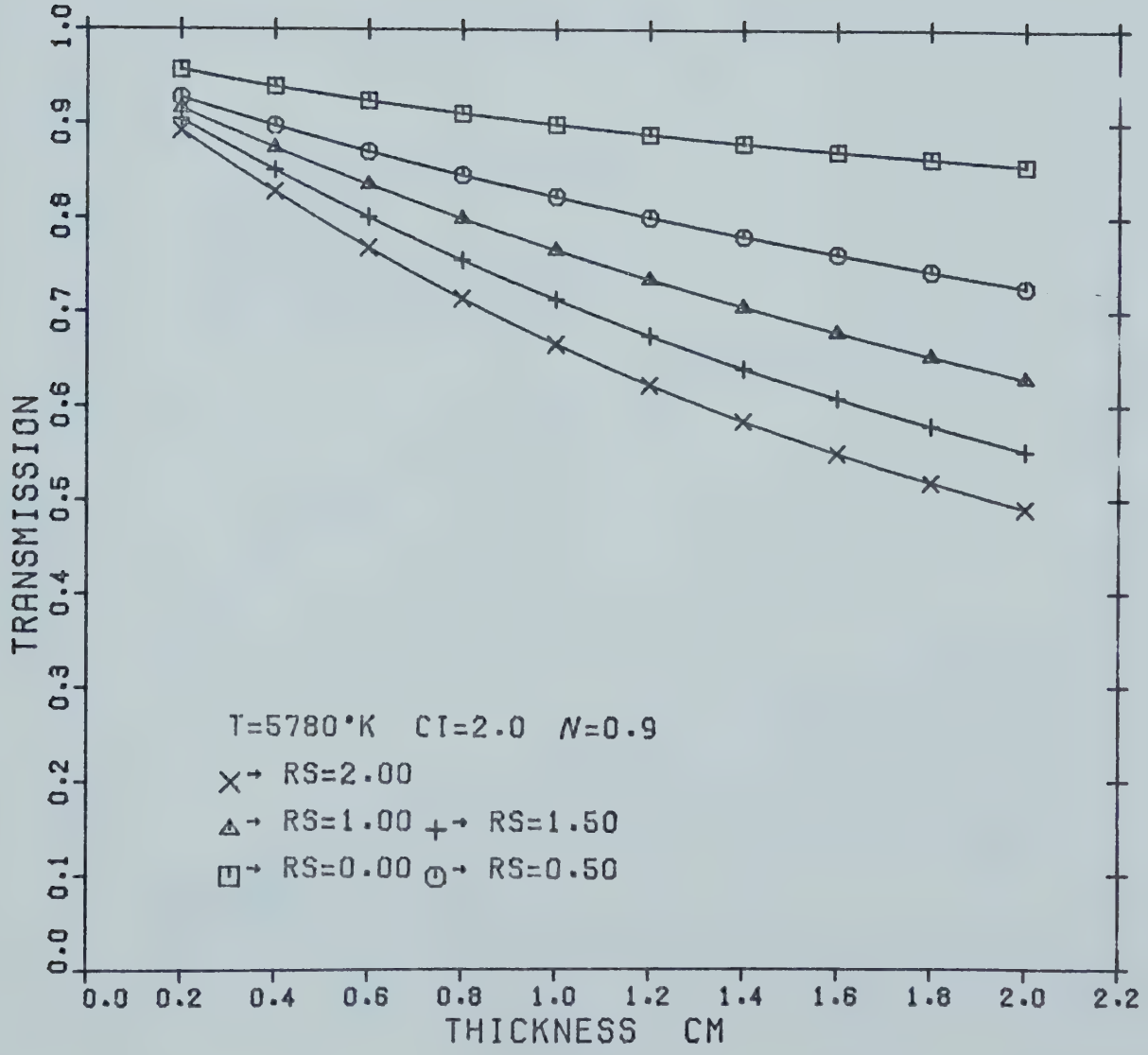

ICE SHEET EFFECTS ON THERMAL RADIATION

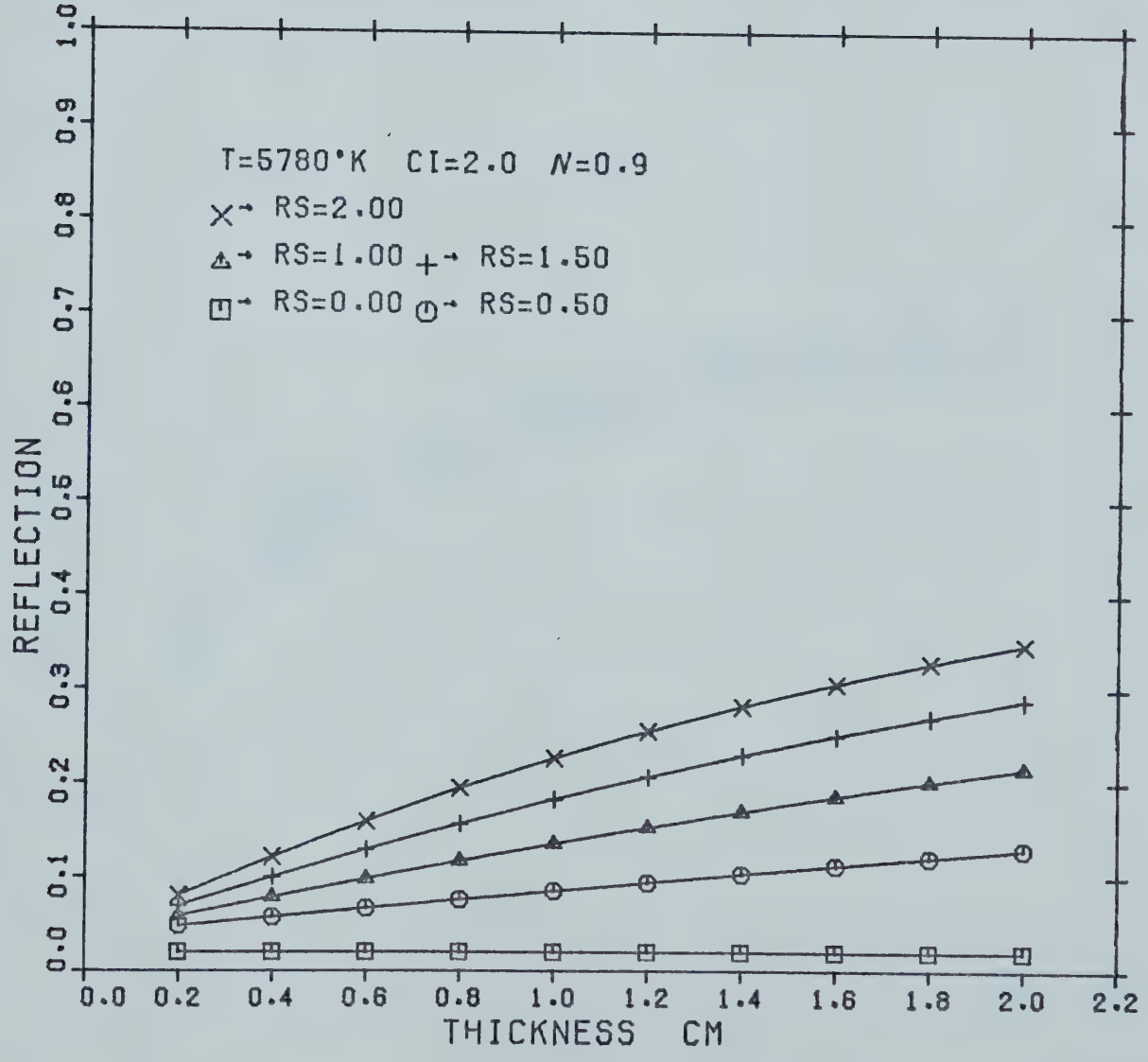

ICE SHEET EFFECTS ON THERMAL RADIATION

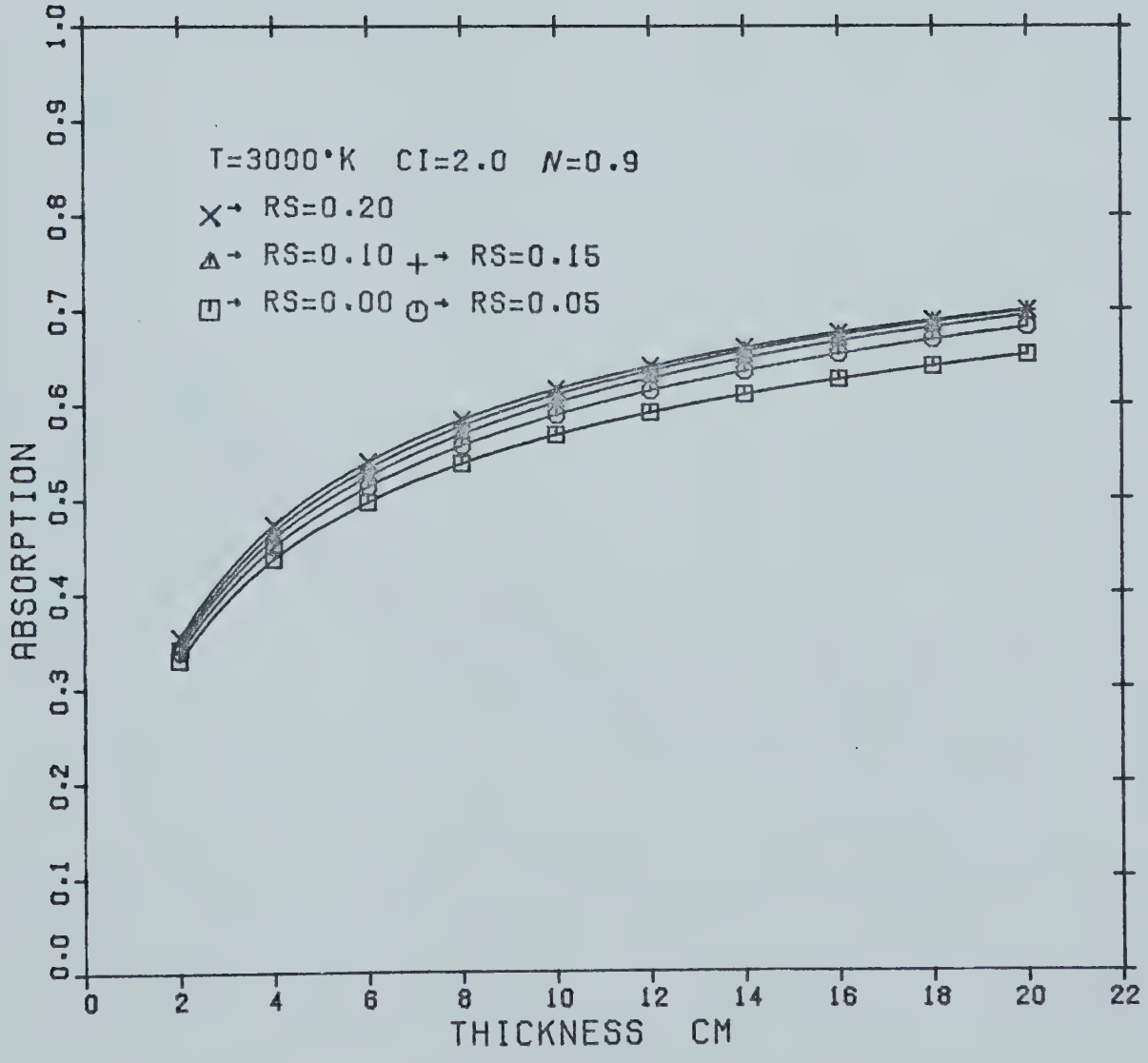

ICE SHEET EFFECTS ON THERMAL RADIATION

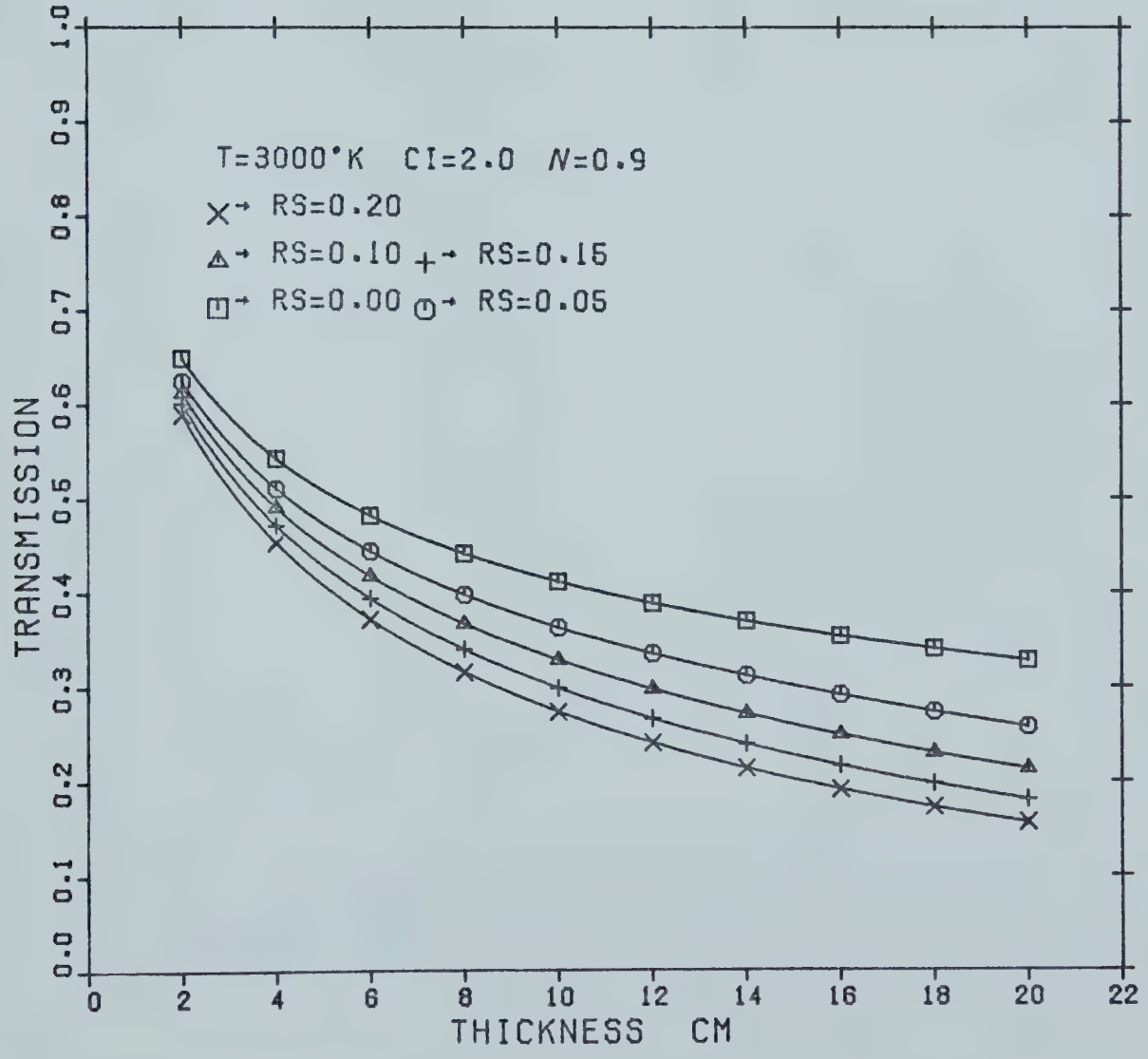

ICE SHEET EFFECTS ON THERMAL RADIATION

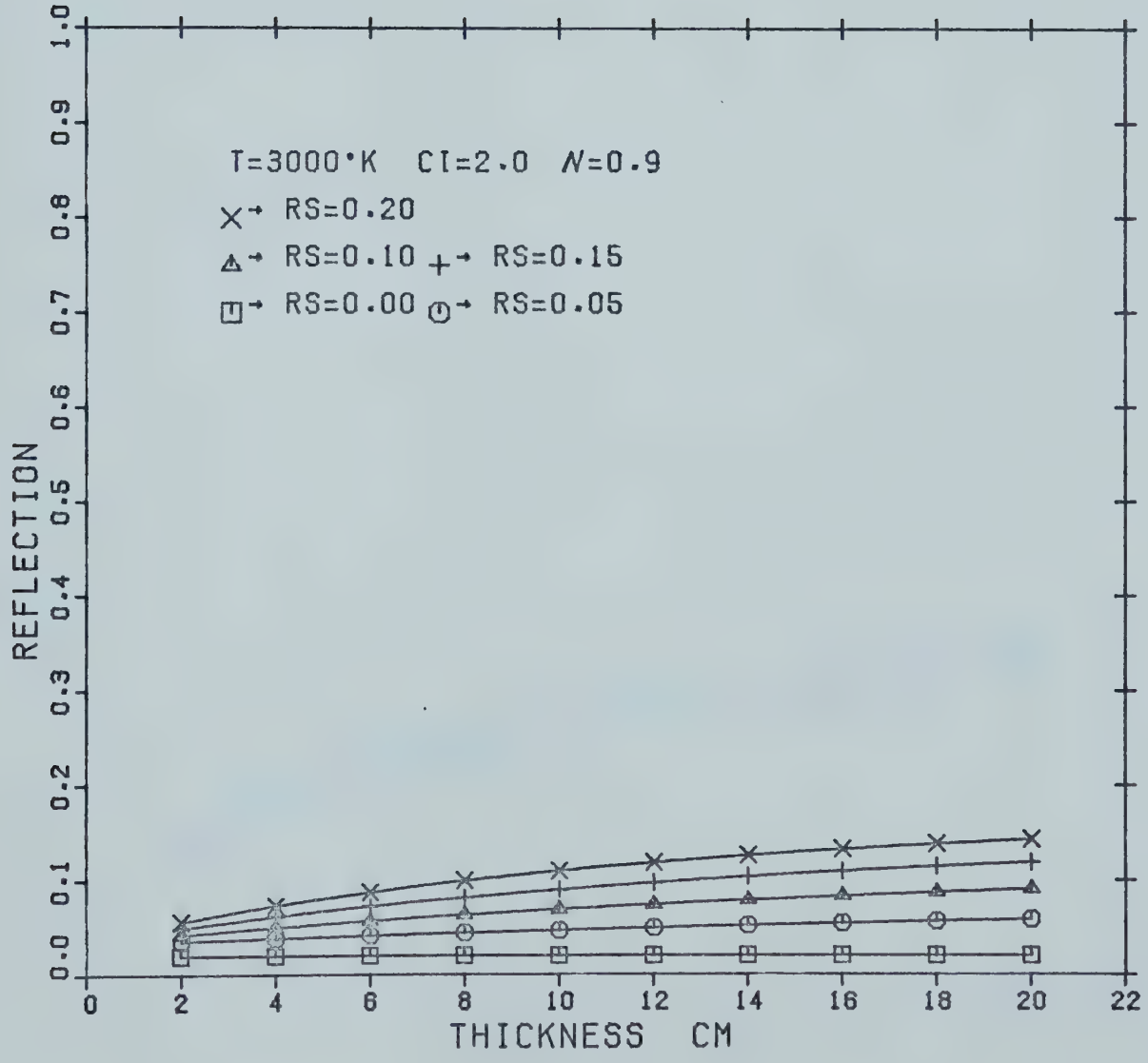

ICE SHEET EFFECTS ON THERMAL RADIATION

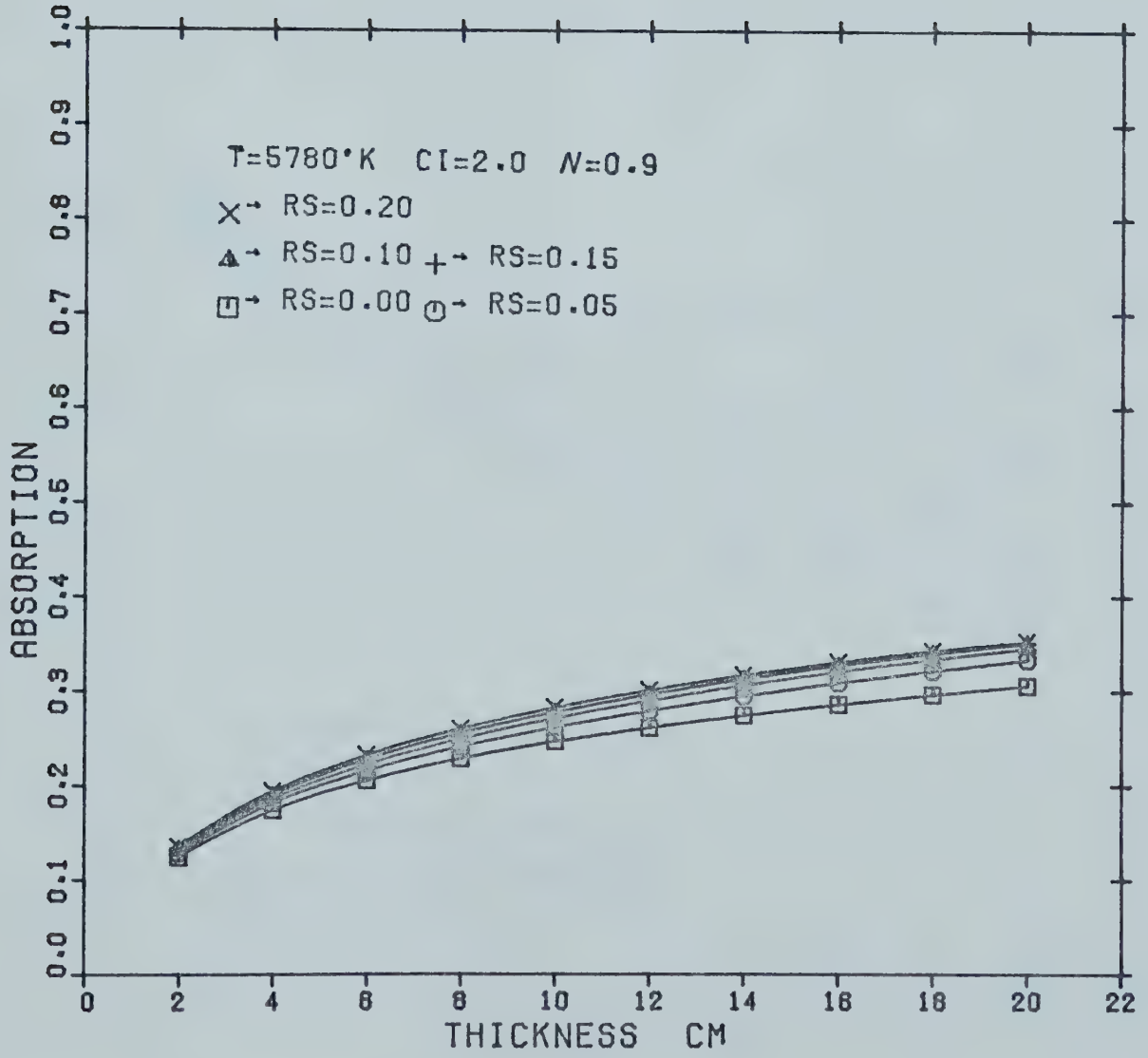

ICE SHEET EFFECTS ON THERMAL RADIATION

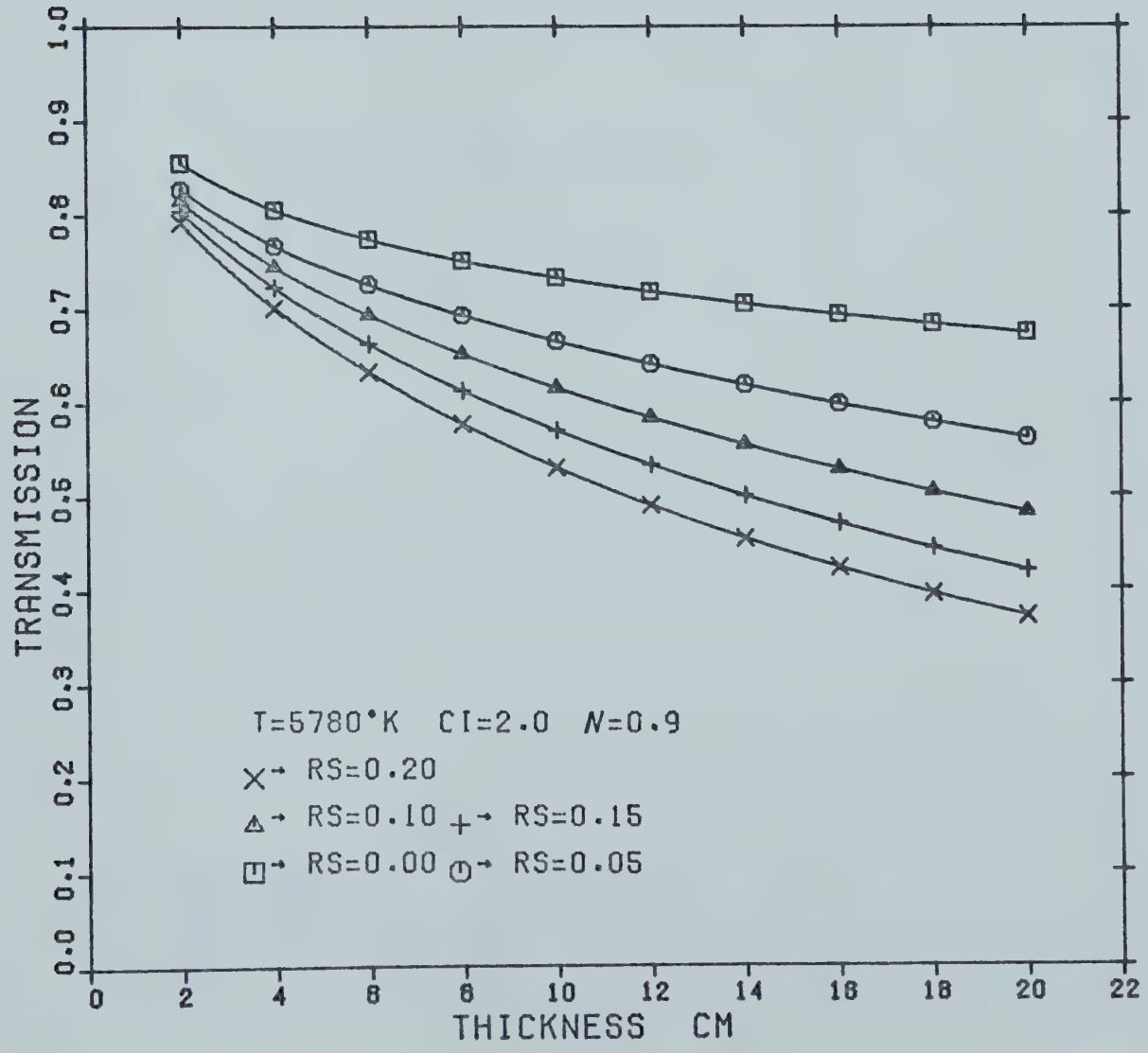

ICE SHEET EFFECTS ON THERMAL RADIATION

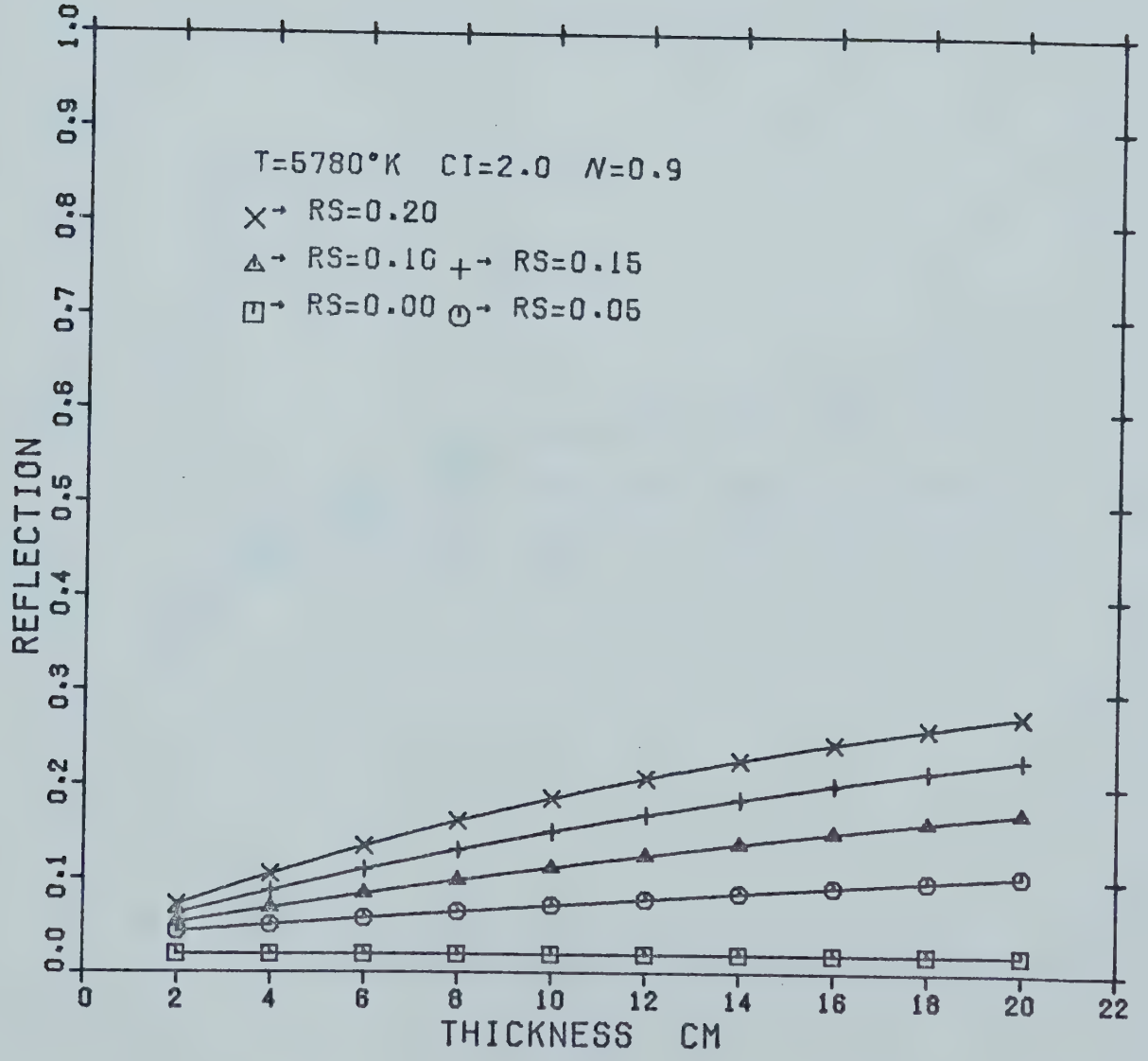

ICE SHEET EFFECTS ON THERMAL RADIATION

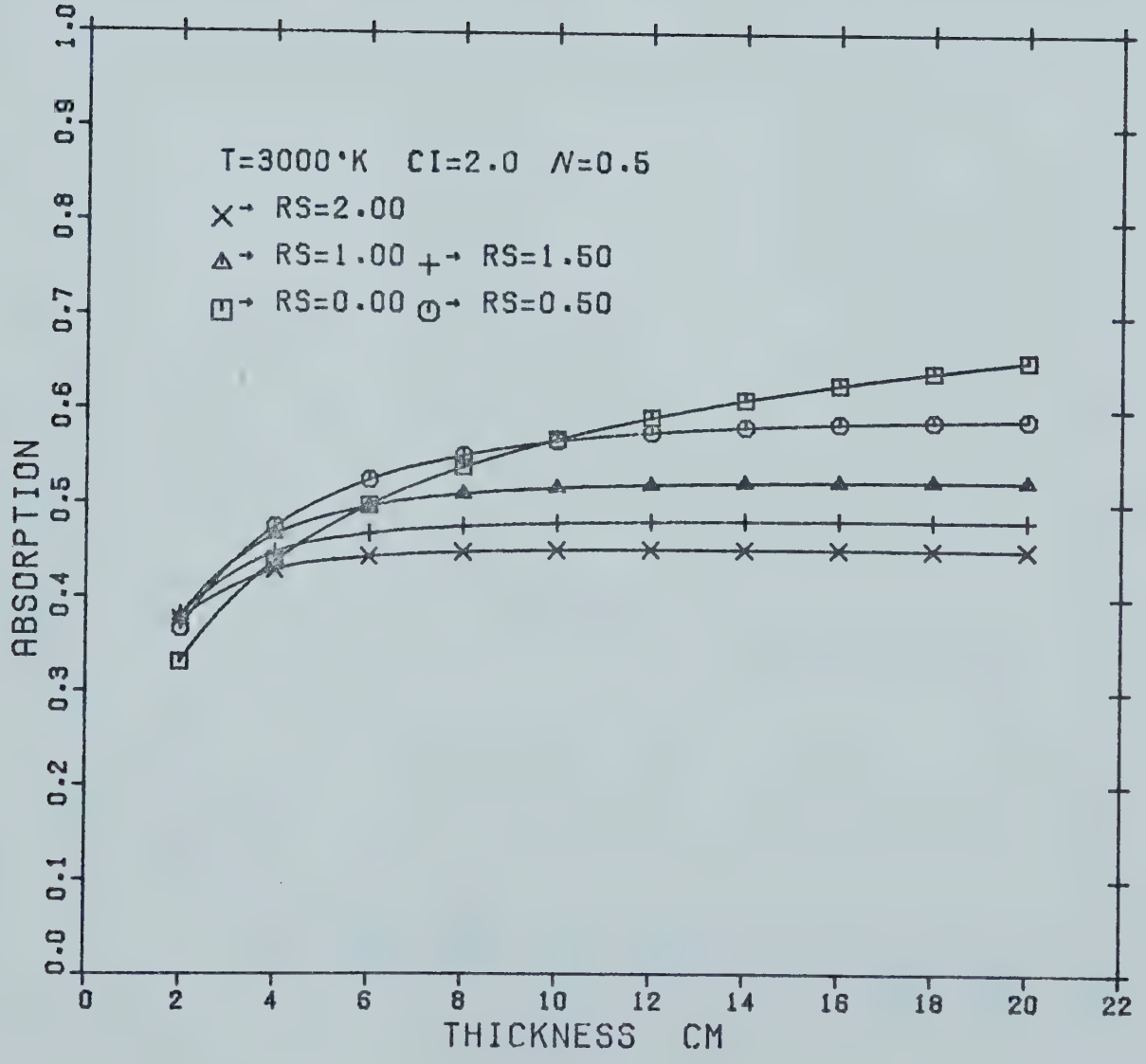

ICE SHEET EFFECTS ON THERMAL RADIATION

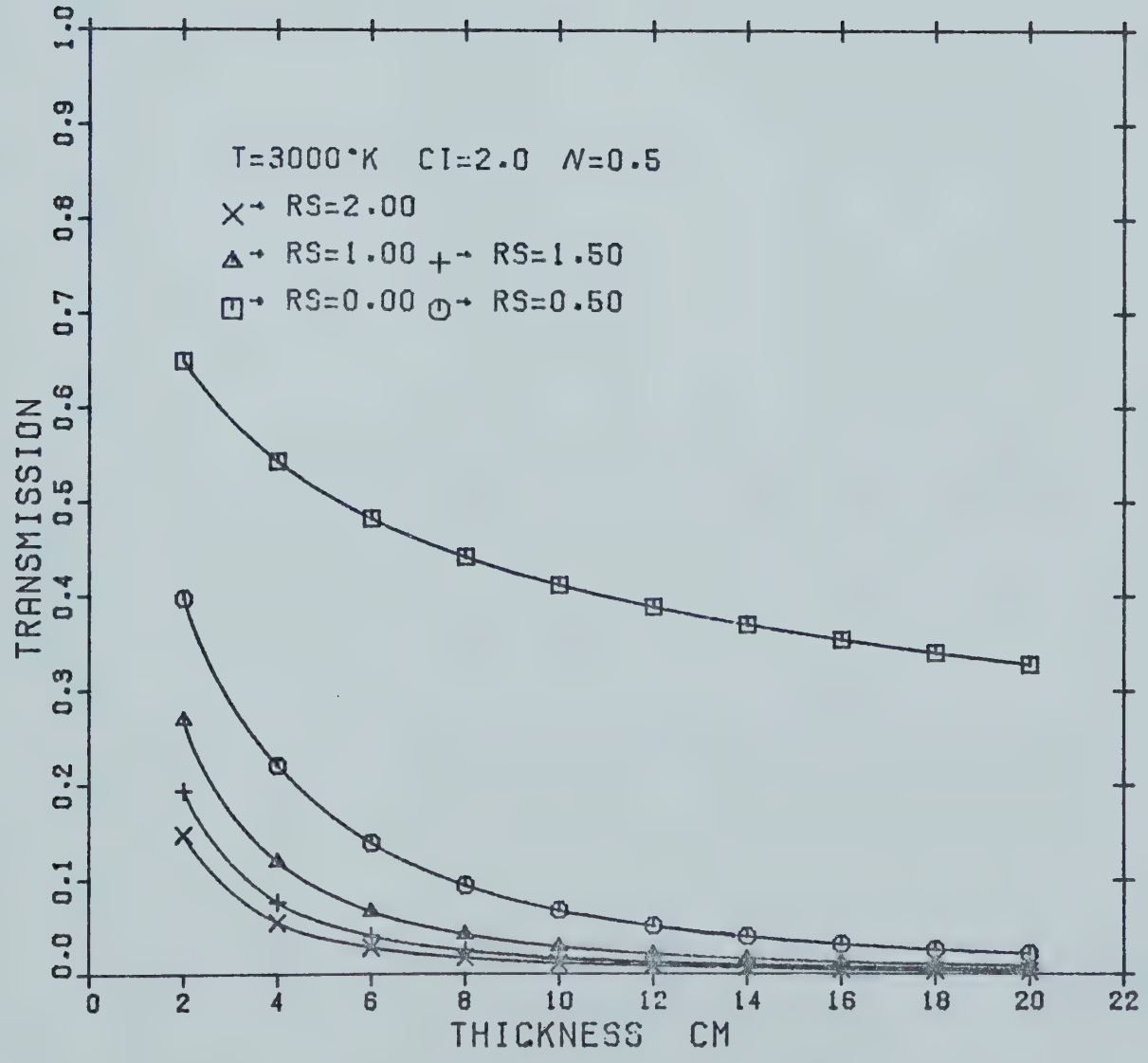

ICE SHEET EFFECTS ON THERMAL RADIATION

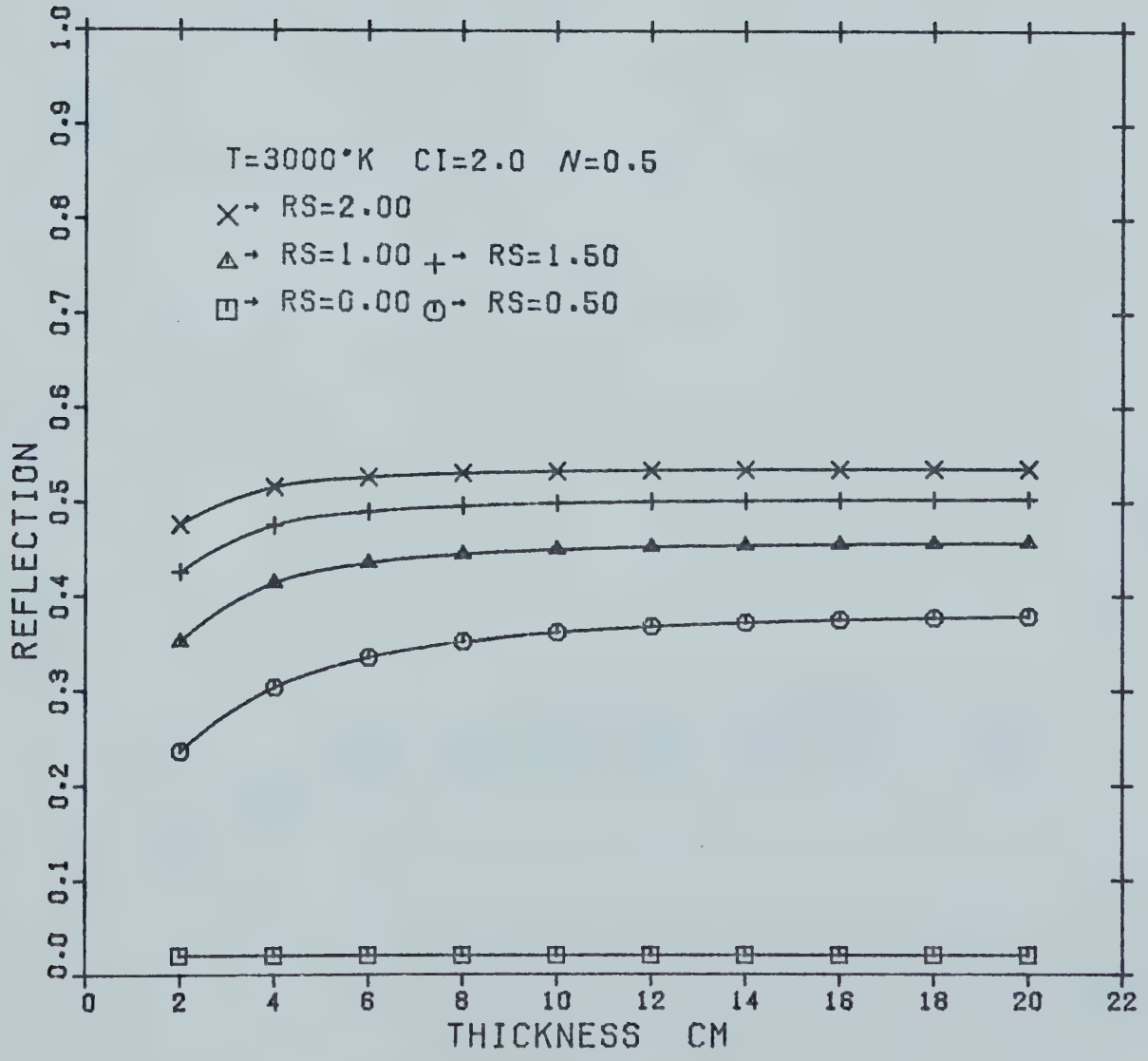

ICE SHEET EFFECTS ON THERMAL RADIATION

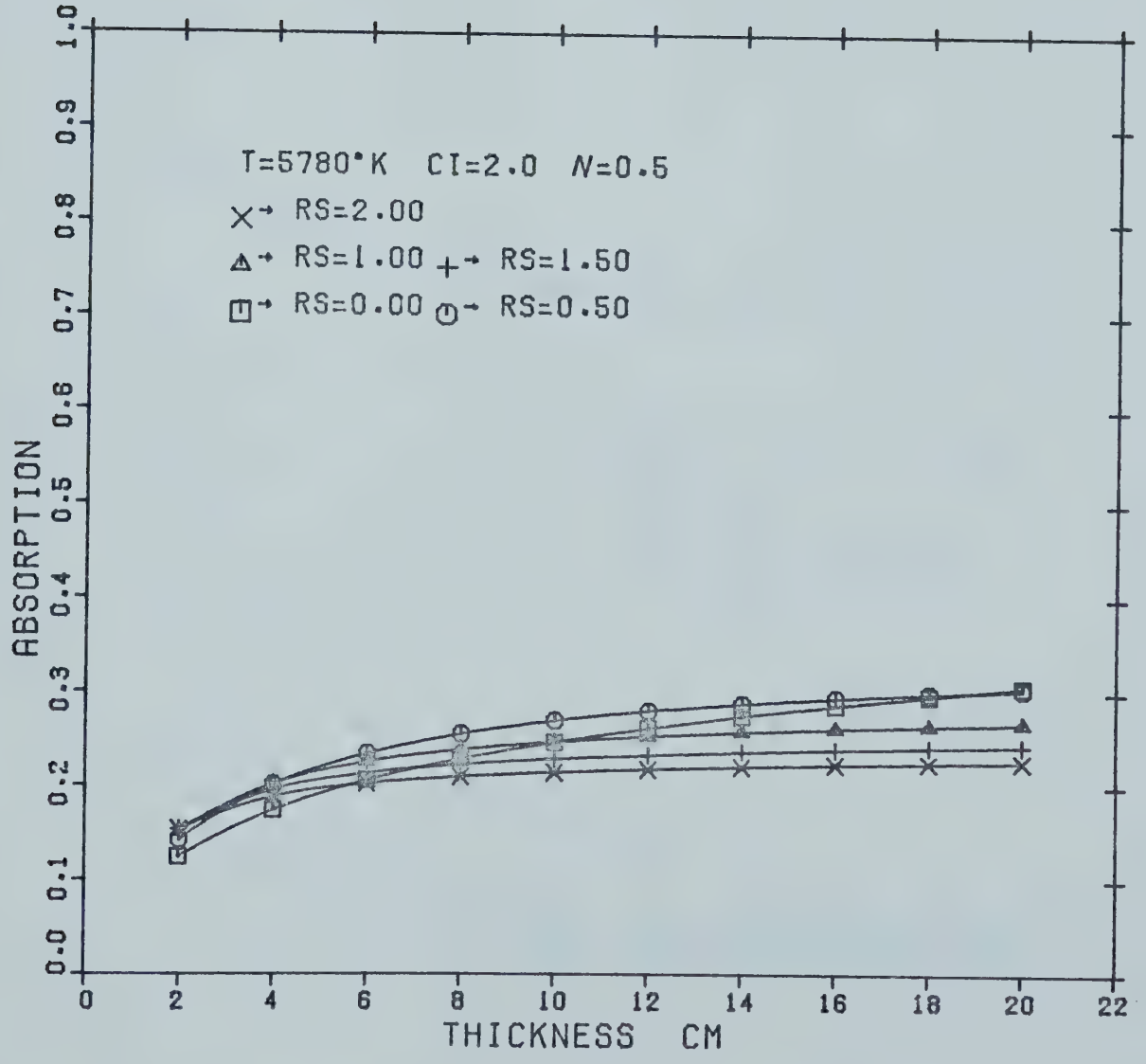

ICE SHEET EFFECTS ON THERMAL RADIATION

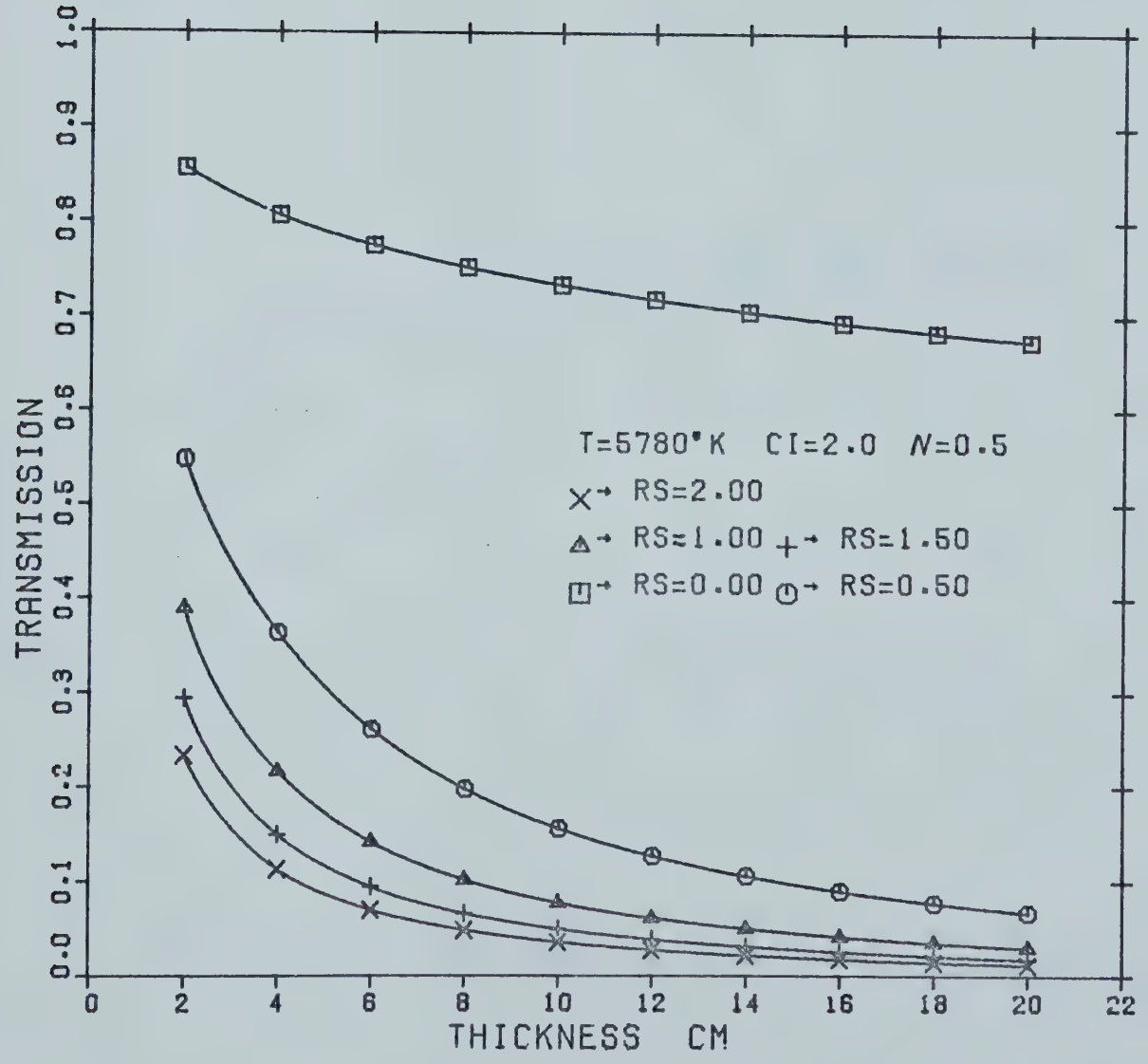

ICE SHEET EFFECTS ON THERMAL RADIATION

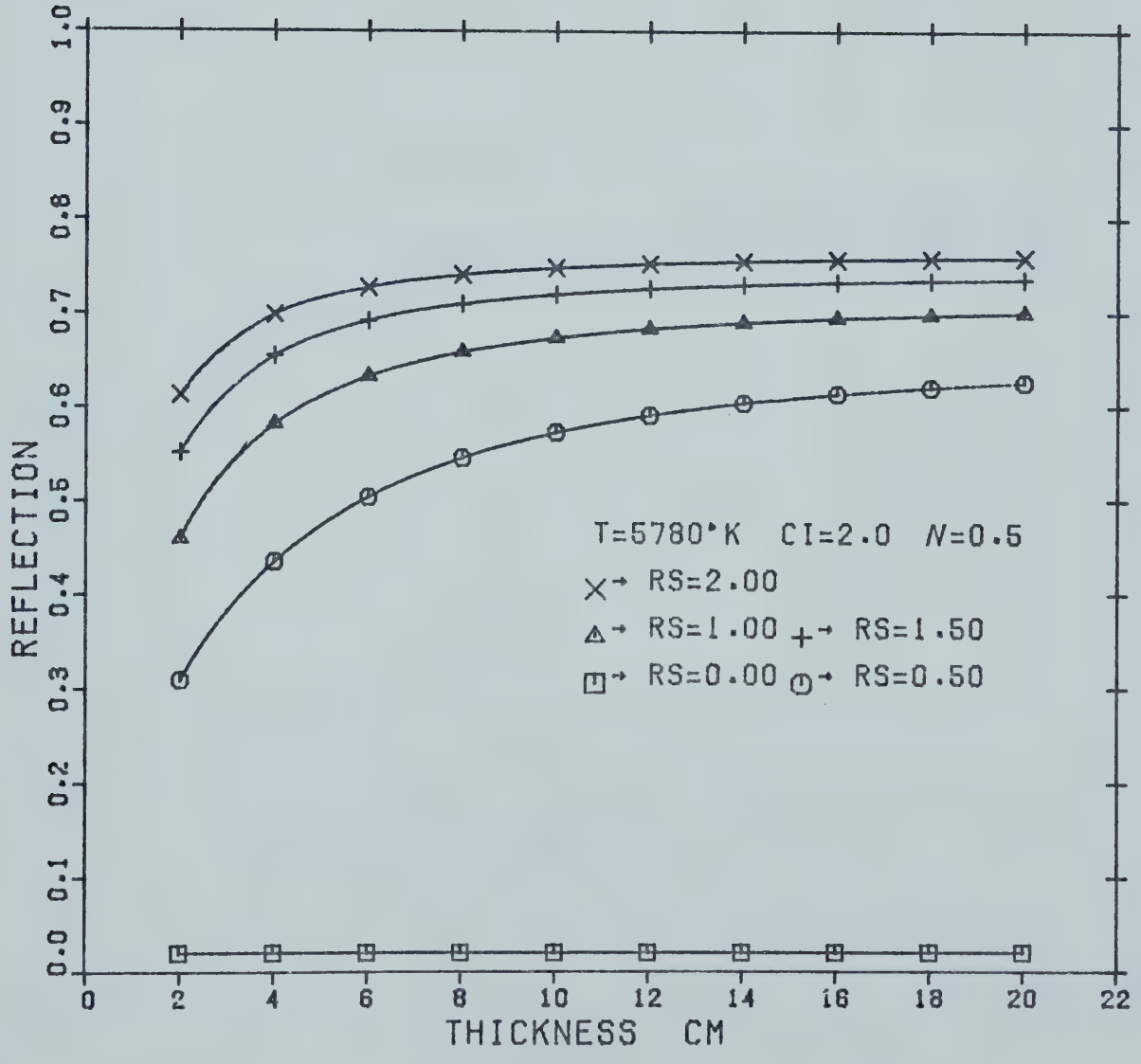

ICE SHEET EFFECTS ON THERMAL RADIATION

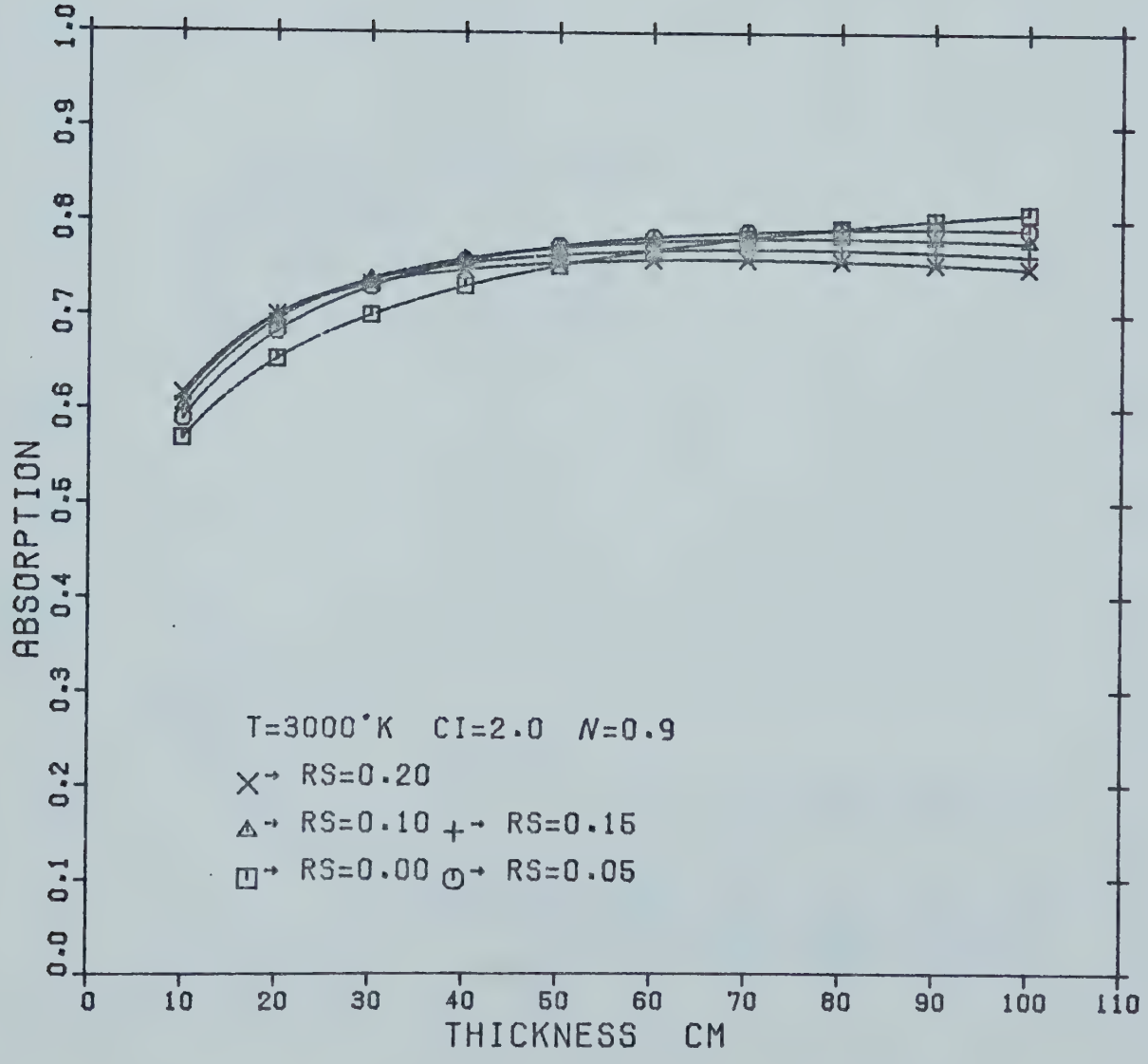

ICE SHEET EFFECTS ON THERMAL RADIATION

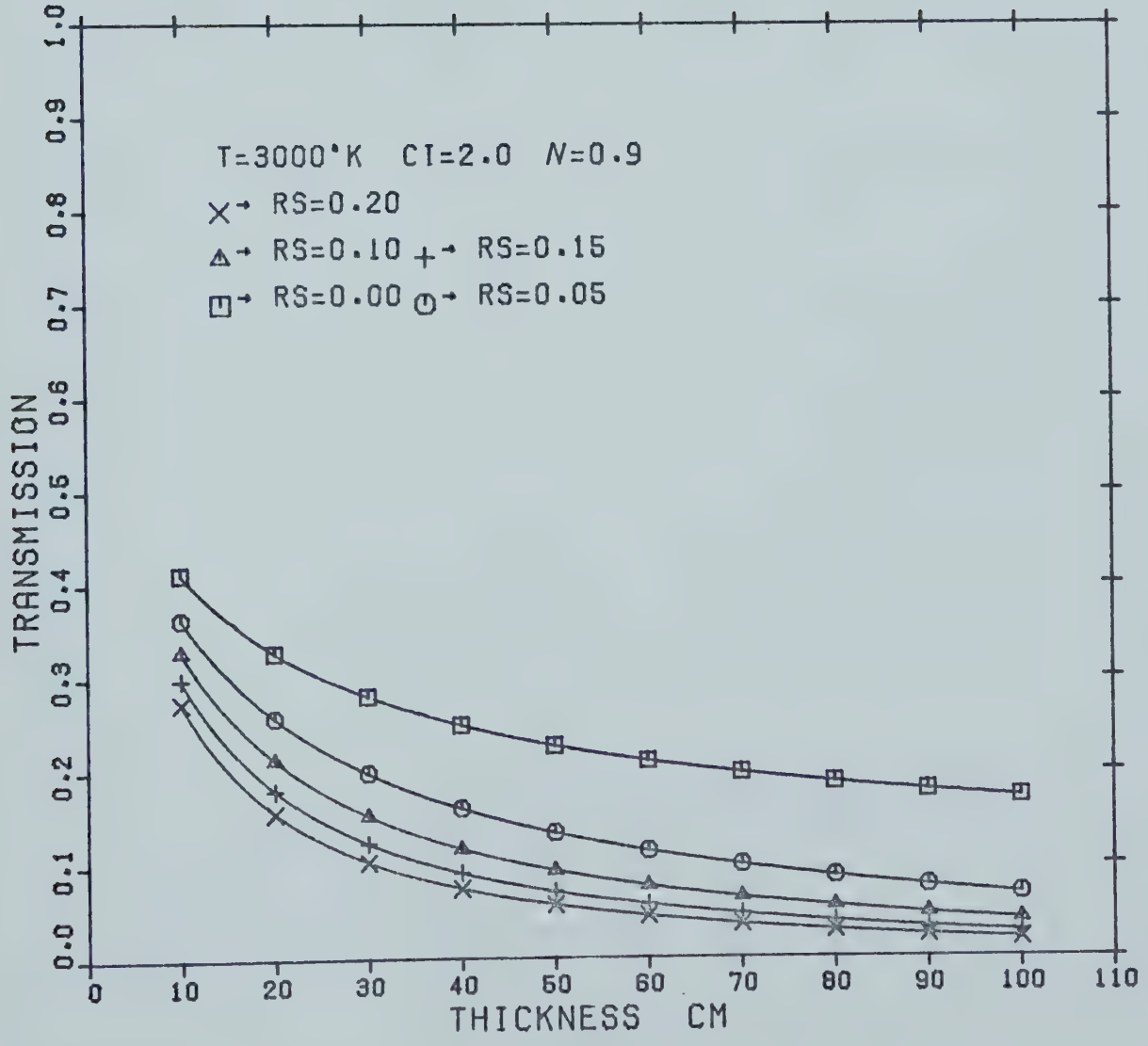

ICE SHEET EFFECTS ON THERMAL RADIATION

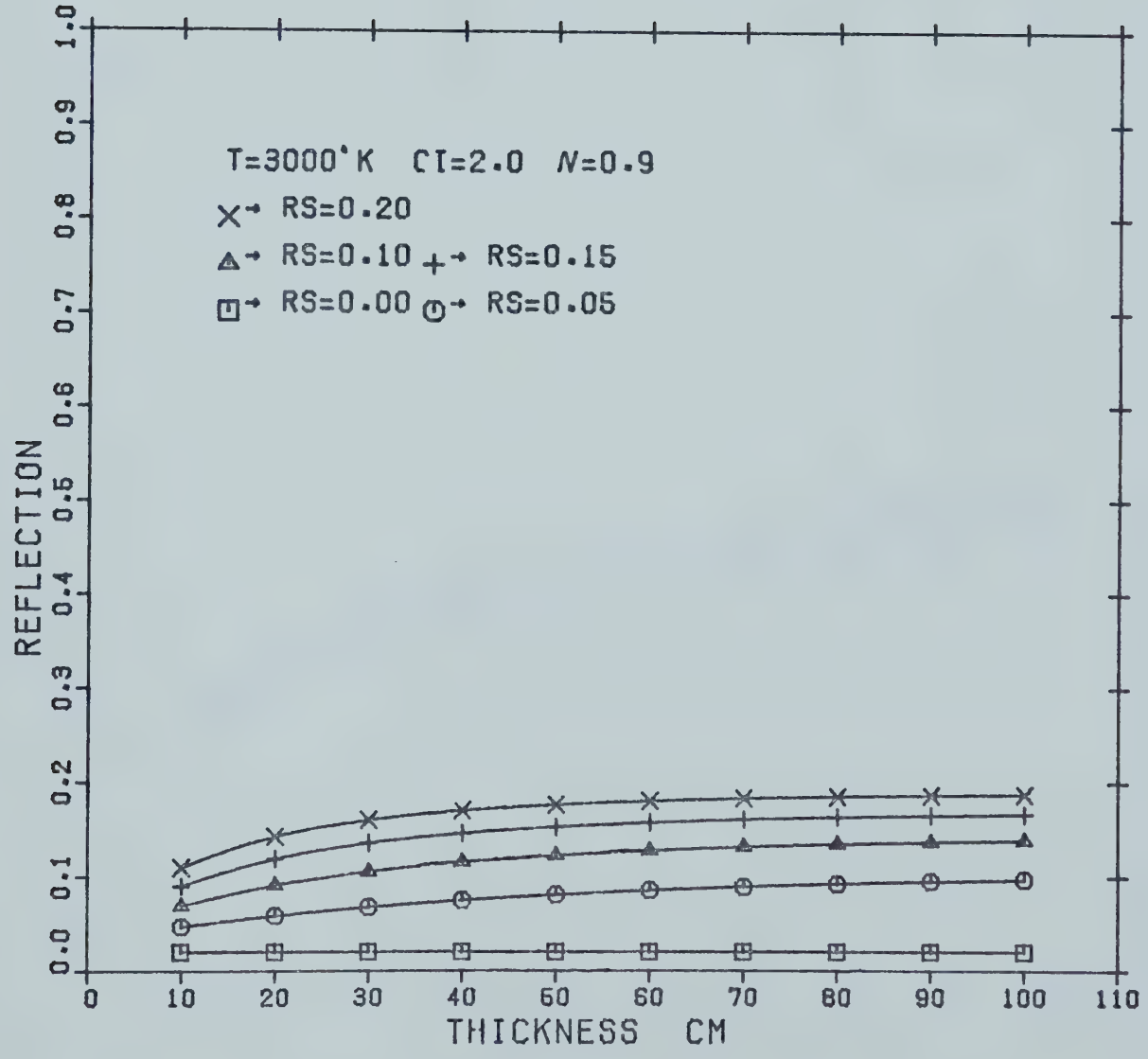

ICE SHEET EFFECTS ON THERMAL RADIATION

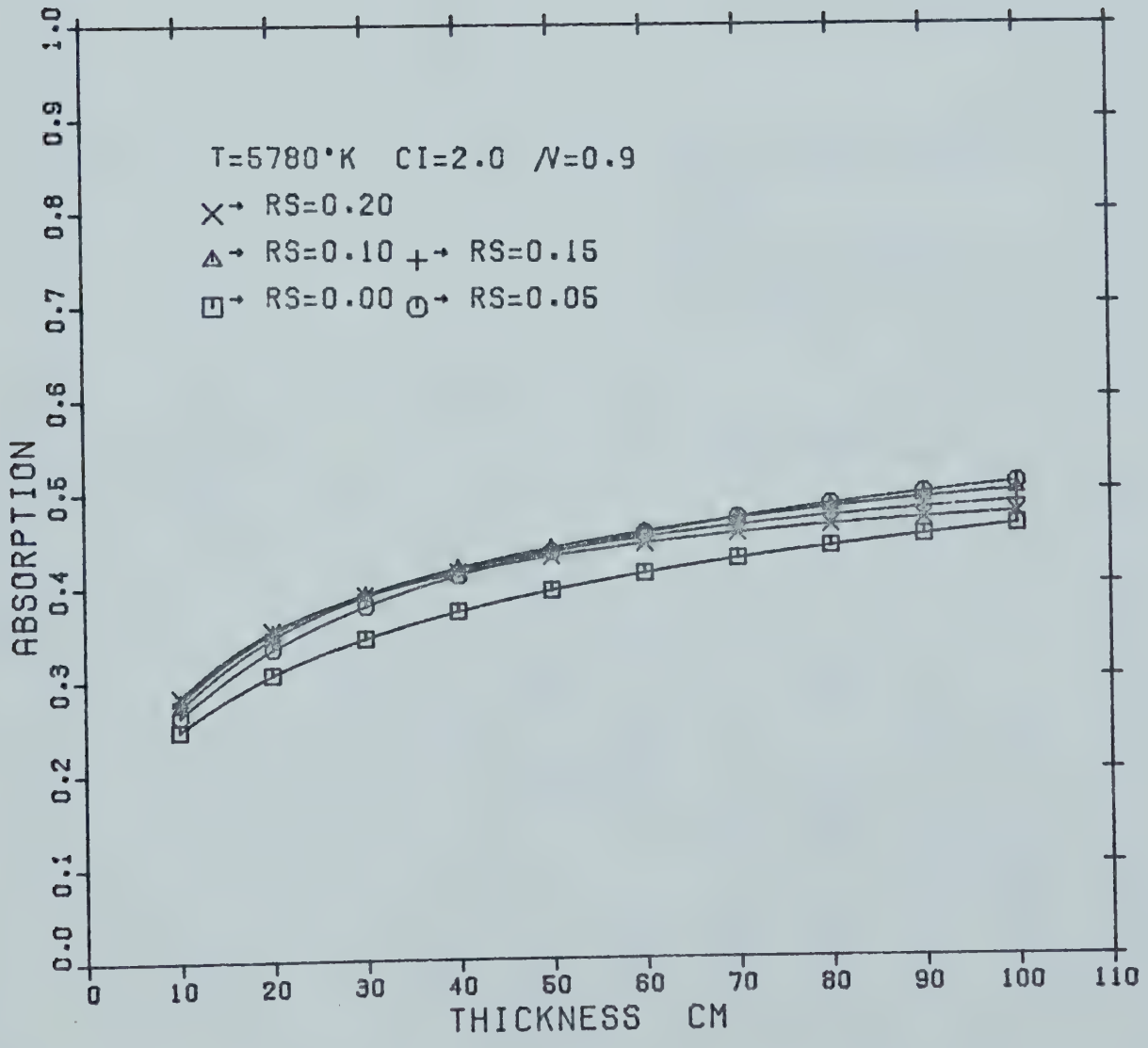

ICE SHEET EFFECTS ON THERMAL RADIATION

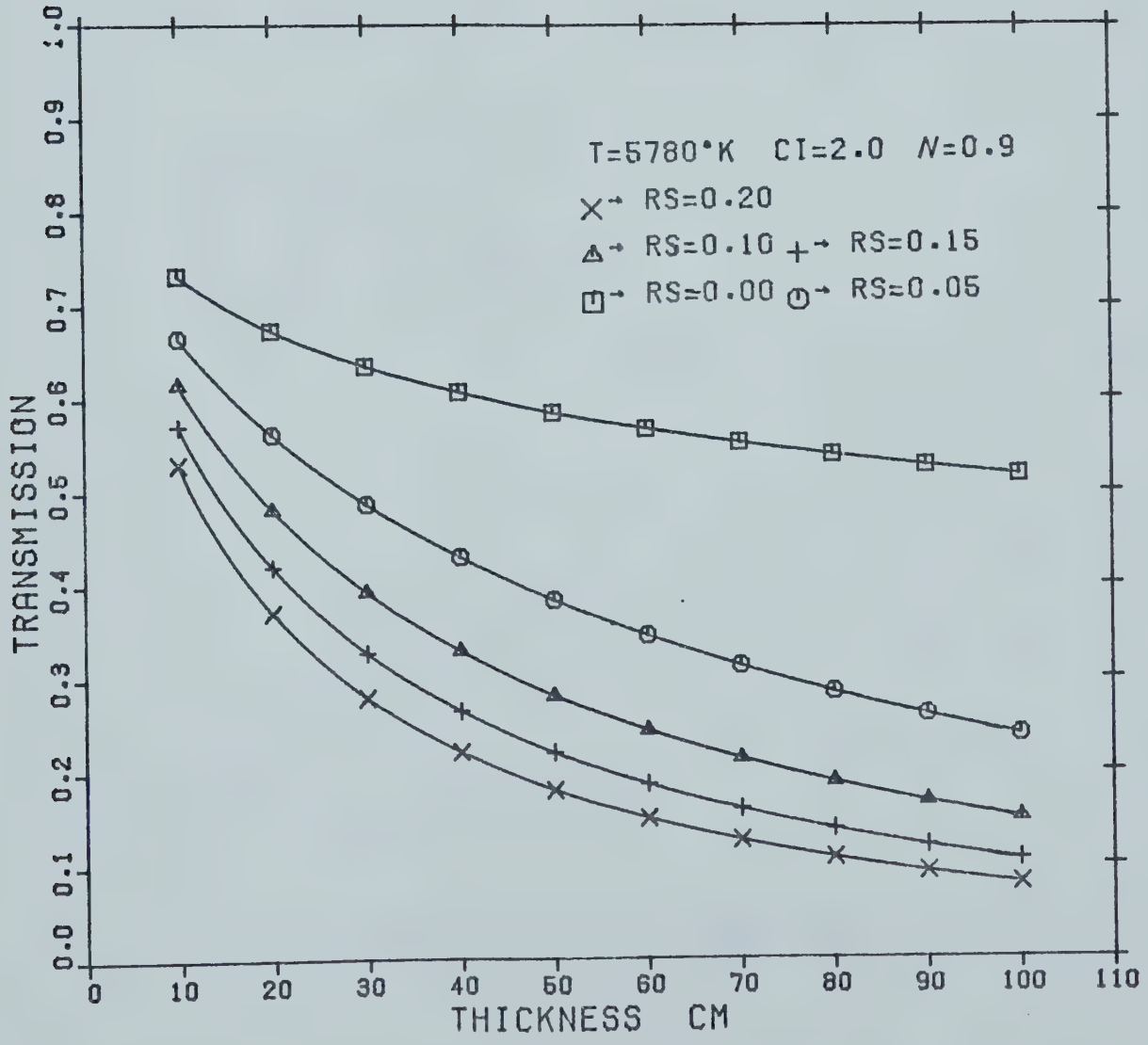

ICE SHEET EFFECTS ON THERMAL RADIATION

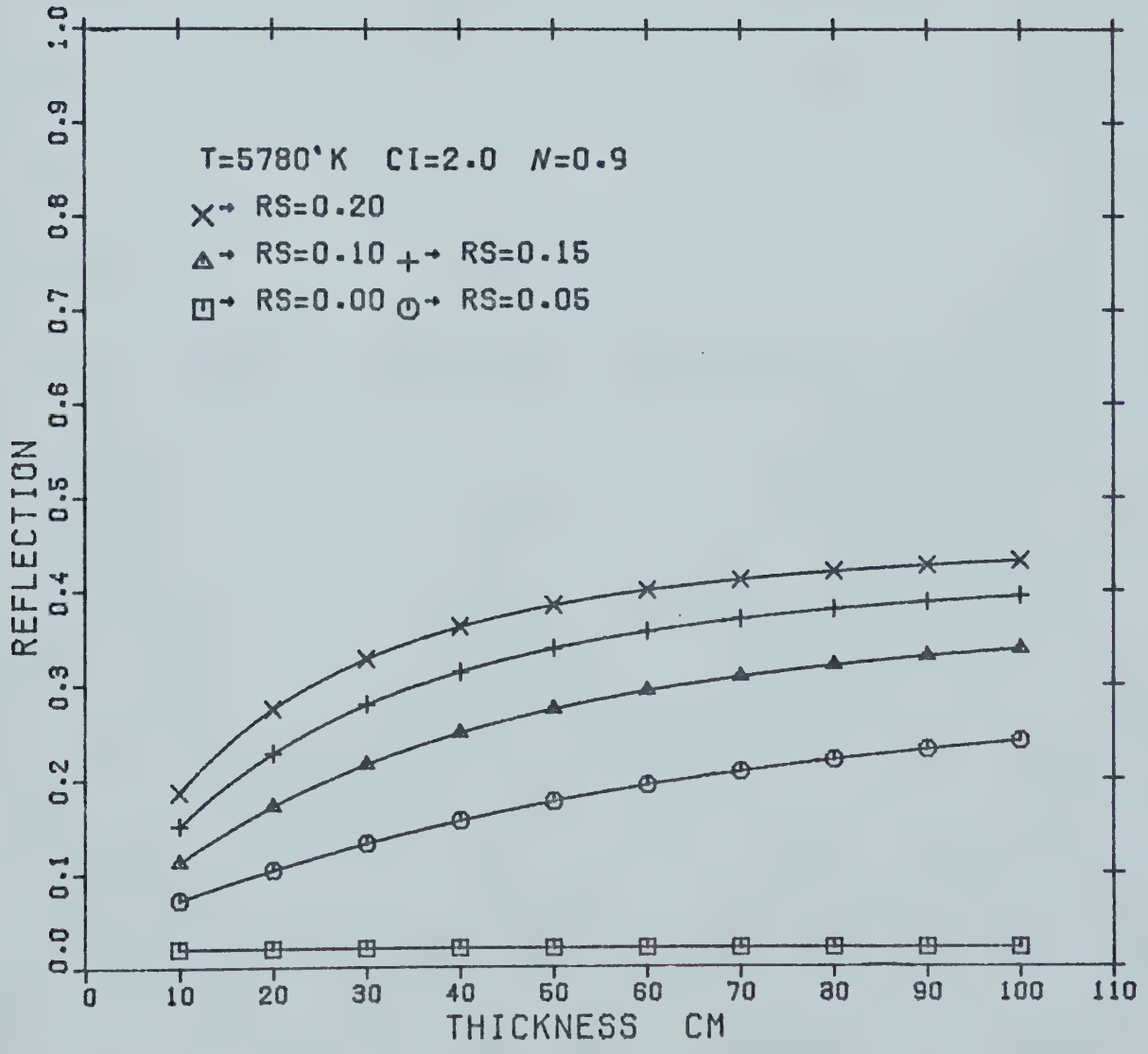

ICE SHEET EFFECTS ON THERMAL RADIATION

APPENDIX C

ATTENUATION IN AN ICE SHEET WITH DEPTH

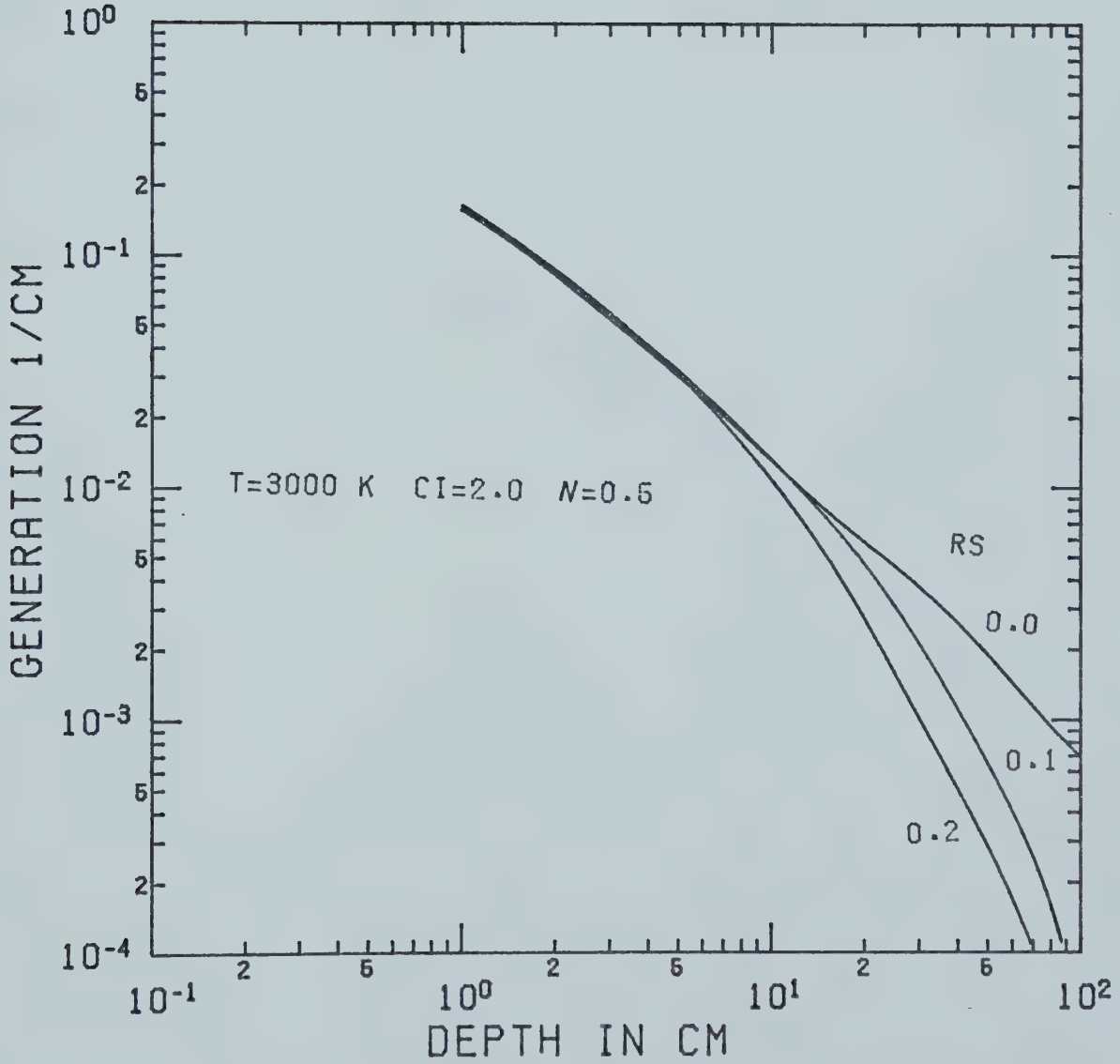

ATTENUATION IN AN ICE SHEET WITH DEPTH

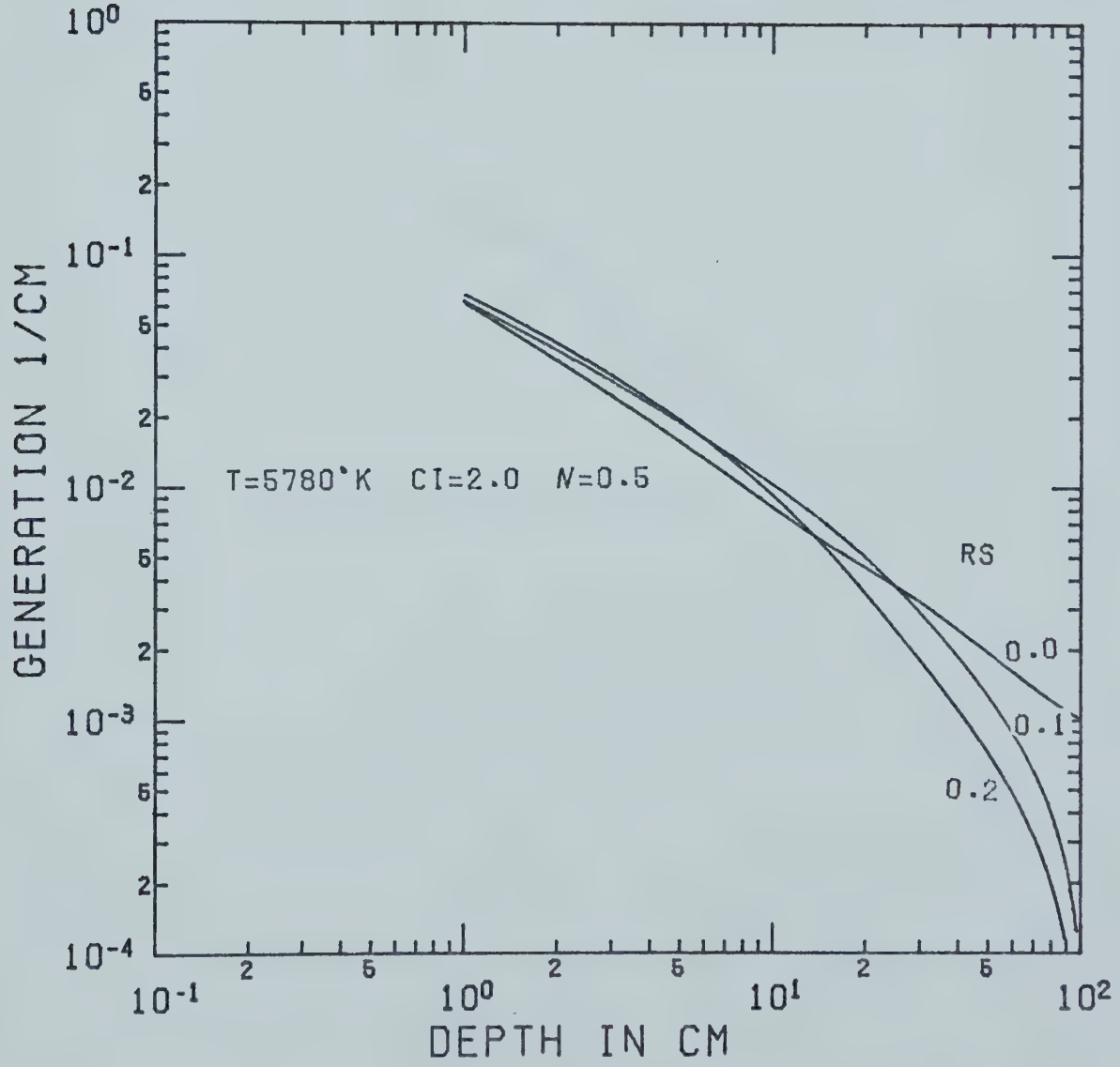

ATTENUATION IN AN ICE SHEET WITH DEPTH

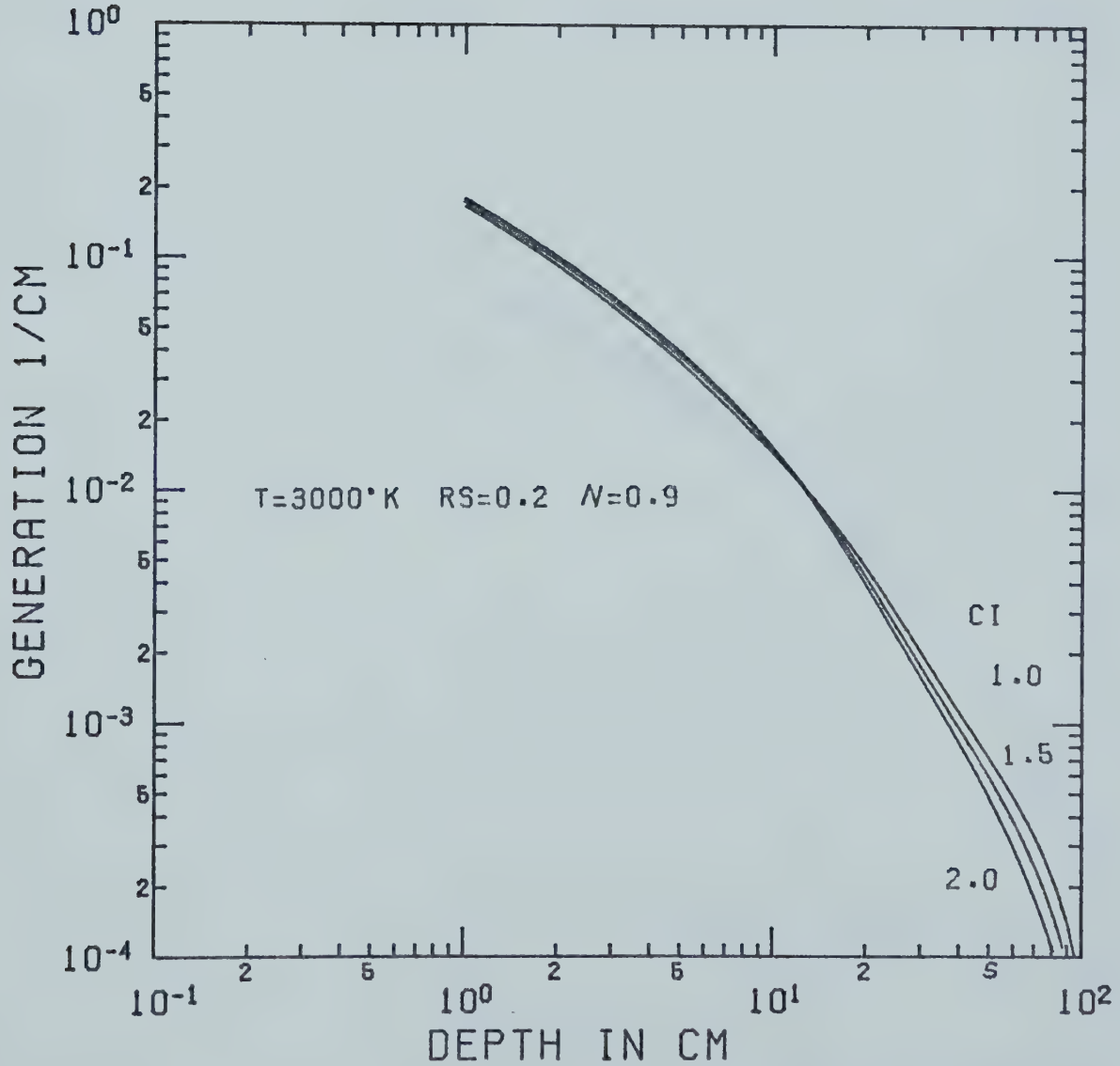

ATTENUATION IN AN ICE SHEET WITH DEPTH

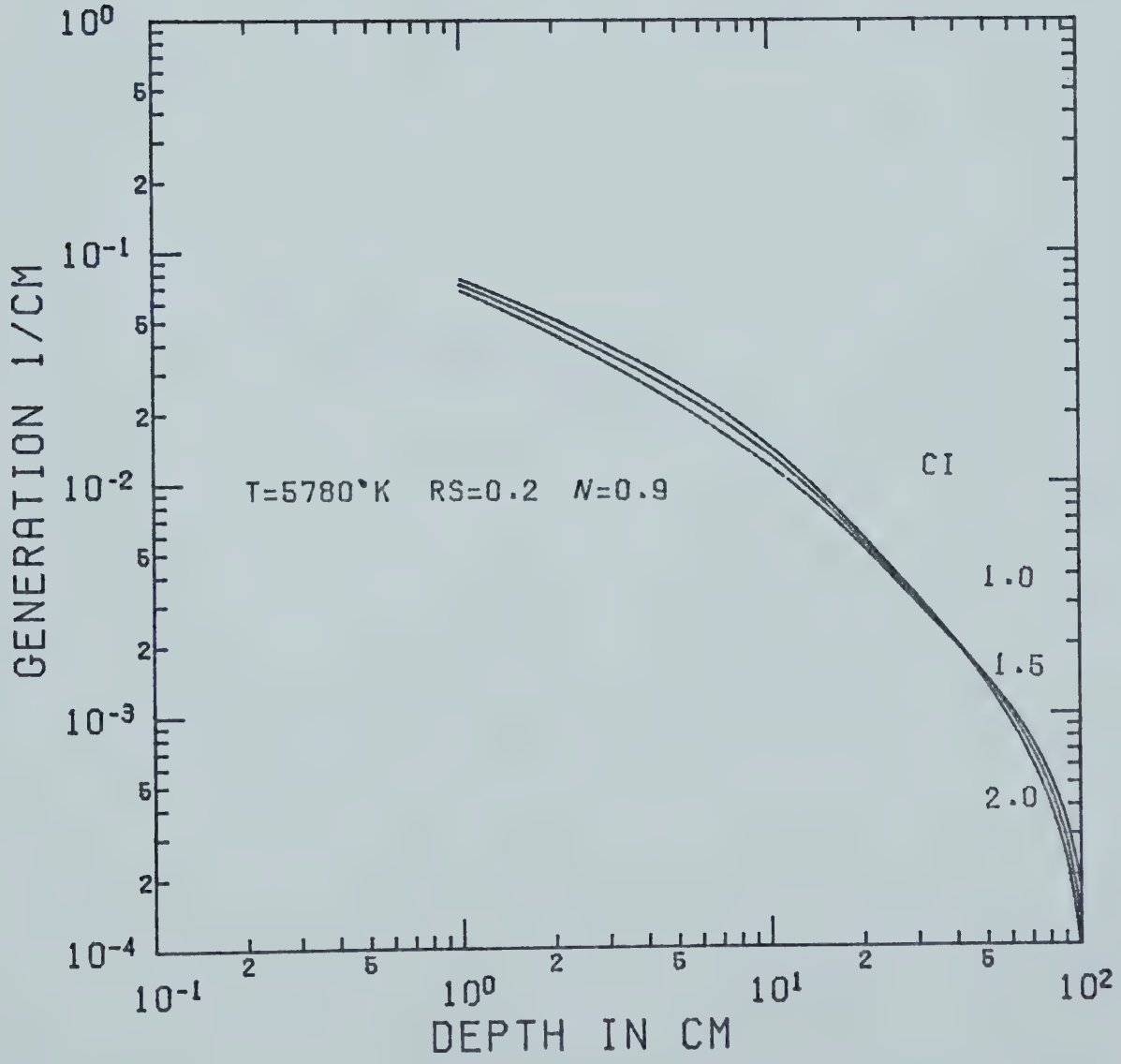

ATTENUATION IN AN ICE SHEET WITH DEPTH

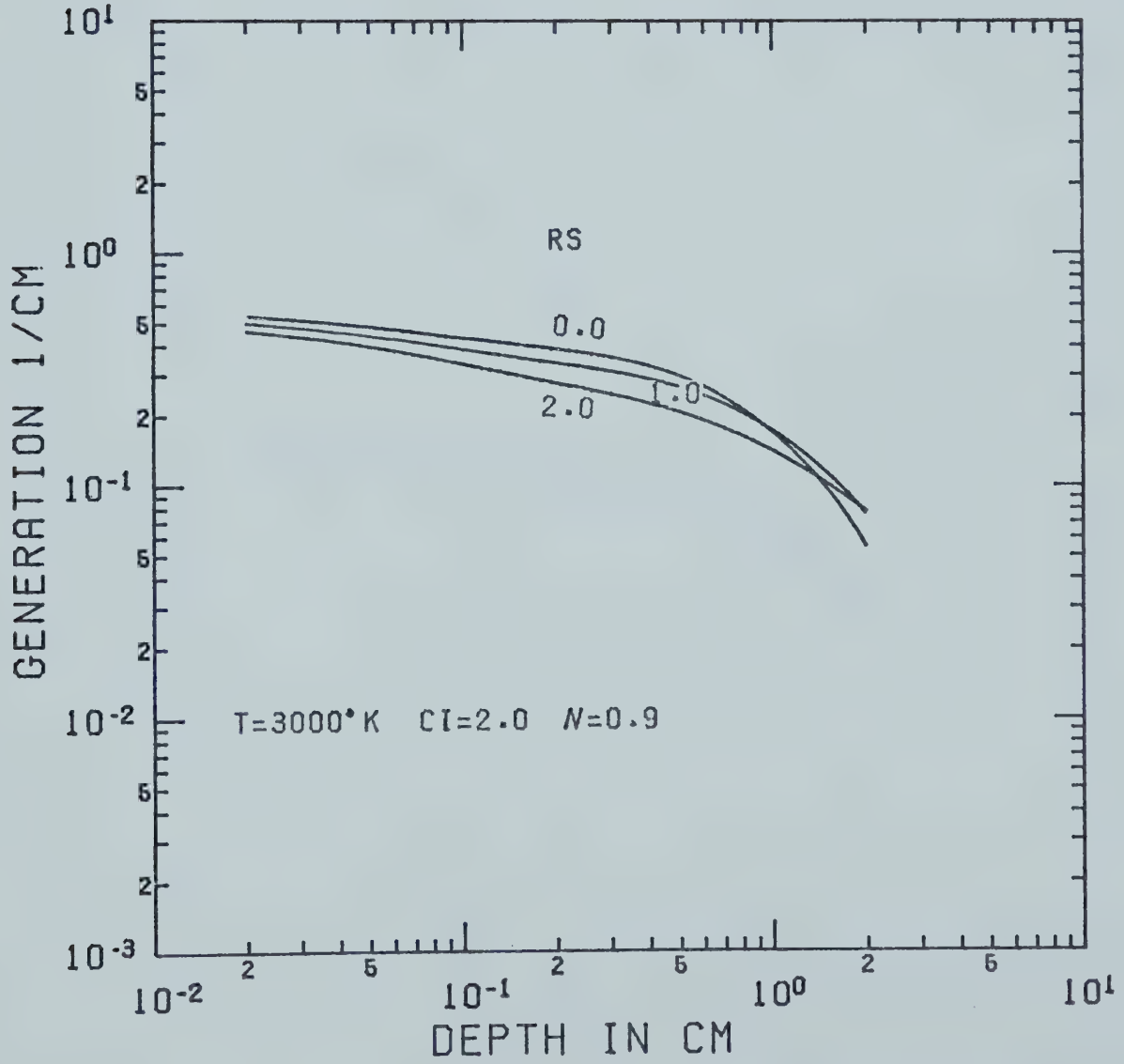

ATTENUATION IN AN ICE SHEET WITH DEPTH

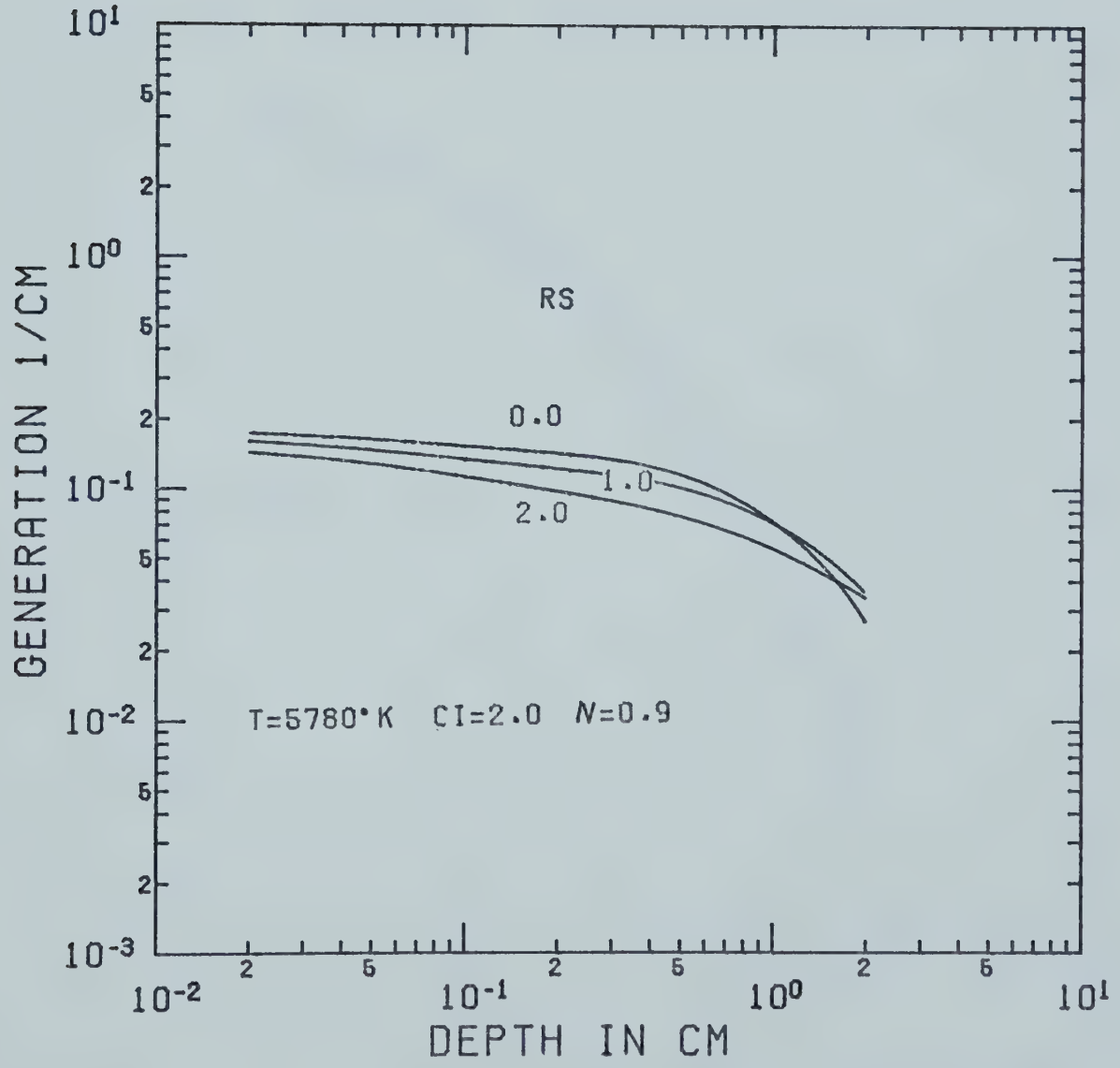

ATTENUATION IN AN ICE SHEET WITH DEPTH

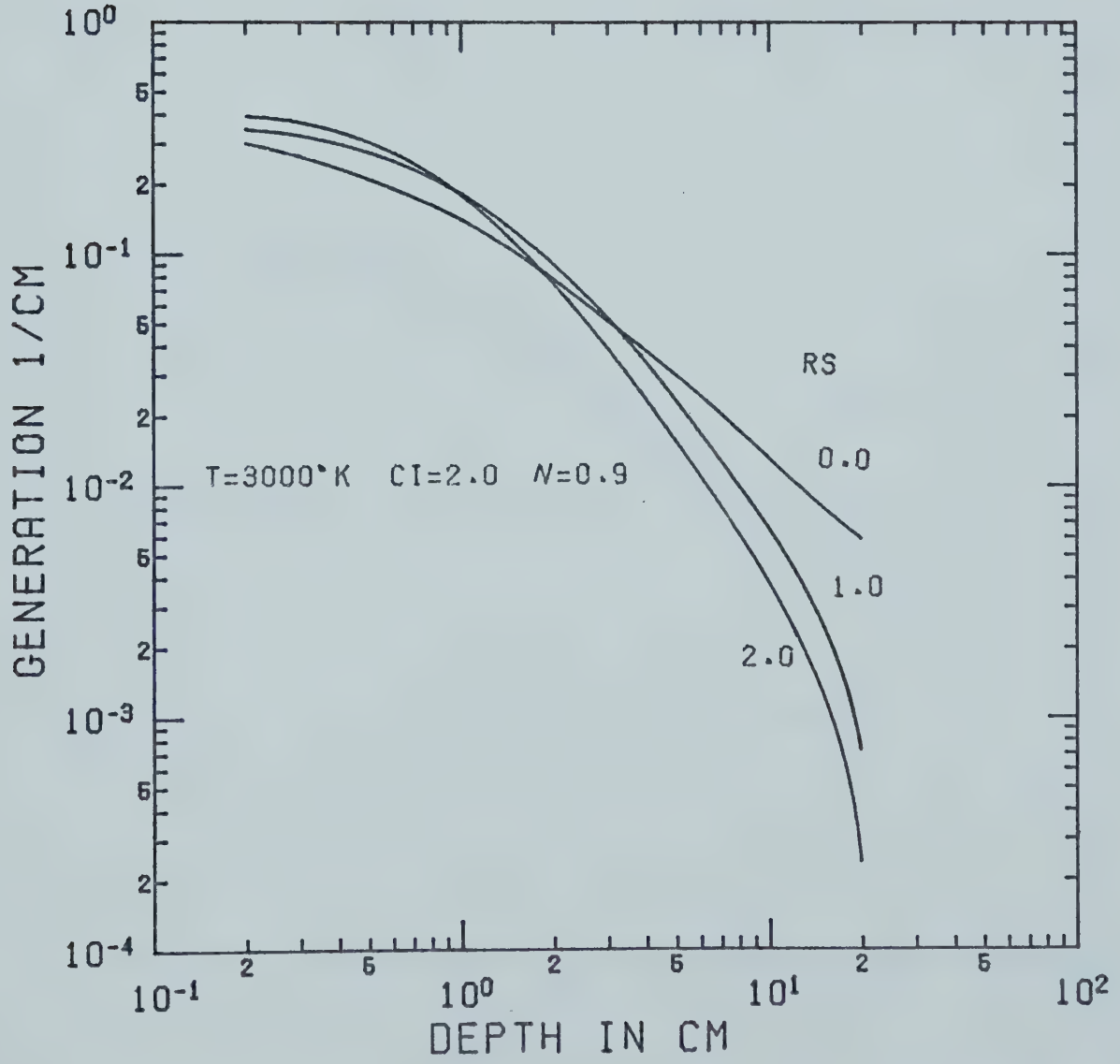

ATTENUATION IN AN ICE SHEET WITH DEPTH

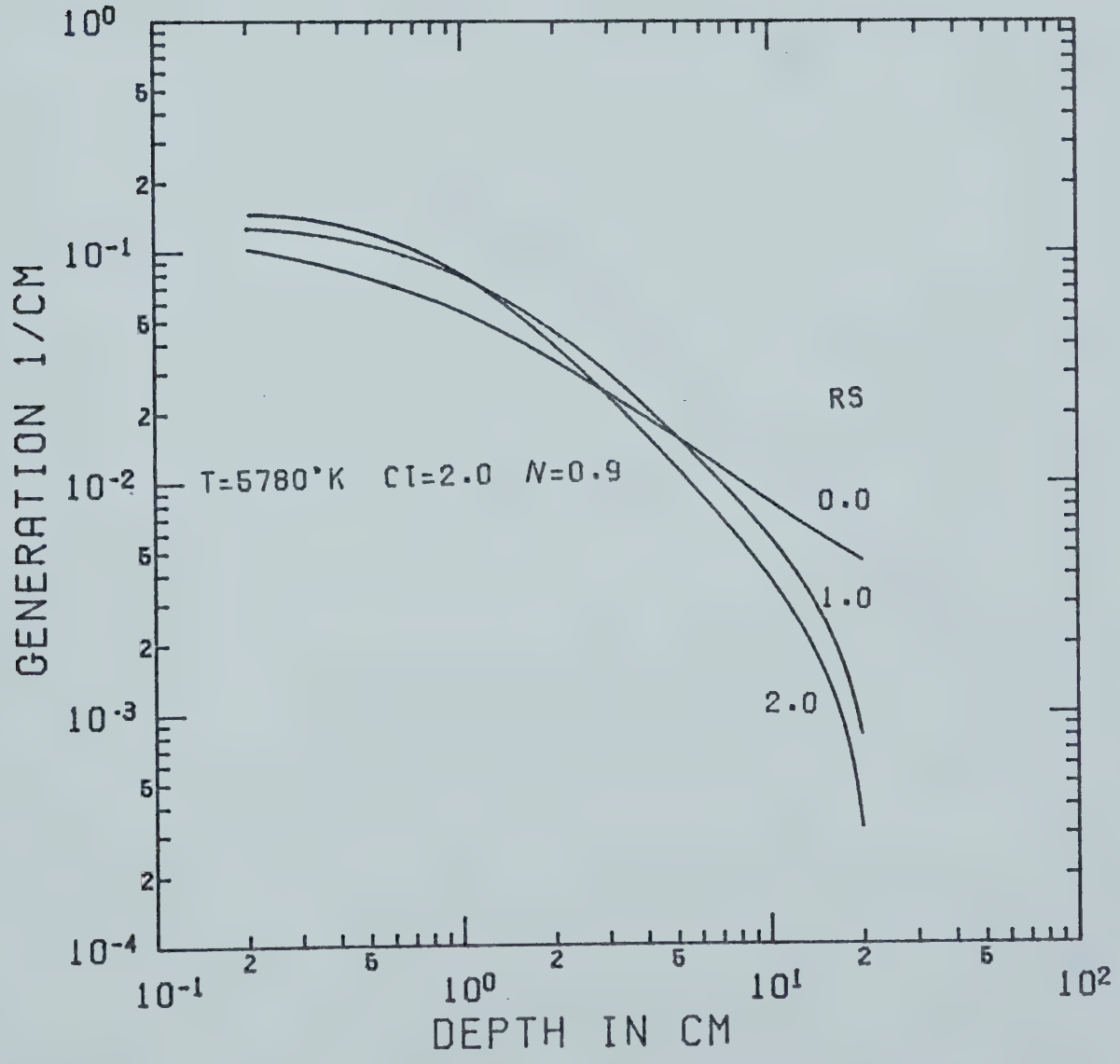

ATTENUATION IN AN ICE SHEET WITH DEPTH

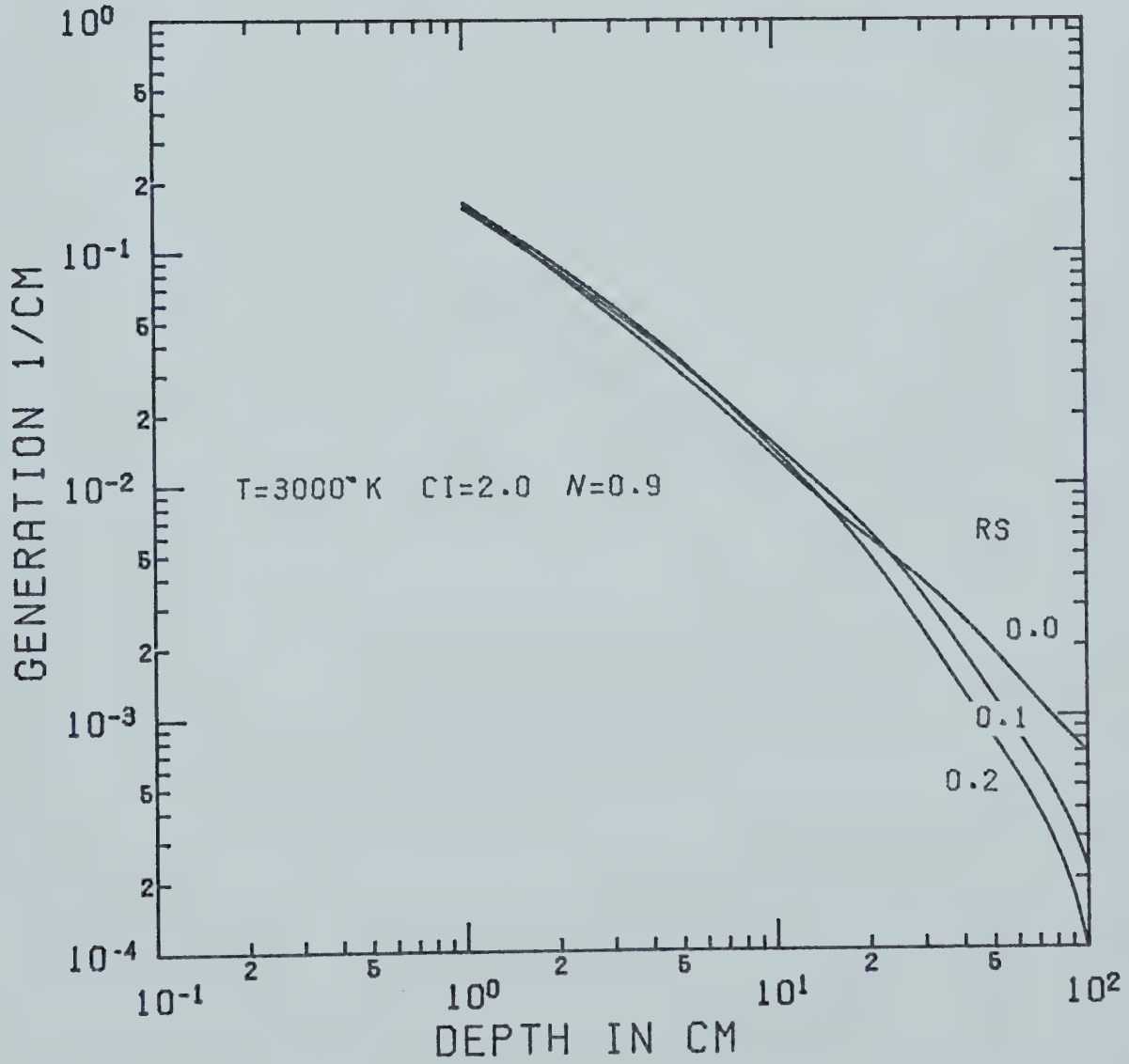

ATTENUATION IN AN ICE SHEET WITH DEPTH

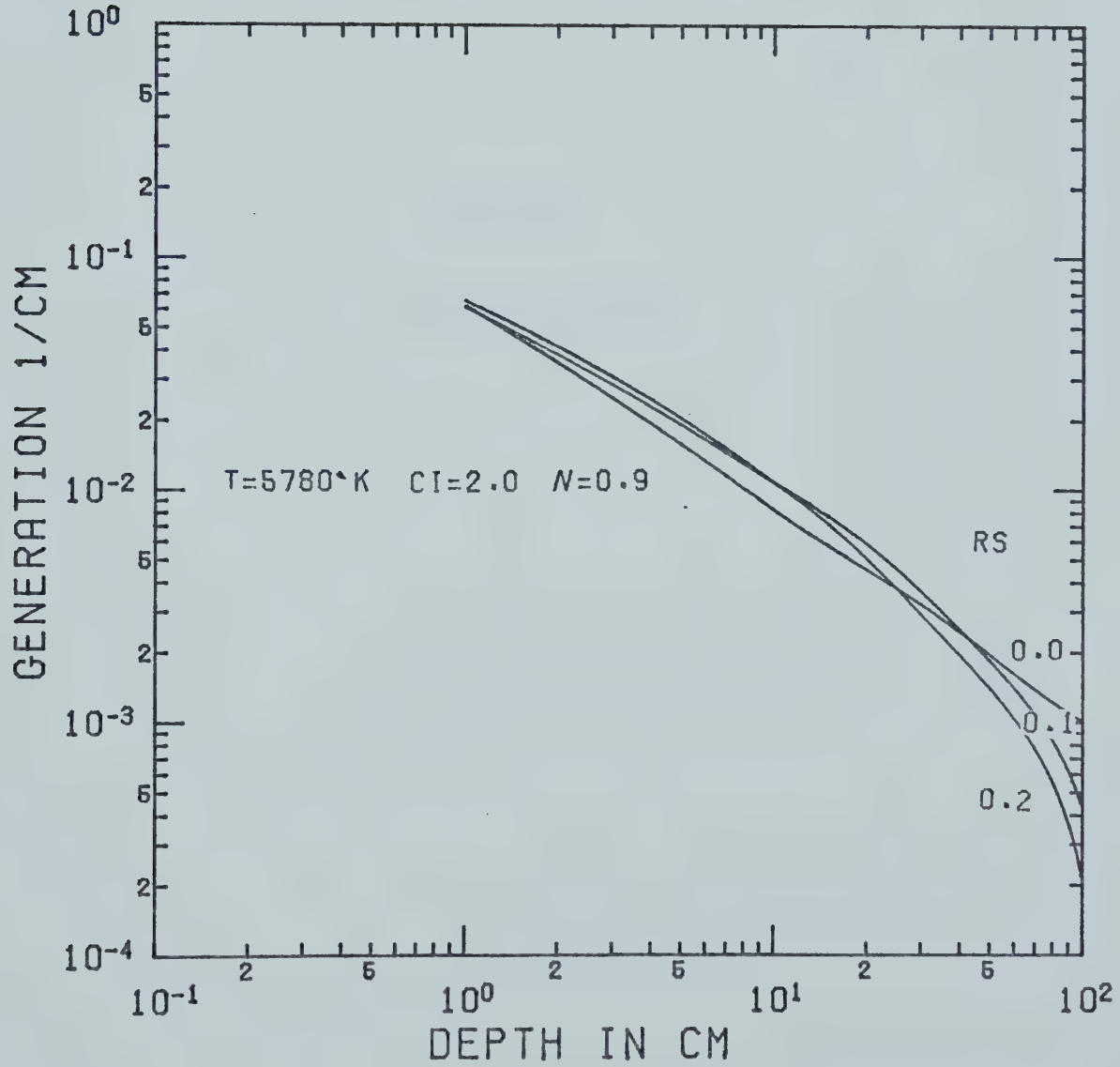

ATTENUATION IN AN ICE SHEET WITH DEPTH

APPENDIX D

INSTRUMENTATION

Type of Equipment Used	Description
1. Blackbody Source	In order to calibrate the thermal radiometer, a known intensity of radiation was produced by a Blackbody Radiation Source Model WS143 made by Electro Optical Industries, Inc. The selected source temperatures were maintained by a Temperature Controller Model 215B produced by the same company.
2. Chart Recorder	A Hewlett Packard strip chart recorder Model 7100B was used on the 0.5 millivolt and 1.0 millivolt scales to record thermocouple outputs.
3. Laser	The specific laser used was a Spectra Physics Model 130B. This laser was of helium-neon-gas phase type producing continuous emmission at a wavelength of 0.6328 μ.
4. Radiation Probes	To measure radiation intensities two types of radiometers were used. They are a Cintra Quantum Radiometer Model 101 and a Cintra Thermal Radiometer Model 202.

Type of Equipment Used	Description
	To detect the radiation intensities the quantum radiometer used a Cintra Probe #1114 while the thermal radiometer used a Cintra Probe #2000.
5. Radiation Sources	The tungsten lamp (3000°K) consisted of a Sylvania Tungsten Halogen Lamp type DVG rated at 650 watts surrounded by a parabolic reflector. To simulate the solar spectrum, a Metro-Lite Model ME-4 carbon arc lamp was employed.
6. Thermocouple Calibration	To calibrate the thermocouples, a platinum resistance thermometer cat. #8163-QB produced by Leeds and Northrup was employed. Outputs from the copper constantan thermocouples and resistance thermometer, that were obtained by placing them in a temperature controlled bath, are compared using Potentiometer #7555 Type K-5 and a Guarded Nanovolt Detector #9383-1 also produced by Leeds and Northrup.